NUREG/IA-0163


# International Agreement Report

# A Study of the Dispersed Flow Interfacial Heat Transfer Model of RELAP5/MOD2.5 and RELAP5/MOD3

Prepared by
M. Andreani*
G. Th. Analytis
S. N. Aksan

Thermal-Hydraulics Laboratory
Paul Scherrer Institute (PSI)
CH–5232 Villigen PSI, Switzerland

*ETHZ, Nuclear Engineering Laboratory
Swiss Federal Institute of Technology (ETH)
8092 Zurich, Switzerland

**Office of Nuclear Regulatory Research**
**U.S. Nuclear Regulatory Commission**
**Washington, DC 20555–0001**

**April 1999**

Prepared as part of
The Agreement on Research Participation and Technical Exchange
under the International Code Application and Maintenance Program (CAMP)

**Published by**
**U.S. Nuclear Regulatory Commission**

# AVAILABILITY NOTICE

## Availability of Reference Materials Cited in NRC Publications

NRC publications in the NUREG series, NRC regulations, and *Title 10, Energy,* of the *Code of Federal Regulations,* may be purchased from one of the following sources:

1. The Superintendent of Documents
   U.S. Government Printing Office
   P.O. Box 37082
   Washington, DC 20402–9328
   <http://www.access.gpo.gov/su_docs>
   202–512–1800

2. The National Technical Information Service
   Springfield, VA 22161–0002
   <http://www.ntis.gov/ordernow>
   703–487–4650

The NUREG series comprises (1) brochures (NUREG/BR-XXXX), (2) proceedings of conferences (NUREG/CP-XXXX), (3) reports resulting from international agreements (NUREG/IA-XXXX), (4) technical and administrative reports and books [(NUREG-XXXX) or (NUREG/CR-XXXX)], and (5) compilations of legal decisions and orders of the Commission and Atomic and Safety Licensing Boards and of Office Directors' decisions under Section 2.206 of NRC's regulations (NUREG-XXXX).

A single copy of each NRC draft report is available free, to the extent of supply, upon written request as follows:

Address: Office of the Chief Information Officer
Reproduction and Distribution
Services Section
U.S. Nuclear Regulatory Commission
Washington, DC 20555–0001
E-mail: <DISTRIBUTION@nrc.gov>
Facsimile: 301–415–2289

A portion of NRC regulatory and technical information is available at NRC's World Wide Web site:

<http://www.nrc.gov>

All NRC documents released to the public are available for inspection or copying for a fee, in paper, microfiche, or, in some cases, diskette, from the Public Document Room (PDR):

NRC Public Document Room
2120 L Street, N.W., Lower Level
Washington, DC 20555–0001
<http://www.nrc.gov/NRC/PDR/pdr1.htm>
1–800–397–4209 or locally 202–634–3273

Microfiche of most NRC documents made publicly available since January 1981 may be found in the Local Public Document Rooms (LPDRs) located in the vicinity of nuclear power plants. The locations of the LPDRs may be obtained from the PDR (see previous paragraph) or through:

<http://www.nrc.gov/NRC/NUREGS/SR1350/V9/lpdr/html>

Publicly released documents include, to name a few, NUREG-series reports; *Federal Register* notices; applicant, licensee, and vendor documents and correspondence; NRC correspondence and internal memoranda; bulletins and information notices; inspection and investigation reports; licensee event reports; and Commission papers and their attachments.

Documents available from public and special technical libraries include all open literature items, such as books, journal articles, and transactions, *Federal Register* notices, Federal and State legislation; and congressional reports. Such documents as theses, dissertations, foreign reports and translations, and non-NRC conference proceedings may be purchased from their sponsoring organization.

Copies of industry codes and standards used in a substantive manner in the NRC regulatory process are maintained at the NRC Library, Two White Flint North, 11545 Rockville Pike, Rockville, MD 20852–2738. These standards are available in the library for reference use by the public. Codes and standards are usually copyrighted and may be purchased from the originating organization or, if they are American National Standards, from—

American National Standards Institute
11 West 42nd Street
New York, NY 10036–8002
<http://www.ansi.org>
212–642–4900

NUREG/IA-0163


# International Agreement Report

# A Study of the Dispersed Flow Interfacial Heat Transfer Model of RELAP5/MOD2.5 and RELAP5/MOD3

Prepared by
M. Andreani*
G. Th. Analytis
S. N. Aksan

Thermal-Hydraulics Laboratory
Paul Scherrer Institute (PSI)
CH-5232 Villigen PSI, Switzerland

*ETHZ, Nuclear Engineering Laboratory
Swiss Federal Institute of Technology (ETH)
8092 Zurich, Switzerland

**Office of Nuclear Regulatory Research**
**U.S. Nuclear Regulatory Commission**
**Washington, DC 20555-0001**

**April 1999**

Prepared as part of
The Agreement on Research Participation and Technical Exchange
under the International Code Application and Maintenance Program (CAMP)

**Published by**
**U.S. Nuclear Regulatory Commission**

# A Study of the Dispersed Flow Interfacial Heat Transfer Model of RELAP5/MOD2.5 and RELAP5/MOD3.

M. Andreani*, G. Th. Analytis, S. N. Aksan
Thermal-Hydraulics Laboratory,
Paul Scherrer Institute (PSI),
CH-5232 Villigen PSI, Switzerland

## Abstract

In this work, the model of interfacial heat transfer for the dispersed flow regime used in the RELAP5 computer code is investigated. The validity of the 1-D approach used for calculating the heat exchange between the droplets and the vapour in the dispersed flow region above a quench front was shown to be questionable for conditions of low quality at the quench front and low mass flux. Under such conditions, the interfacial heat transfer calculated assuming a uniform distribution of droplets over the cross-sectional area of the channel is necessarily overpredicted, and the vapour superheat is strongly underpredicted. The purpose of the present paper is to show that the limitations of the 1-D approach, obtained from the steady-state anlyses of slow reflooding experiments, has some impact on the performance of the 1-D transient computer codes like RELAP5/MOD2.5 and RELAP5/MOD3. As an example, the transient analysis of a low flooding rate experiment in a tube was performed. An early completion of the quench process and a fast desuperheating of the vapour at the tube exit was obtained by both codes. The too high quench front velocity (four times higher than in the experiment) could not, however, be put univocally in relation to the underprediction of the vapour temperature, and the consequent increase of the precursory cooling, as many coupled thermal and hydraulic transient effects prevailed. Quasi steady-state anlyses of two runs, where the boundary conditions for the the post-dryout region could be better controlled for a predetermined position of the quench front, were thus performed. These analyses show that the vapour superheat at the tube exit is strongly underpredicted, confirming the limitations of the 1-D model for interfacial heat transfer in the dispersed flow region.

* ETHZ, Nuclear Engineering Laboratory Swiss Federal Insitute of Technology (ETH),
8092 Zürich, Switzerland

# Contents

# List of Figures

# List of Tables

# 1 Introduction

An extensive work of assessment, development and applications of the RELAP5 and TRAC/B reactor safety computer programs has been underway for some time at the Thermal-Hydraulics Laboratory of the Paul Scherrer Institute (PSI). One of the reactor safety issues to which the research has been specially addressed is the reflooding phase of the LOCA: indeed, the accurate calculation of the rod temperature during this period is of importance for the estimation of the safety margins required for the reactor operation.

The main results of this research [1],[2],[3],[4] and the contributions to the code development in the areas of wall heat transfer [5],[6], interfacial drag [2],[6], and numerical techniques [6],[7] have been fully documented and examples of references have been provided here. For several reflooding experiments, it has been observed that both the trend and the values of the calculated results (wall and vapour temperatures, entrainment, collapsed liquid level, etc.) obtained by the 'frozen' version of the codes were very different to the measured experimental data. The discrepancies between the calculations and the data were noticeably large, especially for low flooding rate conditions. Low flooding rate experiments are characterized by very high void fractions all over the region above the QF for long time periods; in this zone droplets are dispersed in a stream of superheated vapour. The incorrect calculation of either the vapour superheat or the wall heat transfer coefficient resulted in the poor predictions of the 'frozen' versions of the codes.

The implementation of more consistent packages of correlations for wall heat transfer and interfacial shear (for both the wet and dry wall regions), the accurate selection of several empirical constants entering in the various models on the base of sensitivity studies, and the modification of interpolation schemes and numerical techniques lead to improved versions of the programs, which successfully simulate most experiments with *bundles* [2],[3],[5],[6],[7].

Modifications to the closure laws (largest droplet size, interfacial heat transfer) related to the dispersed flow regime above the Quench Front (QF) have also played a role in the achievement of good results, and more research is underway in this area. These studies are important contributions to the development of reliable calculation tools for reactor safety assessment, as the test facilities considered for the assessment are closely reproducing the conditions expected in the nuclear cores.

However, since a few quantities (average temperatures, entrainment rate, quench front velocity, etc.) are measured and can be used for the assessment, the adequacy of the closure laws used for the individual submodels can seldom be demonstrated. In principle, a fortuitous compensation of errors and the lumping of different effects in one single 'best fit' parameter, could mask the deficiencies in the models implemented in the codes. For instance, the lack of the representation of the spacer grids and an incorrect model for interfacial heat transfer and interfacial shear could be 'compensated' by a proper, although unphysical, choice of the empirical criterion for defining the droplet diameter.

In the present report, a different approach to the analysis of the reflooding process is presented, which is more suitable for evaluating the capabilities of one of the submodels used in the codes, namely that for interfacial heat transfer in the dispersed flow region. The attention to this particular model is motivated by the results of a recent investigation [8],[9] on post-CHF heat transfer with dispersed flow during reflooding. It has been shown that, under conditions of low mass flux and low quality at the QF, the interfacial heat transfer must be overpredicted by the 1-D models and some 3-D (such as those implemented in RELAP and TRAC* series of codes) and this results in large underpredictions of the vapour superheat. It was argued that the neglect of the cross-sectional distribution of the droplets can be the reason for these discrepancies. The clustering of the droplets around the centre with the consequent reduction in the interfacial heat transfer has been proposed [8],[9] as a possible mechanism for explaining the high superheating rates (close to those admissible for 'frozen flow') at some distance from the QF observed in several tube experiments [10]: this conclusion was obtained using the commonly accepted closure laws for interfacial drag and droplet diameter.

The present analysis using RELAP5 is, therefore, aiming at a verification of such a general statement by a specific application of the 1-D approach. In this respect, the most interesting variable for judging the

*The TRAC code is often quoted as 3-D code, as it can provide information on the 3-D distributions *in the core*; the large sizes of the radial mesh which can practically be used, however, do not allow to calculate the radial profiles *inside the individual sub-channels*.

capability of the model is the vapour temperature at the exit of the test section, and this will be the main object of the discussions of the results.

For this purpose, it is convenient to assess the codes against data obtained in single-tube experiments; the simpler tube geometry allows to better test the interfacial heat transfer model, as the 'spurious' effects of the grids (which cannot be quantified and cannot be taken into consideration by the code, but are present in the experiments with bundles) on the droplet size and other variables, will not bias the comparison between the calculated vapour temperature and the experimental data. The exercise presented in this work is the transient analysis of the low flooding rate experiment 3051 at 2 bar in the single tube test section of the University of California-Berkeley (UCB) by means of frozen versions of RELAP5/MOD2.5 (Mod2, cycle 36.06)[11] and RELAP5/MOD3 (7vj)[12]; this experiment was chosen because the separate steady-state analyses [9] showed severe difficulties of the 1-D approach.

However, while the transient analysis of the core is the only important application of the reactor safety codes, much deeper insight in the influence of the interfacial heat transfer on the mixture evolution is made possible by considering 'snapshots' at different times during the transient. The values of several variables are considered constant over a short time period, and the analysis is referred to such a 'frozen' picture. The rationale for the consequent 'quasi steady-state analysis' is shortly outlined here, and discussed more in depth in §3. For the 'steady-state' calculation, the conditions above the QF must be imposed (approximately) constant over a short time, and the wall heat flux over the tube length above the QF must be given as input: if good predictions for both liquid and vapour mass flow rates are obtained, the resulting vapour temperature at the tube exit (which depends on the total heat exchanged with the droplets) will give a direct estimate of the adequacy of the interfacial heat transfer closure law used in the code. Indeed, the uniform heat flux which characterizes the single-tube experiments leads to slowly changing axial wall temperature distributions and allows a sufficiently good estimate of the local heat flux at all elevations. This, in turn, allows a rather accurate evaluation of the total power input to the mixture above the QF (on which the vapour superheat strongly depends) at any selected time, so that one of the unknowns which complicates the interpretation of the results of the transient analyses, namely the instantaneous 'actual' power input, can be eliminated.

Therefore, in the present work the quasi-steady state analyses of two UCB experiments (Run 3051 at 2 bar and Run 3053 at 3 bar) for the time of the mid-height quench are also carried-out.

## 2 Test cases used for the assessment

Well documented experimental results for the reflooding of tubes were obtained at the University of California at Berkeley [13],[14]. The diagram of the experimental test facility is shown in Fig. 1. The test section used for the second series of experiments at 2 and 3 bar was a 14.25 mm inside diameter (0.83 mm thickness) tube, 3.67 m in length. It was quenched by bottom injection of water at flooding rates from 25 to 180 mm/s: the water subcooling, about 80 K, was the same for all the experiments. Constant electrical heat input was used, and the cooling of the tube was initiated after an equilibrium condition had been reached: initial wall temperatures ranged between 316 °C and 760 °C. The tube was *not* insulated, and large heat losses have been allowed. The transient was initiated from a condition of constant wall temperatures, the power input being balanced by the heat losses. The initial axial wall temperature profile was practically flat.

The temporal variation of the tube wall temperature at different elevations and of the fluid temperature at the tube exit were obtained: the vapour temperature was measured by a sheathed microthermocouple (0.254 mm) located at about 5 cm above the tube exit. The flows of liquid and vapour at the tube exit were separated by means of a carefully designed separator, and the entrained liquid was collected in a tank. The vapour mass flow was also measured. Moreover, the water collected inside the test section (from which the collapsed liquid level can be calculated) was obtained by measuring the pressure difference between inlet and outlet of the test section, and neglecting friction and acceleration pressure drops.

During many tests, the wall temperatures at some distance from the QF set to nearly constant values for long times, being the heat input balanced by the heat losses and the heat transfer to the fluid: typical wall temperature time-histories are shown for Run 3051 (experimental conditions specified below) in Fig. 2.

In the present investigation, the conditions at the earliest time such a steady condition (the quality at the QF being positive) for the wall temperatures at the higher elevations is attained are chosen for the 'quasi steady-state' analyses.

In Table 1 the experimental conditions of the two runs used for assessing the codes are summarized.

For the quasi steady-state analyses, the additional information on the equilibrium quality at the QF $x_{QF}$ and the axial distribution of the net heat input to the fluid $q''_{in}$ at the selected time are also required.

The equilibrium quality immediately above the quench front $x_{QF}$ is calculated [15] by adding to the quality immediately below the Quench Front $x^-$ (calculated by an energy balance over the wet region) the quality change across the Quench Front due to the intense vaporization caused by the release of the heat stored in the tube wall:

$$x^+ = x^- + \frac{C_w A_w (T^+ - T^-) U_{QF}}{H_{fg} G A} \tag{1}$$

with:

$$x^- = \frac{P_{tot} \left(\frac{z_{QF}}{L}\right)}{H_{fg} G A} + \frac{\Delta H_{sub}}{H_{fg}}$$

where $C_w$ is the volumetric heat capacity of the wall, $A_w$ the cross sectional area of the wall, $U_{QF}$ the quench front velocity, $H_{fg}$ the vaporization enthalpy, $G$ the total mass flux, $A$ the cross sectional area of the channel, $T^+$ and $T^-$ the wall temperatures above and below the quench front, $\Delta H_{sub}$ the liquid subcooling at the inlet of the test section, $L$ the total length of the tube test section, $z_{QF}$ the distance of the QF from the tube inlet, and $P_{tot}$ the input power.

The net heat flux $q''_{in}$ at each elevation is obtained by subtracting from the inside-wall 'imposed' heat flux $q''_o$ ($P_{tot}$ divided by the internal surface area), the heat losses $q''_{L,iw}$ (referred to the inside-wall surface area) and the sensible heat stored in the wall:

$$q''_{in} = q''_o - q''_{L,iw} - C'_w \frac{dT'_w}{dt} \tag{2}$$

where $C'_w$ is wall heat capacity per unit inside wall area and $T'_w$ the value of the wall temperature (in K) obtained by polynomial interpolation of the experimental temperatures. The outside heat flux (losses) is:

$$q''_L = h_L (T'_w - T_{amb}) \tag{3}$$

where $h_L$ is the global heat transfer coefficient (HTC) from the wall to the surroundings, assumed to be at temperature $T_{amb}$=294 K. The experimental values of $h_L$ could be correlated by the formula:

$$h_L = 11.949\, e^{[2.592 \cdot 10^{-3} (T'_w - T_{amb})]} \quad (\mathrm{W/m^2\ K}) \tag{4}$$

The heat losses per unit area (heat flux to the ambient) referred to the inside-wall heat transfer area is obtained by:

$$q''_{L,iw} = q''_L \frac{D_e}{D}$$

where $D_e$ and $D$ are the external and internal diameters, respectively.

The total heat input to the fluid in the dry region above the Quench Front $P_{dry}$ is calculated by integrating $q''_{in}$ over the wall heat exchange area.

The values of the several variables required for the quasi steady state analyses are given in Table 2 together with the transient times to which they refer.

| Run No. | $p$ bar | $G$ kg/m$^2$ s | $P_{tot}$ kW | $T_{w,in}$ K |
|---|---|---|---|---|
| 3051 | 2. | 25.1 | 4.326 | 812. |
| 3053 | 3. | 25. | 4.326 | 812. |

Table 1: Experimental conditions for test cases UCB-3051 and UCB-3053

| Run No. | t s | $z_{QF}$ m | $U_{QF}$ mm/s | $T^-$ K | $T^+$ K | $x^-$ | $x_{QF}$ | $P_{dry}$ W | $q''_{in}$ z(m) | $q''_{in}$ kW/m$^2$ |
|---|---|---|---|---|---|---|---|---|---|---|
| 3051 | 150. | 1.90 | 7.3 | 401. | 593. | 0.10 | .12 | 923. | 2.00 | 16.91 |
| | | | | | | | | | 2.20 | 15.45 |
| | | | | | | | | | 2.40 | 13.92 |
| | | | | | | | | | 2.60 | 12.38 |
| | | | | | | | | | 2.80 | 10.97 |
| | | | | | | | | | 3.00 | 9.69 |
| | | | | | | | | | 3.20 | 8.83 |
| | | | | | | | | | 3.40 | 8.19 |
| | | | | | | | | | 3.58 | 8.19 |
| 3053 | 150. | 2.05 | 7.5 | 414. | 593. | 0.12 | .14 | 874. | 2.20 | 15.19 |
| | | | | | | | | | 2.40 | 14.20 |
| | | | | | | | | | 2.60 | 13.60 |
| | | | | | | | | | 2.80 | 12.98 |
| | | | | | | | | | 3.00 | 12.10 |
| | | | | | | | | | 3.20 | 10.97 |
| | | | | | | | | | 3.40 | 9.90 |
| | | | | | | | | | 3.58 | 9.89 |

Table 2: Calculated variables used for the steady-state analyses.

# 3 Transient analysis of test case 3051

The basic nodalization scheme for the analysis of Run 3051 is shown in Fig. 3. It consists of one pipe (component 120) with 19 cells for the test section, one time-dependent junction (110) for the bottom injection, one junction (125) representing the tube exit, and two time-dependent volumes (105 and 130). The heated wall of the test section is represented by the same number of heat slabs (19), and uniform linear power generation is imposed. The heat losses (calculated from a temperature-dependent heat transfer coefficient $h_L$) to the ambient depend on the external wall temperature, according to correlations (3) and (4). The values of the heat transfer coefficient $h_L$ has been calculated for several temperatures, and a table of $h_L$ vs temperature has been used for the input deck. The ambient temperature has been imposed constant and equal to 294 K. At the beginning of the transient (t=0 s) the test section is filled with superheated steam in thermal equilibrium with the wall of the tube ($T_g$=$T_{w,in}$=812 K). The transient is initiated by starting (t=0 s) the bottom injection of water.

The transient was calculated with the 'frozen' versions of both RELAP5/MOD2.5 and RELAP5/MOD3. For both calculations the correlation for interfacial drag in tubes was chosen. The reflooding option was chosen for the calculation with both versions of RELAP5, so that moving fine heat structure meshes were used in the wall heat transfer calculation. The reflooding heat transfer package was then utilized in the calculation with RELAP5/MOD2.5, whereas this option does not affect the correlations used by RELAP5/MOD3, as a unique heat transfer package is used for all conditions. The input decks for the two calculations are given in App. I.

The calculation by RELAP5/MOD2.5 could not be completed using the nodalization with 19 vols. shown in Fig. 3 (left), as a condition of error (which could not be explained) occurred, at about 160 s, in the subroutine QFMOVE, which calculates the advancement of the quench front(at this time, the quench front elevation was already above 2.44 m). Reduction of maximum and minimum time steps, and changes in the number of radial meshes and maximum number of fine meshes only provoked a negligible time shift of the error condition. Eventually, the solution was to halve the size of the hydrodynamic nodes (from 0.2 to 0.1 m) and, correspondingly, of the heat slabs. The resulting nodalization with 36 vols. is also shown in Fig. 3.

The comparisons of the wall temperatures calculated by both codes with the measurements are shown in Figs. 4 and 5. Even though some minor differences can be observed in the results of the two calculations, the most striking outcome of the analysis is the very large discrepancy between calculated and measured wall temperatures, as in [4]. The test section quenches completely in about 550 s, while both codes predict complete quench within 160 s. While RELAP5/MOD3 predicts correctly a gradual bottom quench progression, RELAP5/MOD2.5 calculates a second quench front, propagating from the top of the test section, as it can be recognized (Fig. 5) from the early quench at 3.35 m (highest measurement station). The results are somewhat surprising, if one recalls that most of the analyses with bundles (e.g., NEPTUN with cosine-shaped heat flux profiles, but also with several spacer grids) indicated the tendency of RELAP5/MOD2.5 to *overpredict* the quench times and the wall peak temperatures, especially at the highest elevations [4]. These results are also in conflict with recent assessment work using data from the Lehigh bundle reflooding experiments, where a uniformly heated bundle was used: for these cases RELAP5/MOD2.5 was generally predicting peak temperatures and quench times with acceptable agreement in comparison to experimental data, and the only underpredictions were found for low elevations [4]. This last assessment work can, however, be barely associated to the previous ones, because of the short length of the test section; in fact, the analysis was focussed on lower elevations than in the NEPTUN case.

RELAP5/MOD3, on the contrary, behaves in accordance with the previous experience [4]: it overpredicts the quench front velocity (or rather the 'cooling front' velocity, as no evident temperature 'knee' can be observed). For the present tube experiment the effect is amplified, as the QF velocity is four times higher than in the experiment.

Moreover, it can be observed (Fig. 6) that early in the transient (30 s for the MOD2.5 and 100 s for the MOD3), the calculated vapour temperatures in the uppermost node drop to low values (about 420-450 K) close to the saturation temperature (about 400 K), whereas the experimental value sets for a long time to a value of around 600 K.

The reason for such a large disagreement between the predicted and the measured quench front velocities is not easy to single out, as several effects can contribute to the inaccuracy of the predictions. On the one hand, too large wall heat fluxes might have driven the wall to rewetting conditions, with consequent drop in the vapour temperature to the saturation value. Moreover, large mass flow oscillations affect both code versions (in Figs. 7 and 8 the vapour and liquid carry-out, as well as the total mass flow rate at the tube exit are shown), and most probably contribute to the excessively fast propagation of the quench front. On the other hand, the large temperature difference between the wall and the vapour might have resulted in an additional increase of the already over-predicted wall heat flux [6] and, consequently in an overprediction of the precursory cooling.

From the comparison of the calculated mass accumulated inside the tube, the collapsed liquid level, the vapour flowing out of the test section and the total liquid carry-out (Fig. 9), with their respective experimental counterparts, one can conclude that both code versions predict the 'average' hydraulic behaviour of the system fairly well.

It should be noted here that the calculation of the total liquid carry-out by RELAP5/MOD2.5 is actually better than what appears in Fig. 9, as the control variable (cntrlvar) which integrates the liquid expelled over the time is affected by an error, and underestimates the total liquid carry-out. A short explanation can be given as follows. The mass flow rate of the phase $k$ at a junction $j$ (in the specific case the junction 125) is obtained from:

$$\dot{M}_{kj} = \rho_{kj}\alpha_{kj}v_{kj}A$$

and the total mass flow can be calculated by summing up the gas and the liquid mass flows. The total mass expelled out of the test section $\dot{M}_{out}$ is then:

$$\dot{M}_{out} = \text{int(cntrlvar)} = \int_0^t (\dot{M}_{f,j} + \dot{M}_{g,j})\, dt \tag{5}$$

On the other hand, the total carry-out can be calculated by integrating directly the total mass flow at the tube exit $\dot{M}_j$, which is also calculated by the code:

$$\dot{M}_{out} = \text{int(mflowj1250000)} = \int_0^t \dot{M}_j dt \tag{6}$$

The comparison of the results of the two expressions is given in Fig. 10: it is observed that a 10% difference exists in the RELAP5/MOD2.5 calculation, while a much smaller discrepancy appears in the RELAP5/MOD3 calculation. As the value of $\dot{M}_{out}$ calculated by Eq. (6) satisfies the mass balance with a high accuracy, it can be concluded that the mass flows calculated by Eq. (5) underestimate the 'actual' mass flows. Indeed, under rather unstable liquid mass flow conditions, the spikes in the mass flow rate (due to the spikes in the liquid mass flow rate) calculated by Eq. (5) are much lower than those present in the mass flow time-history of the variable mflowj1250000 (see Figs. 7 and 8). This can be explained by the different numerical techniques used for obtaining the time and space averages of the various quantities at the junctions in these two different versions of the code.

Even though the comparison between calculations and experiment regards only the exit conditions, it can be assumed that both wall and interfacial drag are correctly predicted over the transient[b] and that the axial liquid mass distribution has also been captured with a good approximation.

Using the hypothesis that the low vapour temperatures drive the wall heat flux increase and the wall temperatures drop (and not vice versa), one could then argue that the failure of the RELAP5/MOD3 in predicting vapour and wall temperature, is an overprediction of the interfacial heat transfer, which results in an anticipated desuperheating of the vapour up to large distances from the quench front. An indication in favour of this explanation can be obtained from observing, for example, that at the time of the quench at 2.58 m (t=93 s, interpolated value) the vapour temperature at the tube exit (1.2 m downstream) is about 550 K, whereas

[b]This does not necessarily imply that interfacial and wall drag models are correct.

in the experiment at the time this happens (t=298 s) the vapour temperature was 50 K higher. However, the comparison is not fully meaningful as one cannot compare the actual quality at the quench front (highly oscillating in the calculation because of the high heat transfer rates across it) and the total heat input to the vapour in the dry region. In fact, one also observes that, because of the high cooling rates (due also to the large wall-to-liquid heat transfer) at large distances from the QF, the calculated and experimental wall temperatures and temperature decrease rates in the dry region are quite different at the time of the 2.58 m quench. This implies different values of the local heat fluxes and, then, of the total heat input to the vapour.

Therefore, because of the complex interactions between the different heat transfer processes, the transient effects and the history-dependent thermal-hydraulic conditions, the boundary conditions which influence the vapour superheating rate are different in the calculation and in the experiment, so that the model for interfacial heat transfer in the dispersed flow regime cannot be judged conclusively.

In the case of the MOD2.5 calculation, the occurrence of top quench confuses the picture even more, as the sudden decrease of the vapour temperature close to the exit is not due to the excessive interfacial heat transfer, but to the fact that the vapour cannot receive heat from the wet wall any longer and a large quantity of saturated vapour is generated from the direct wall-to-liquid heat exchange.

From the analysis of this tube experiment, it can be deduced that:

1. The analysis of experiments with tubes can yield rather different results than those obtained for bundles, even for very similar conditions. The results for tubes, even though they are not truly representative of the conditions in a nuclear reactor, provide a useful test for the adequacy of the correlations used in the computer codes, as most of the models implemented are primarily derived for circular channels (the application to bundles implies the use of some 'equivalent' diameter). This can be recognized from the excellent prediction of the hydraulics.

2. The calculated quench front progression is much faster than in the experiment for both versions of the codes. The discrepancy is due to a too large wall heat flux [6] in the post-CHF regime, to which the underprediction of the vapour temperature also contributes.

3. Run 3051 provides a very severe test for the codes. The difficulty of the 1-D approach in predicting interfacial heat transfer demonstrated for more specific conditions [9], cannot be definitely confirmed here, but the large discrepancy in the calculated vapour temperature seems to be consistent with those phenomenological considerations. In particular the MOD3 calculations seem to be affected by the overprediction of interfacial heat transfer, but both calculations are probably dominated by deficiencies in the wall heat transfer models.

4. The transient analysis above does not allow to draw any conclusion about the correctness of the individual models, as they (and their numerical implementation) interact with each other.

With respect to the main goal of the present work, namely the assessment of the interfacial heat transfer model for Dispersed Flow, not much can be concluded from the transient analysis; hence, the analysis of experiment 3053 (for which results similar to those obtained for test 3051 are expected) was not carried-out.

# 4 Quasi-steady state analysis of Run 3051

The basic idea behind the quasi steady-state analysis has already been introduced in §1; here the mathematical formulation of this approach, as well as the conditions which must be fulfilled in order to arrive to the evaluation of the capabilities of the interfacial heat transfer model using only the experimental vapour temperature at the tube exit, are discussed.

When the quenching process progresses slowly and at constant rate, as usual when the quality at the QF is positive, the thermal-hydraulic conditions at any point in the channel downstream from the QF (wall and fluid temperatures, mass flows, qualities, etc.) vary slowly as well. The quasi steady-state condition is thus realized if the time necessary to the QF to move a significant distance (e.g., the distance between the centres

of the volumes above and below the 'nominal' position of the QF) is larger than the residence time of the droplet in the post-CHF region. If this prerequisite is satisfied, any slow variation of the QF position (and quality) will lead to slow variations of the hydrodynamic variables downstream. Under this condition, the evolution of the mixture can be described by the usual conservation equations, dropping the time-derivatives.

The steady-state form of the vapour continuity and energy equation can be written for a straight tube (like in the RELAP5 code [11], but neglecting dissipation and using the enthalpy instead of the internal energy) of cross-sectional area $A$ as:

$$\frac{d}{dz}(< \alpha_g >< \rho_g > U_g) = \frac{dG_g}{dz} =< \Gamma > \tag{7}$$

$$< \alpha_g >< \rho_g > U_g \frac{dH_b}{dz} = G_g \frac{dH_b}{dz} = Q_{wg} + < Q_{ig} > - < \Gamma > (H_b - H_{g,s}) \tag{8}$$

where $U_g$, $H_b$, $G_g$, $Q_{wg}$ and $< Q_{ig} >$ are the cross-sectionally averaged axial vapour velocity, the bulk vapour enthalpy, the vapour mass flux, the phasic wall heat transfer rate per unit volume and the cross-sectionally averaged interfacial heat transfer rate per unit volume, respectively.

By integrating between the QF elevation $z_{QF}$ and the tube exit elevation $z^T$ Eq. (8) multiplied by the tube flow area $A$, one obtains:

$$\int_{z_{QF}}^{z^T} AG_g \frac{dH_b}{dz} dz = \int_{z_{QF}}^{z^T} Q_{wg} A dz + \int_{z_{QF}}^{z^T} < Q_{ig} > A dz - \int_{z_{QF}}^{z^T} \Gamma (H_b - H_{g,s}) A dz$$

and, integrating by parts the first term in the Left Hand Side of the equation:

$$\begin{aligned} AG_g^T H_b^T - AG_{g,QF} H_{g,QF} - \int_{z_{QF}}^{z^T} AH_b \frac{dG_g}{dz} dz \;=\; & \int_{z_{QF}}^{z^T} Q_{wg} A dz + \\ & \int_{z_{QF}}^{z^T} < Q_{ig} > A dz + \\ & - \int_{z_{QF}}^{z^T} \Gamma (H_b - H_{g,s}) A dz \end{aligned}$$

Using the continuity equation (7) and replacing $G_g A$ by the vapour mass flow rate $\dot{M}_g$, it follows:

$$\begin{aligned} \dot{M}_g^T H_b^T - \dot{M}_{g,QF} H_{b,QF} \;=\; & \int_{z_{QF}}^{z^T} Q_{wg} A dz + \int_{z_{QF}}^{z^T} < Q_{ig} > A dz + \int_{z_{QF}}^{z^T} \Gamma H_b A dz \\ & - \int_{z_{QF}}^{z^T} \Gamma (H_b - H_{g,s}) A dz \end{aligned}$$

Observing that:

$$\int_{z_{QF}}^{z^T} \Gamma A dz = \dot{M}_g^T - \dot{M}_{g,QF}$$

one can write (assuming saturated vapour at the QF):

$$\dot{M}_g^T H_b^T = \dot{M}_{g,QF} H_{b,QF} + P_{g,dry} + \int_{z_{QF}}^{z^T} < Q_{ig} > A dz + (\dot{M}_g^T - \dot{M}_{g,QF}) H_{g,s} \tag{9}$$

where $P_{g,dry}$ is the total heat transfer rate to the vapour alone in the dry-wall region. If all the droplet population is represented by an average diameter $d$, the average interfacial heat transfer rate per unit volume is:

$$< Q_{ig} >= \frac{6h_i}{d} < (1-\alpha_g)(T-T_s) > \tag{10}$$

Since in a 1-D model the droplet concentration is assumed uniform over the cross section and the distribution coefficient is taken equal to unity, the relation:

$$< (1-\alpha_g)(T-T_s) > \equiv < (1-\alpha_g) >< (T-T_s) > \equiv < (1-\alpha_g) > (T_b - T_s) \tag{11}$$

leads to:

$$< Q_{ig} >= \frac{6h_i}{d} < (1-\alpha_g) >< (T_b - T_s) \tag{12}$$

*This is the relation* that under low mass flux and low quality conditions, will lead to the overprediction of the interfacial heat transfer, and the underprediction of the vapour temperature [9]. To show that RELAP5 is affected by large inaccuracies in the prediction of the vapour temperatures because of the large interfacial heat transfers, and then that Eq. (12) does not hold, is the goal of the following analysis.

From Eq. (9) one easily realizes that if the gas mass flow rate at the QF and the tube exit calculated by the computer code are (approximately) equal to the experimental ones, and the total wall-to-vapour heat transfer is the same as in the experiment, any deviation of the exit enthalpy (temperature) can be attributed to the incorrect prediction of the interfacial heat transfer. This estimation can be done *irrespective of the wall-to-liquid heat transfer* and the consequent vapour production at the wall.

Therefore, for the quasi steady-state analysis four conditions (Fig. 11) must be fulfilled in the calculation:

1. the time needed by the the QF to advance a substantial length about the 'reference' QF position is much longer than the droplet residence time $t_r$ ($\equiv (z^T - z_{QF})/\bar{U}_l$). The average values of the variables during this time (which we will call 'averaging period' $t_{av}$) can be compared with the values obtained by a steady-state analysis.
2. same (approximately) $x_{QF}$ ($\dot{M}_{g,QF}$) as in the experiment during the averaging period $t_{av}$.
3. total heat input to the vapour equal to the experimental one.
4. same $\dot{M}_g^T$ as in the experiment.

The first two conditions can be imposed by restricting the analysis to a section of the tube including the region downstream of the 'nominal' position of the QF and a short length upstream of it. The fluid injected at the bottom of this 'reduced' length section is a mixture with a quality close to that inferred from the experiment. The QF progresses from the inlet of the section up to the nominal location of the QF (and the quality at the QF changes accordingly), for which the tube exit vapour temperature must be compared with the experimental value. From this time on, and until the time the first node above $z_{QF}$ quenches, the values of the various variables of interest are considered.

With respect to the third condition, certain assumptions and approximations are needed, since only the total heat flux to the mixture is known at the few measurement stations. As the experimental wall temperatures reach nearly steady values at some time during the run, and drop suddenly only when the QF is very close to the measurement location, the interpolation of the heat fluxes for any elevation of the tube can be calculated with good accuracy, and the total heat input to the mixture in the dry region of the tube can then be estimated with reasonable confidence: with this procedure the values in Table 2 were obtained. Still the partition between the two phases is unknown, so that two approaches can be used in the calculation:

- Impose the total heat flux equal to the experimental one, and let the code partition the heat between the phases. If this option is chosen, the wall-to-liquid heat transfer must be small at least at some distance from the QF, otherwise an underprediction of the vapour temperature can be due to the low heat input to the vapour rather than to the overprediction of the interfacial heat transfer.

- If the code calculates a too large wall-to-liquid heat transfer, increase the total heat flux as much as necessary to transfer to the vapour an amount of heat equal (approximately) to the total experimental one. This second option assumes no wall-to-liquid heat transfer in the experiment. Therefore, this procedure uses the upper limit for the heat input to the vapour, and, if the vapour temperature is still underpredicted, the deficiency in the approach for calculating the interfacial heat transfer will become more evident.

For the fourth condition, namely calculated vapour mass flow close to the experimental value, one can only hope that the computer program predicts liquid and vapour carry-out flow rates close to the experimental ones at the time of the mid-height quench. This expectation is conforted by the results of the transient analysis above, where both calculated liquid and vapour carry-out were in excellent agreement with the measured ones. For the purpose of testing the interfacial heat transfer model, lower vapour mass flows than in the experiment can also be accepted, as the calculated vapour superheat is enhanced by a reduced vapour mass flow. Similarly, the liquid carry-out must be approximately equal to or lower than the experimental value. A calculated liquid mass flow much higher than in the experiment would imply a large concentration of liquid at high elevation: the consequent vapour desuperheating effect could not be related to the 1-D approach for the interfacial heat transfer.

In order to avoid misunderstandings, it is appropriate to repeat here that, as RELAP5 is a transient code, our 'steady-state' analysis consists in running the program over the short time period needed by the QF to advance from the inlet of the tube to the node immediately above the elevation $z_{QF}$, chosen for the analysis.

In summary: The analysis will be restricted to a shorter tube length. The quench front moves from the inlet to a certain predetermined elevation above $z_{QF}$. From the time the QF is close to $z_{QF}$, the quality immediately above must be close to $x_{QF}$, and the power input to the vapour in the dry region must be equal to $P_{g,dry}$; this last condition can be approximated by imposing that the total heat transfer rate to the mixture is equal to the (experimental) $P_{dry}$. The mass flows at the tube exit will be observed; if they are in close agreement with the experimental data (obtained by differentiating the experimental water and vapour carry-out), the vapour temperature at the tube exit will be compared with the experimental data.

## 4.1 Calculation with RELAP5/MOD2.5

In Fig. 12 the nodalization used for the 'steady-state' analysis with the MOD2.5 is shown. It consists of ten short (0.03 m) cells below $z_{QF}$, and nine cells representing the above-QF region having the same size as in the 19 vols. nodalization (Fig. 3). The inlet quality $x_{in}$ was set by a trial-and-error procedure, by checking the value of $x_{QF}$ at the end of the transient, as calculated from an energy balance performed by means of a control variable; at the end $x_{in}$ has been set equal to about 6%. The need for this procedure is due to the oscillations in the calculation of the mass flows immediately above the QF, which render the direct estimation of the quality impossible.

The heat flux at the wall was initially imposed according to Table 2, the initial vapour temperature in the dry region was given a linear profile (the experimental temperature at t=150 s being used for the highest node), and the experimental wall temperature was imposed to the heat structures. Unfortunately, the calculation stopped after a few seconds, and the reason was easily found: the vapour temperature upstream of the quench front was exceeding 3000 K. This happened because a very large amount of heat was transferred directly to the vapour, in spite of the fact that a bubbly flow regime was predicted. It was realized that RELAP5, for imposed heat flux conditions, calculates the heat fluxes to the two phases by splitting the total heat input into two *equal* parts, irrespective of the flow regime.

It was then necessary to change our approach of imposing the heat flux, and other boundary conditions were used:

- Impose the power generation.
- Impose the experimental heat losses at t=150 s.

- Impose the axial temperature profile. As the heat flux is then calculated by the reflooding heat transfer package, the total heat input to vapour is not controlled, but varies during the short period of time of the 'quasi steady-state' analysis, and depends mainly on the initial wall temperature. Therefore, three different axial wall temperature profiles are imposed, and the resulting heat input to the vapour is calculated. The three axial wall temperature profiles, shown in Fig. 13, are:

1. **exp**: experimental wall temperature distribution.
2. **low**: temperatures decreasing with the distance from the QF. These values have been found (by trial and error) to yield (approximately) the desired axial heat flux distribution (Fig. 14).
3. **high**: temperatures higher than those experimentally observed.

The resulting wall heat fluxes averaged over the last 5 s of the calculations are shown in Fig. 14. The input deck for the calculation using the experimental temperature distribution is given in App. II.

The results of the three computations are shown in Figs 15-21. In Fig. 15 the wall temperatures at several elevations are shown for the low initial wall temperature distribution. The temperature time-histories in the other two cases were similar. Two remarks can be done: 1) the wall temperatures at some distance from the QF ($z \geq 2.2$ m) are practically constant during the calculation time, and 2) in the time period between 10 and 15 s the QF lies somewhere between 1.855 m and 2.0 m. The time needed for the QF to advance from 1.855 m to 2.0 m was found to be larger than the droplet residence time $t_r$ ($\simeq$ 1-2 s), so that the first requirement for the 'steady-state' analysis is satisfied.

It is first observed that the equilibrium quality at the QF (Fig. 16) varies during the transient time, but is close to the experimental value at least for times larger than 10 s.

The vapour mass flow (Fig. 17) at the tube exit is also in close agreement with the experimental value. On the contrary, the liquid mass flow rate (Fig. 17) exhibits large oscillations: their, amplitude, however, do not exceed 30% of the measured average flow rate. The fact that the average values (between 10 and 15 s) of the total mass flow rate and exit quality (Fig. 18) are quite close to the experimental values, suggest that the hydraulic behaviour is in general well predicted.

The total power input to the vapour (Fig. 19) is, in all cases, at least as high as the total heat input to the mixture, so that also the thermal boundary condition on the vapour superheat evolution is satisfied in both cases.

Under the conditions mentioned above, the average values of the several quantities of interest for our analysis during the time period from 10 to 15 s are thus comparable with those obtained by a steady-state analysis for QF 'frozen' at 1.89 m; then, it does make sense to compare the calculated vapour temperature with the measured one. In Fig. 20, it can be observed that after 10 s the vapour temperature (while being unstable) is always underpredicted by at least 50 K, even when the power input to the vapour is twice as much as the experimental total heat transfer rate to the mixture (Fig. 19). It is easily realized that the spikes are due to instantaneous increases of the void fraction due to sudden drops in the liquid mass flow rate (liquid carry-out). In Fig. 21 the average value of the vapour temperature is shown, and the large underprediction (150 K) observed for the initial wall temperature distribution which yields value of $P_{dry}$ close to the experimental ones is in fairly good agreement with that expected on the base of the quasi steady-state separate model [9].

From the RELAP5/MOD2.5 calculations, we can thus conclude that the interfacial heat transfer must be overpredicted. Let us discuss the possible sources contributing to the overprediction:

1. The liquid fraction might have been overestimated. This, however, can be almost excluded by the fairly good prediction of the liquid carry-out, which suggests a correct estimate of the axial liquid distribution.
2. The interfacial heat transfer coefficient ($h_i$) is possibly overpredicted because of a large average value of the phase velocity difference. Indeed, one can suspect that large oscillations in the liquid velocity (leading even to negative velocities) can still be compatible with a correct average value of the liquid

mass flow, but yield (because of the non-linear dependence of the heat transfer coefficient on the phase velocity difference ($U_g - U_l$)) large values of $h_i$. This can be also excluded by observing that the velocity difference at two elevations (Fig. 22) are quite stable.

3. The droplet diameter might be underpredicted. The separate steady-state analyses [8] show, however, that for a wide range of droplet diameters the results are very similar to those obtained using the RELAP5/MOD2.5 criterion.

4. The only possibility that is left is, thus, that the interfacial heat transfer rate is based on the incorrect assumption of a uniform droplet concentration over the cross-sectional area.

Other calculations (not shown) have been carried-out using the normal (blowdown) heat transfer package, and slowing down the propagation of the quench front by increasing the thickness of the heat slabs in the region below the QF. The vapour temperature at the tube exit was still underpredicted by at least 100 K.

Furthermore, a version of the code was generated, in which the wall-to-liquid heat transfer was forced to go to zero within 30 cm from QF. The axial wall temperature profile was imposed in such a way to preserve the total experimental power input to the dry region ($P_{dry}$), so that the heat transfer rate to the vapour ($P_{g,dry}$) was practically equal to the total experimental one. Even under these conditions, the calculated vapour temperature was still much lower than in the experiment.

## 4.2 Calculation with RELAP5/MOD3

For the analysis with RELAP5/MOD3, the nodalization had to be slightly modified. This was due to the reason that the first calculation (not shown by a figure) showed that the quench front was progressing much faster than in the corresponding RELAP5/MOD2.5 calculation. Under these circumstances, the time necessary for the QF to propagate from the node below $z_{QF}$ to the node above it (time $t_{av}$ over which the thermal-hydraulic conditions of the post-CHF region can be considered approximately insensitive to the actual location of the quench front around the imposed $z_{QF}$) became comparable with the droplet transit time: the averaging of the variables over the time period $t_{av}$ was consequently becoming of dubious meaning. Therefore, larger nodes (50 mm instead of 30 mm) were used for the section below $z_{QF}$ and the node including $z_{QF}$ (Fig. 23). Moreover, the time, over which the average values of the variables discussed above are calculated, is made dependent on the transient, i.e., the averaging period is between the time the wall temperature in the cell below $z_{QF}$ (cell 9) drops below the quench temperature (580 K) and the time this happens to the first node in the 'dry' zone (cell 11). When the wall temperature in node 11 drops below 580 K the transient is thus terminated.

The first calculation, performed by using initial wall temperatures equal to the experimental ones, also showed a very high heat transfer rate in the dry zone, nearly double as much than in the experiment, and a much larger vapour mass flow, resulting from the large evaporation rates caused by the high wall-to-liquid heat transfer.

Therefore, the low axial wall temperature distribution (Fig. 13) was used for the next calculations. The results are shown in Figs. 24-29. The wall temperatures are shown in Fig. 24: at large distance from the QF they are slowly growing, and the QF lies between 1.825 and 2.0 m for the time between 8 and 12 s. The equilibrium quality at the QF is shown in Fig. 25. It can be remarked that it is highly oscillatory (often, the case found in the RELAP5/MOD3 calculations [4]), due to the large spikes in the heat transfer from the wall to the fluid in the wet region. The lower value of the equilibrium quality, which is representative of the 'steady state' heat transfer rate, is, however, close to the expected value.

The vapour temperature at the tube exit (Fig. 26) is predicted quite well, but one can easily realize from the good prediction of the vapour carry-out (Fig. 27) and the negligible liquid carry-out (Fig. 28) that this is due to the deficiency of liquid in the region far away from the QF. Fig. 29 shows the void fractions at various elevations. The water is accumulated in the region immediately downstream from the QF, so that no heat sink is available to the steam further up. It was originally believed that one of the reasons for the insufficient liquid carry-over could be the larger value of the critical Weber number ($We_{cr}$=12) used in the MOD3 with

respect to that used in the MOD2.5 ($We_{cr}$=3), which implies the calculation of quite large droplets in the mist-flow region and these drops cannot be lifted by the drag force (see below).

It was then decided to perform the calculation with a modified version of the code developed at PSI (version bb) which, among other features, uses the same $We_{cr}$ as in MOD2.5. This modified version has been discussed by Analytis [6], and the description of its features will not be repeated here: it suffices to say that better numerical stability is achieved and several unphysical effects (like the void fraction passing through a minimum immediately below the quench front) are eliminated by the utilization of more physical correlations. The results are shown in Figs. 24-28 and 30. It can be observed that the liquid carry-out (Fig. 28) is a little higher than before, but still much too low: however, the resulting slight modification in the axial void fraction profile (Fig. 30) reduces the average outlet vapour temperature (Fig. 26) by about 30 K.

In order to understand the reasons why the utilization of the same criterion for the droplet size yields different results in RELAP5/MOD2.5 and in RELAP5/MOD3, the overall calculation scheme of the interfacial drag in RELAP5/MOD3 was reviewed. It was realized that, for reflooding calculations, the droplet diameter was bound by a lower limit of 2.5 mm. This value appears arbitrary, and for sensitivity analysis purposes it was changed to 1.25 mm in a new version of the code, which was called UPX. Moreover, it has been found out that the drag coefficient for droplets is defined as:

$$C_D = \min\{C_{D,v}, 0.45\} \tag{13}$$

where the drag coefficient for the viscous regime $C_{D,v}$ is given by:

$$C_{D,v} = \frac{24}{Re}(1. + 0.1Re^{0.687}) \tag{14}$$

It is clear from Eqs. (13)-(14) that for large Re (large droplets) the drag coefficient attains very low values. However, the drag coefficient for a solid sphere is asymptotically approaching the value 0.45 for Re> 1000 (Newton regime), being *higher* for lower values of Re [16]. The value of $C_D$ for fluid particles is even higher, as they get distorted [16]. Eq. (13) is then basically *wrong* and even if one wants to consider the droplets as solid spheres, it must be replaced by the usual criterion:

$$C_D = \max\{C_{D,v}, 0.45\} \tag{15}$$

Eq. (15) was then implemented in the version UPX.

The results of the calculation by version UPX are shown in Figs. 25-28 and 31. It can be remarked that the liquid carry-out (Fig. 28) is now larger than in the previous calculations, but it is still too low. The axial void fraction distribution (Fig. 31) shows a larger presence of liquid at the higher elevations, and this determines lower vapour temperature (Fig. 26).

It can be observed that the calculated heat transfer rate to the mixture (Fig. 32) was always higher than in the experiment, but the heat transfer rate to the vapour was about 30% lower (Fig. 33). However, radiation from wall-to-droplets can account for a significant portion of the wall heat transfer [9], so that the actual heat transfer rate to vapour $P_{g,dry}$ is likely to be predicted realistically.

Further attempts to modify the code in order to get the correct liquid mass flow were not performed. As a trend, it has been already established that, for decreasing values of the droplet diameter, more and more liquid can be carried over, and increasing underprediction of the vapour temperature results.

These results are in agreement with those obtained by RELAP5/MOD2.5 and by the steady-state analyses.

# 5 Quasi-steady state analysis of Run 3053 by RELAP5/MOD2.5

Experiment 3053 was practically the same as Run 3051, the only difference being the higher pressure (3 bar instead of 2). The analysis has been performed only by the RELAP5/MOD2.5, because of the difficulties

in the prediction of the liquid carryout by the MOD3, which render the interpretation of the results more difficult.

The nodalization used for the analysis of run 3053 is shown in Fig. 34. Only, two axial wall temperature distributions (Fig. 35) have been tested. The resulting average axial wall heat flux profiles during the time period between 10 and 14 s are given in Fig. 36.

The transient time for the calculations was 14 s, since the node above the 'nominal' value of $z_{QF}$ quenches at that time. The time-histories of the wall temperature at various elevations for the 'experimental' initial axial wall temperature distribution are shown in Fig. 37. The time span over which the results are representative of a steady quench front at 2.05 m (QF between 2.055 m, vol. 10, and 2.2 m, vol. 12) is between 8 and 14 s.

The results of the calculations are shown in Figs. 38-41. It is noted that the quality at the QF is correctly obtained (Fig. 38) and the heat transfer to the vapour alone is much larger than the experimental *total* power input (Fig. 39). The calculated liquid carry-out (Fig. 40) and the calculated total mass flow at the exit (Fig. 41) decrease from larger values than in the experiment to lower values during the averaging period. The calculated vapour carry-out (Fig. 42) is, however, larger than in the experiment, due to an excessive evaporation in the tube. Therefore, one condition necessary for the fully meaningful comparison (see §3) between calculated and experimental vapour temperature is not satisfied. We note, however, two circumstances: 1) the experimental total mass flow was probably larger than that measured in the test, as a certain error in the mass balance was found [14], and 2) the heat input per unit volume of the flowing vapour is at least as large as in the experiment, since $P_{g,dry}$ is substantially larger than the total experimental heat flux (Fig. 39).

It is thus possible to state that the large underprediction of the vapour temperature at the tube exit (Fig. 43) is again due to the overprediction of the interfacial heat transfer, and not to an overprediction of the vapour mass flow.

# 6 Conclusions

The main goal of the present work was the assessment of the interfacial heat transfer model for the Dispersed Flow Film Boiling region above a quench front implemented in RELAP5/MOD2.5 and RELAP5/MOD3. The interest for this specific aspect of the DFFB model was raised by a separate work [9] which suggested severe limitations of the 1-D models in calculating the interfacial heat transfer rate under low mass flux conditions for low qualities at the quench front.

To this aim, a low-flooding rate reflooding experiment at 2 bar has been analyzed by RELAP5/MOD2.5 and by RELAP5/MOD3. The transient analysis has shown for both codes a large disagreement between the calculated and experimental quench front propagation rates, which can be attributed to an inadequate modelling of the heat transfer phenomena in the vicinity of the QF and confirms other similar analyses, e.g. [4]. In fact the good prediction of the carry-out suggests that the hydrodynamic behaviour is fairly well simulated. The vapour temperature at the tube exit dropped to the saturation value much before than in the experiment, but it could not be conclusively assessed whether a too high interfacial heat transfer was responsible for such bad predictions. This was due to the fact that the total instantaneous power input to the mixture in the post-CHF region at the time the quality at the QF becomes positive, was much larger than in the experiment, as it depends on the axial transient cooling rate distribution and then on the actual wall temperature distribution above the QF, which results from the preceeding transient.

In order to control the power input to the mixture, a quasi-steady state analysis has been performed. A short transient was run, during which the quench front is allowed to advance a short distance around the position of interest, imposing (approximately) the quality at the quench front. The power input to the mixture can be controlled, to a certain extent, by imposing the initial wall temperature distribution above the quench front.

The RELAP5/MOD2.5 calculated correctly the total carry-out and overpredicted the total heat transfer to the vapour. In spite of this, the vapour temperature was substantially underpredicted. It could be so concluded that interfacial heat transfer was overpredicted.

RELAP5/MOD3 showed a large underprediction of the liquid carry-out, and this led to a good prediction of the vapour temperature. However, when the calculation was repeated using two other versions of the code where the closure laws affecting the droplet dynamics were modified in a way to allow a larger carry-out (though still lower than the experimental one), the vapour temperature was again underpredicted.

The steady-state analysis of a second experiment at 3 bar was also performed by RELAP5/MOD2.5, and results similar to those obtained for the test at 2 bar were obtained.

It can be concluded that, as expected from steady-state analysis, computer codes like RELAP5, which calculate the interfacial heat transfer rate between vapour and droplets assuming a homogeneous distribution of the droplets over the cross section, overpredict the desuperheating effect of the liquid, and hence underpredict the vapour temperature at large distances from the quench front. This underprediction of the vapour temperature, does not always lead to the underprediction of wall temperatures, as other deficiencies in the wall heat transfer modelling and/or hydrodynamics often mask the difficulty of the codes to estimate the correct interfacial heat transfer. Nevertheless, we hope that this work will motivate some efforts to develop some empirical approach to calculate the reduction in the interfacial heat transfer rate under low mass flux/low quality conditions, since a detailed 3-D model which can calculate these effects (like that developed by one of the authors [9]) cannot be easily incorporated in a system code.

## Acknowledgements

The interest of Prof. Yadigaroglu for the practical implications of the main results of Andreani's dissertation and his encouragement to carry-out the present investigation were appreciated. The help of M. Sencar in setting up the nodalization and running the codes is gratefully acknowledged.

## References


[1] S.N. Aksan, G.Th. Analytis and D. Lübbesmeyer, 'Switzerland's Code Assessment in support of the International Code Assessment and Application Program (ICAP)', Proceedings of the *16th Water Reactor Safety Information Meeting* (Oct. 1988), NUREG/CP-0097, Vol. 4, pp. 245-273, March 1989.

makebox[20pt][l][2]M. Richner, G.Th. Analytis and S.N. Aksan, 'Assessment of RELAP5/MOD2, cycle 36.02, using NEPTUN Reflooding Experimental Data', NUREG/IA-0054, August 1992 (PSI report No. 104, Oct. 1991)

[3] S.N. Aksan, F. Stierli and G.Th. Analytis, 'Boil-off Experiments with the EIR-NEPTUN Facility: Analysis and Code Assessment Overview Report', NUREG/IA-0040, March 1992 (PSI-Report, No. EIR-629, Sept. 1987).

[4] M. Sencar and S.N. Aksan, 'Evaluation of Reflooding Models in RELAP5/MOD2.5, RELAP5/MOD3/v7j Codes by using Lehigh University and PSI-NEPTUN Bundle Reflooding Experimental Data', Paper presented at the *2nd Code Assessment and Maintenance Program (CAMP) Meeting*, Brussels, Belgium, May 1993.

[5] G.Th. Analytis, 'A Comparative Study of the Post-CHF Wall Heat Transfer Packages of the RELAP5 codes and Preliminary Assessment of Model Changes in RELAP5/MOD3/v7j' Paper presented at the *1st Code Assessment and Maintenance Program (CAMP) Meeting*, Villigen, PSI, Switzerland, June 1992.

[6] G.Th. Analytis, 'A Summary of Model Changes and Options in RELAP5/MOD3' Paper presented at the *2nd Code Assessment and Maintenance Program (CAMP) Meeting*, Brussels, Belgium, May 1993.

[7] G.Th. Analytis and P. Coddington, 'The Effect of Donor Cell Differencing of some Terms of the Momentum Equations of TRAC-BF1 on the Code Predictions', *Proceedings of the 5th International Topical Meeting on Reactor Thermal-Hydraulics (NURETH-5)*, Vol. III, pp. 745-750, Sept. 21-24, 1992, Salt Lake City, Utah, USA.

[8] M. Andreani and G. Yadigaroglu, 'Effect of the Cross-Sectional Droplet Distribution in Dispersed Flow Film Boiling at Low Mass Flux', *Proceedings of the 5th International Topical Meeting on Reactor Thermal-Hydraulics (NURETH-5)*, Vol. III, pp. 823-831, Sept. 21-24, 1992, Salt Lake City, Utah, USA.

[9] M. Andreani, 'Studies of Dispersed Flow Film Boiling with 3-D Lagrangian Hydrodynamics and a 2-D Eulerian Vapour Field', Doctoral Dissertation Nr. 9794, Swiss Federal Institute of Technology, ETHZ, Zurich (1992).

[10] D.G. Evans, S.W. Webb and J.C. Chen, 'Measurement of Axially Varying Non-Equilibrium in Post-Critical-Heat-Flux Boiling in a Vertical Tube', NUREG/CR-3363, Lehigh-Univ., June 1983.

[11] Ransom, V.H. et al. 'RELAP5/MOD2 Code Manual', NUREG/CR-4312, Rev. 1, March 1987.

[12] Carlson, K.E. et al. 'RELAP5/MOD3 Code Manual', Vol. 1, 2, 3, and 4, Draft, NUREG/CR-5535, June 1990.

[13] Seban, R., Grief, R., Yadigaroglu, G., Elias, E., Yu, K., Abdollahian, D. and Peake, W. 'UC-B Reflood Program: Experimental Data Report', EPRI NP-743, 1978.

[14] Seban, R.A. 'Reflooding of a Vertical Tube at 1,2 and 3 Atmospheres', Report EPRI NP-3191, 1983.

[15] Yu, K.P. 'An experimental investigation of the Reflooding of a bare tubular test section', Dissertation, Univ. of California at Berkeley, October 1978.

[16] Ishii, M. and Mishima, K. 'Two-Fluid Models and Hydrodynamic Constitutive Relations', Nucl. Eng. and Design, 82 (1984), 107-126.

# FIGURES

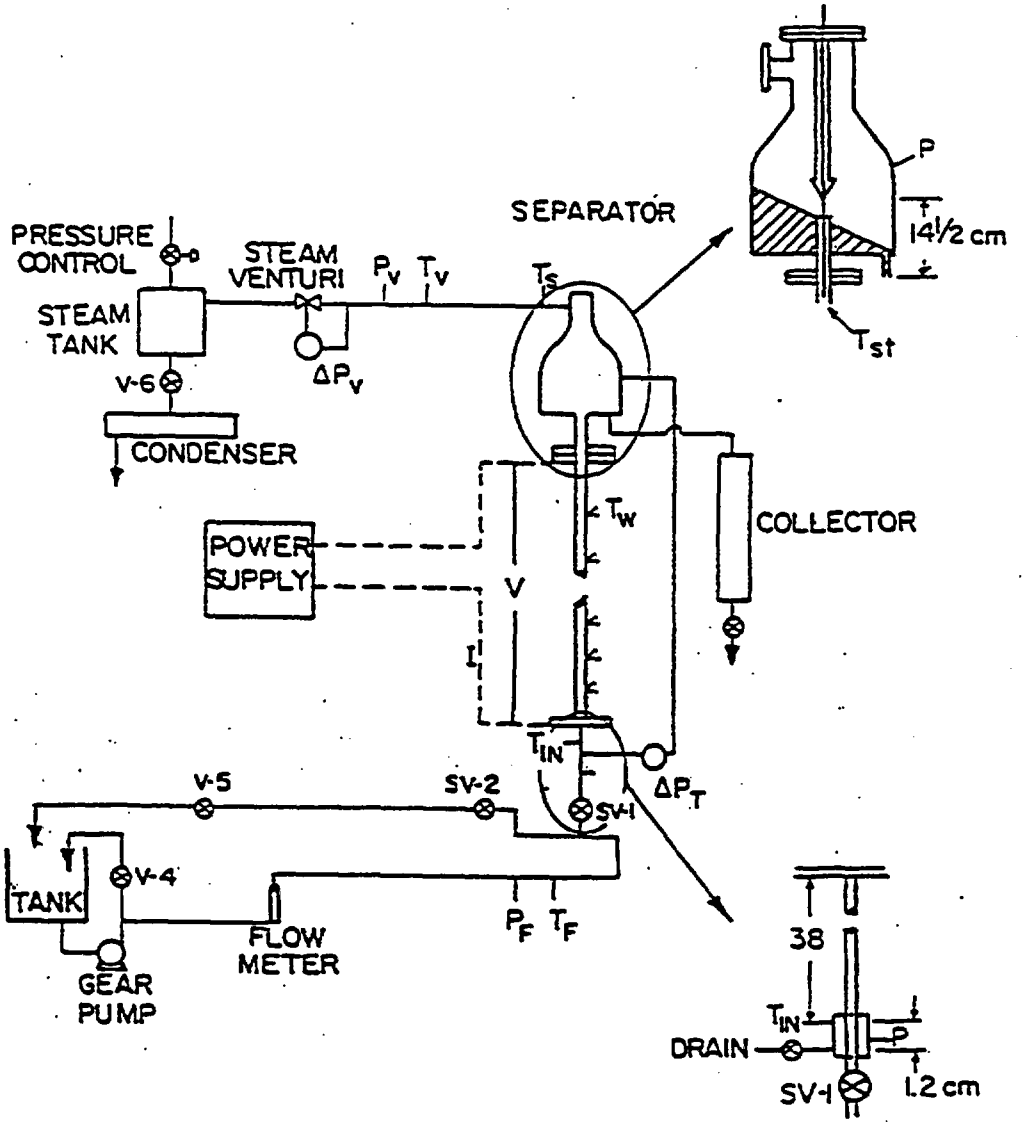


Figure 1: System flow diagram of the UC-B Test facility (Seban et al., 1978).

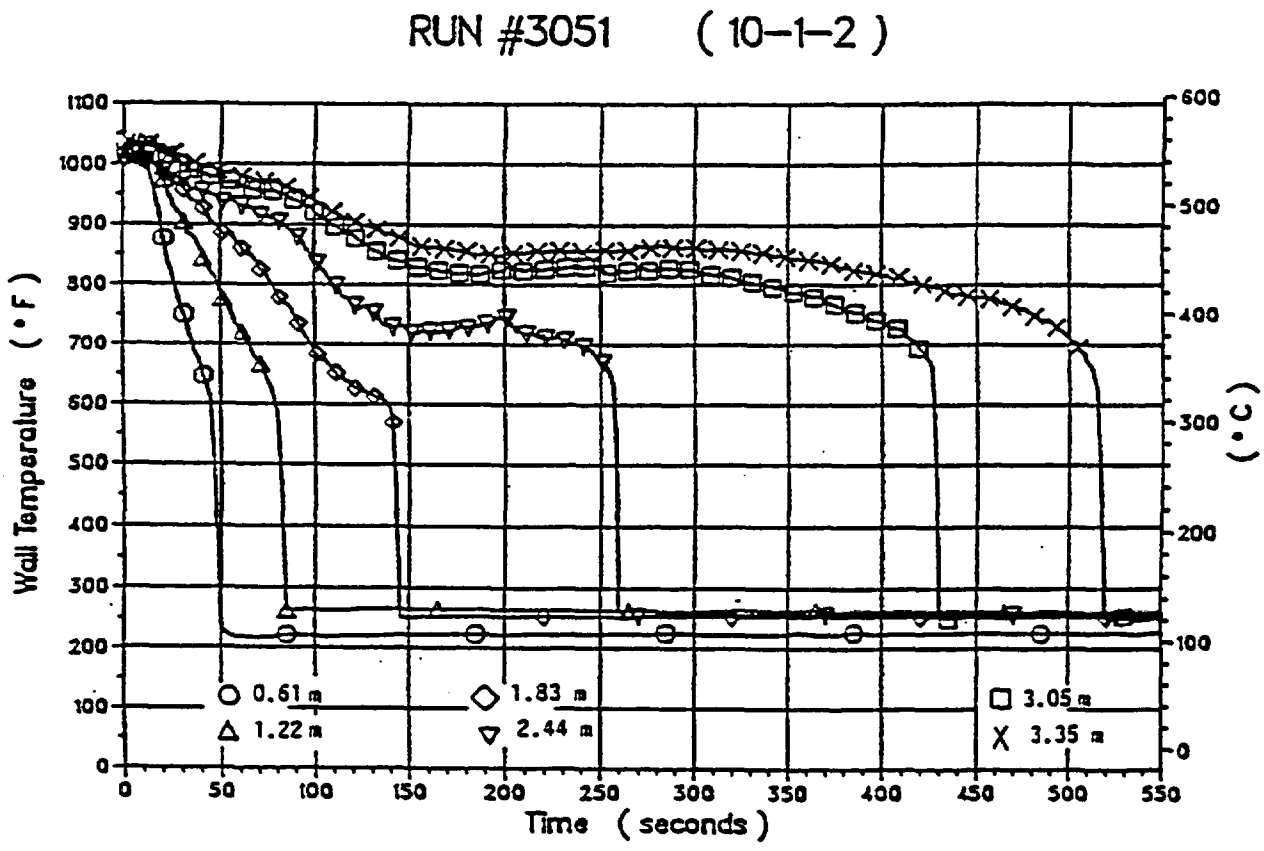


Figure 2: Experimental wall temperatures at various elevations for Run 3051.

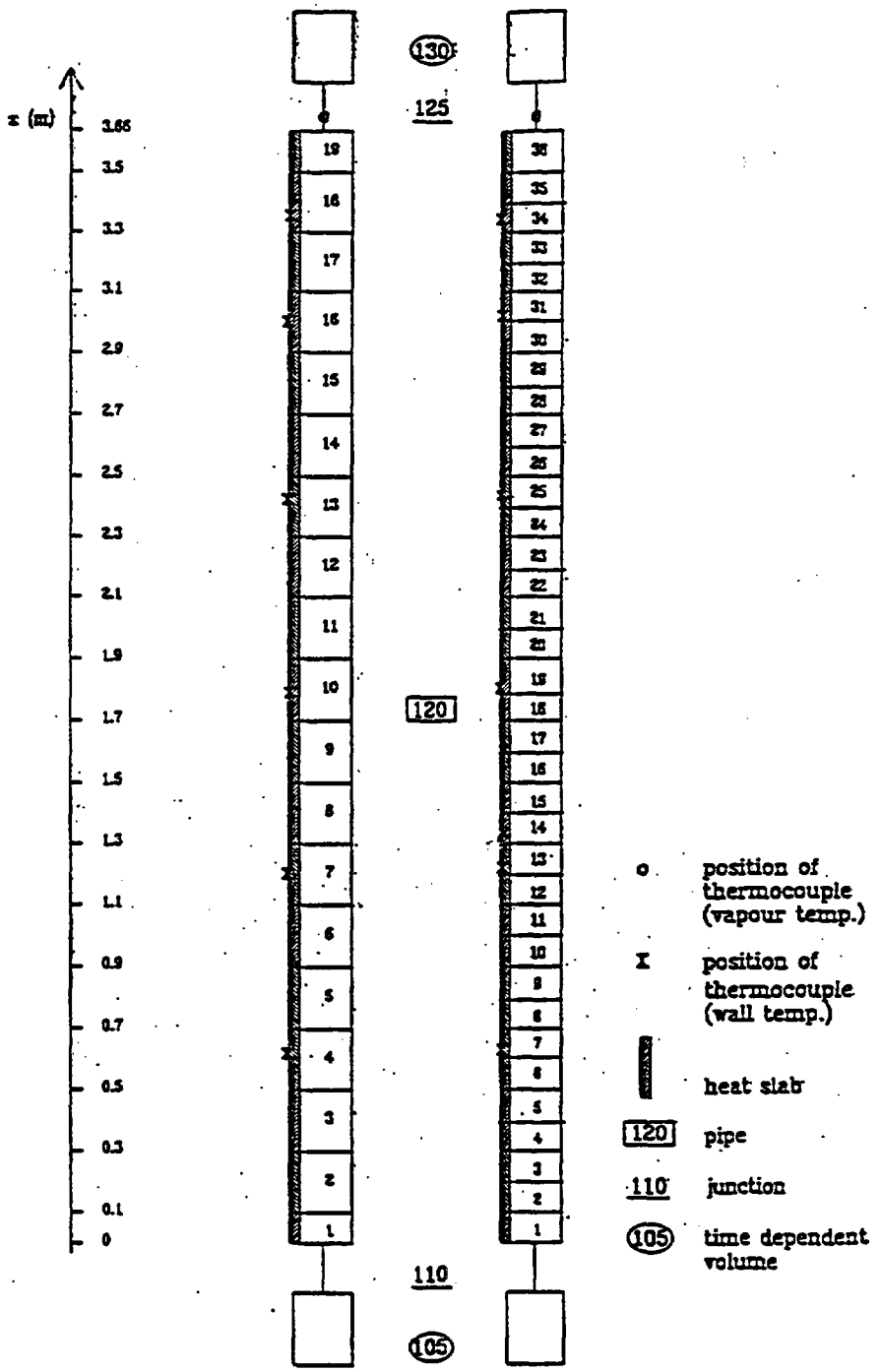


Figure 3: Nodalizations used for the calculations of Run 3051 with RELAP5/MOD2.5 (right) and RELAP5/MOD3 (left).

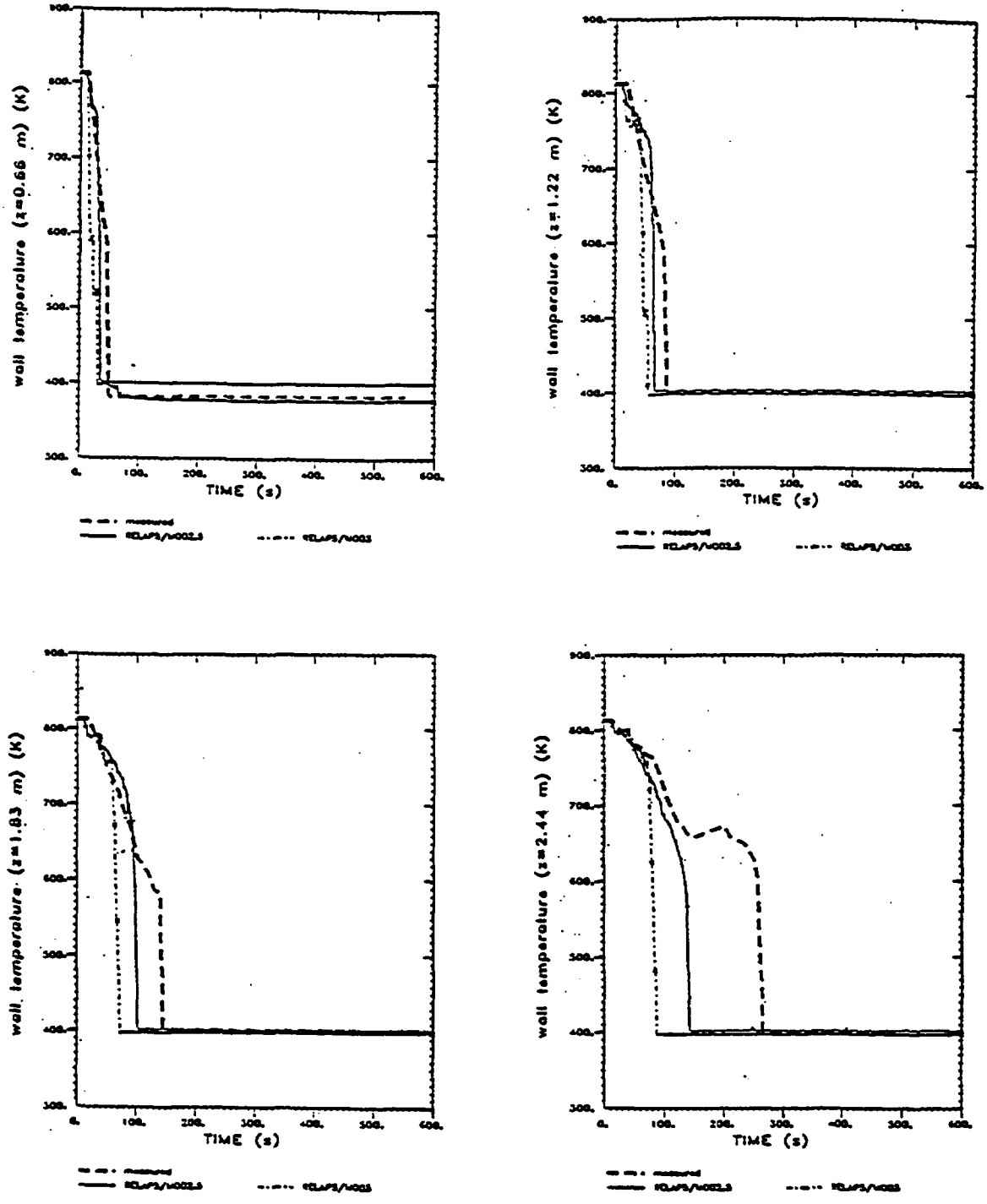


Figure 4: Comparison of the wall temperatures at 0.66, 1.22, 1.83 and 2.44 m calculated by RELAP5/MOD2.5 and RELAP5/MOD3 with the experimental ones for Test 3051.

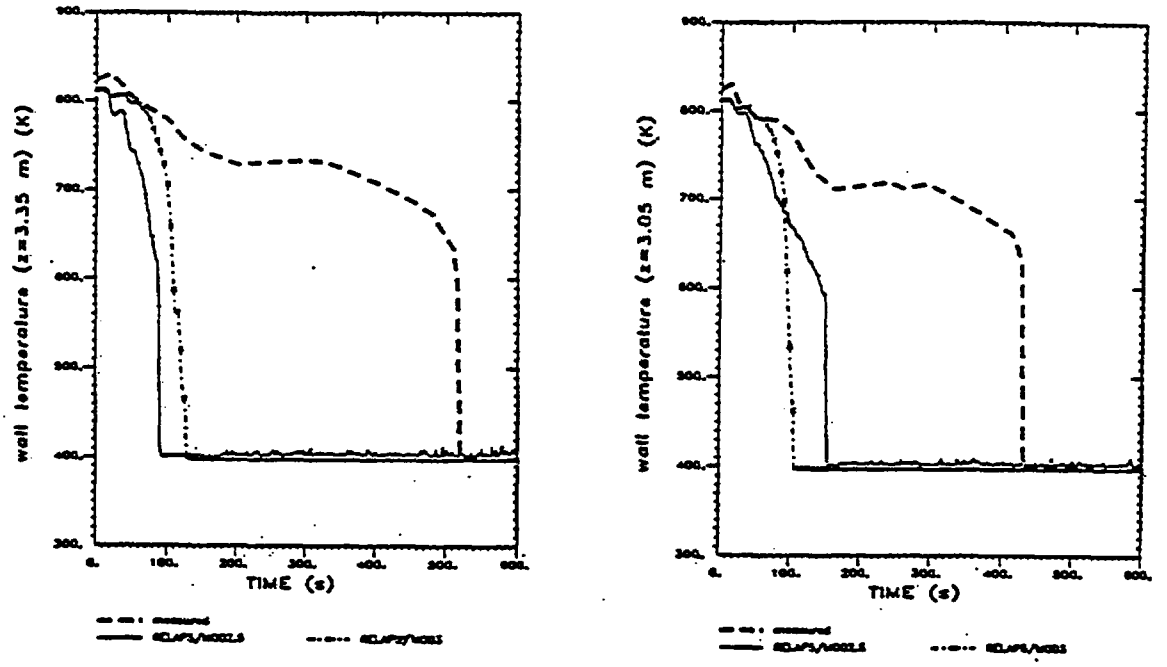


Figure 5: Comparison of the wall temperatures at 3.05 and 3.35 m calculated by RELAP5/MOD2.5 and RELAP5/MOD3 with the experimental ones for Test 3051.

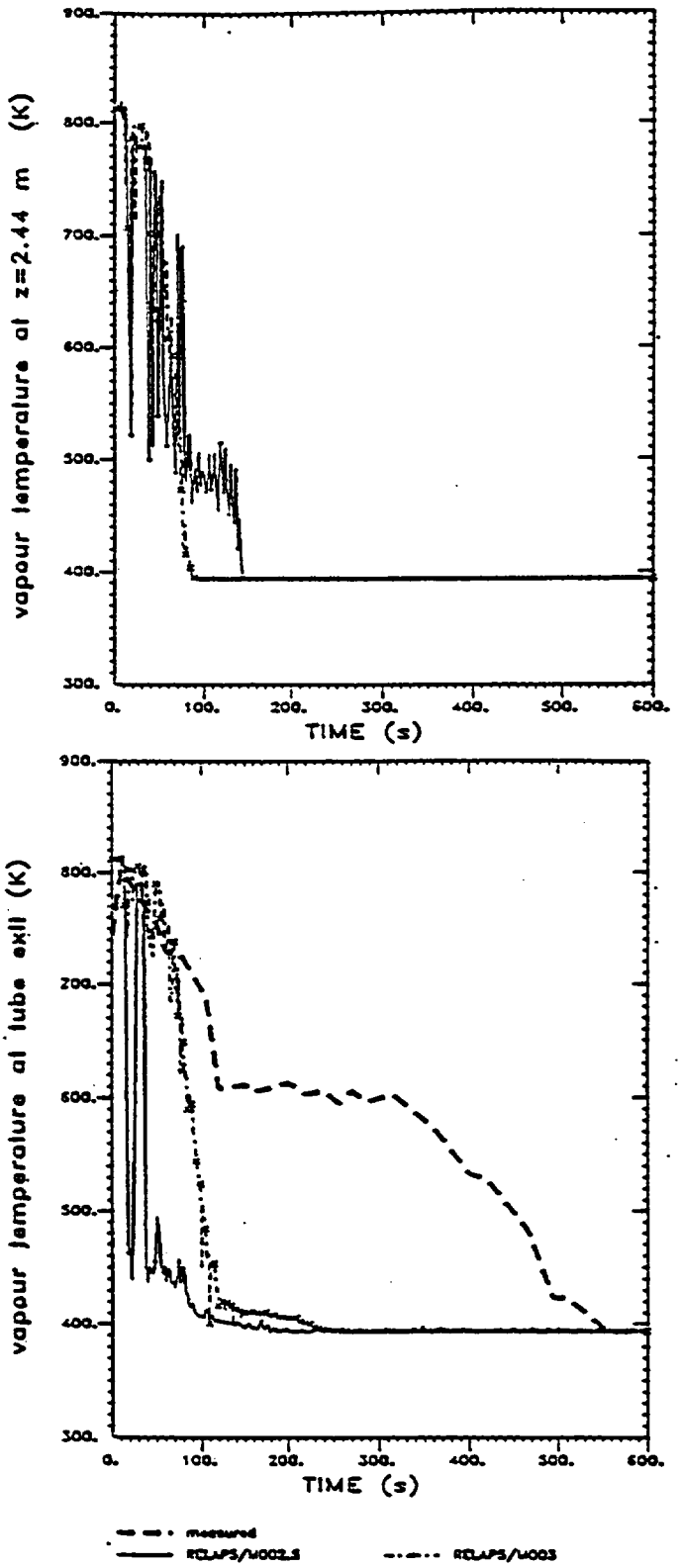


Figure 6: Calculated vapour temperature at 2.44 m and comparison of the calculated vapour temperature at the tube exit with the measured value.

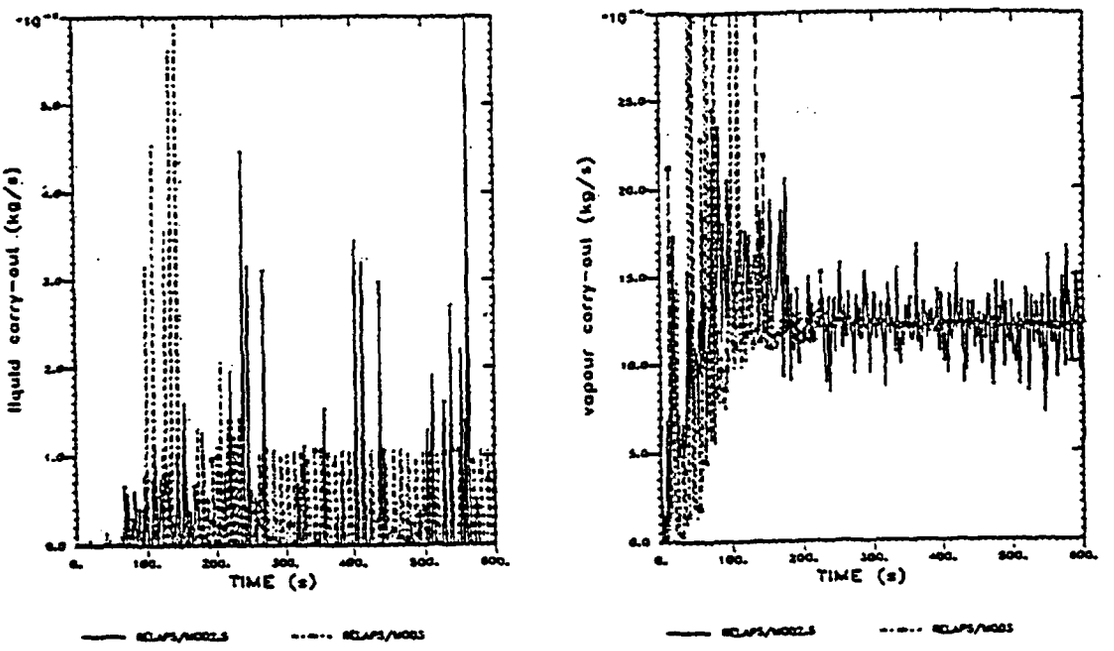


Figure 7: Calculated vapour and liquid carry-out

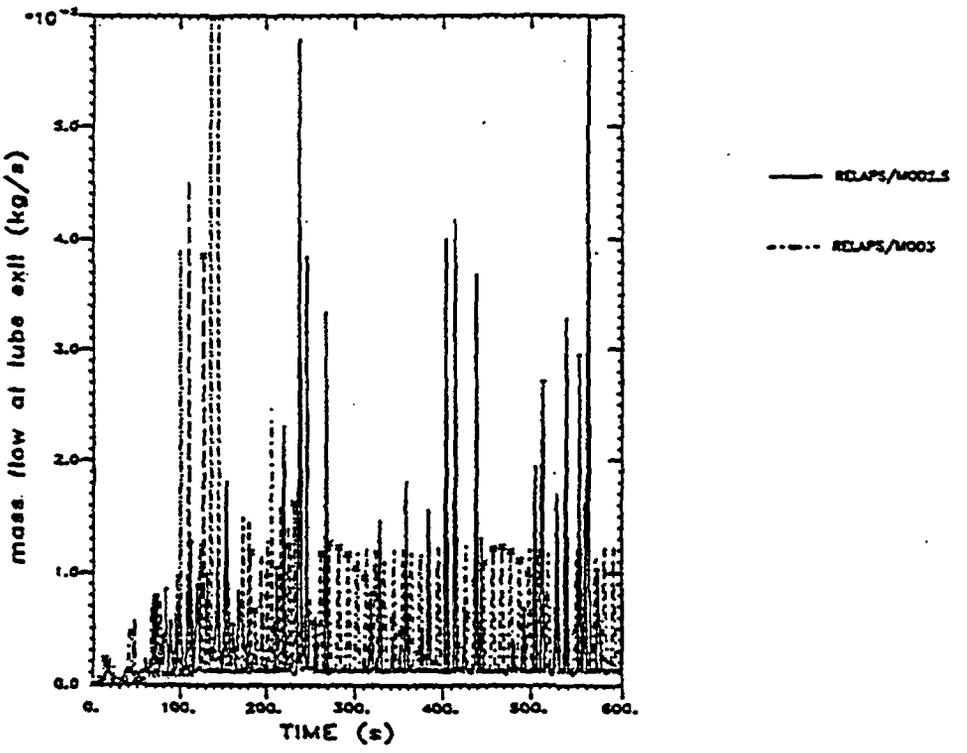


Figure 8: Calculated mass flow rate at the tube exit.

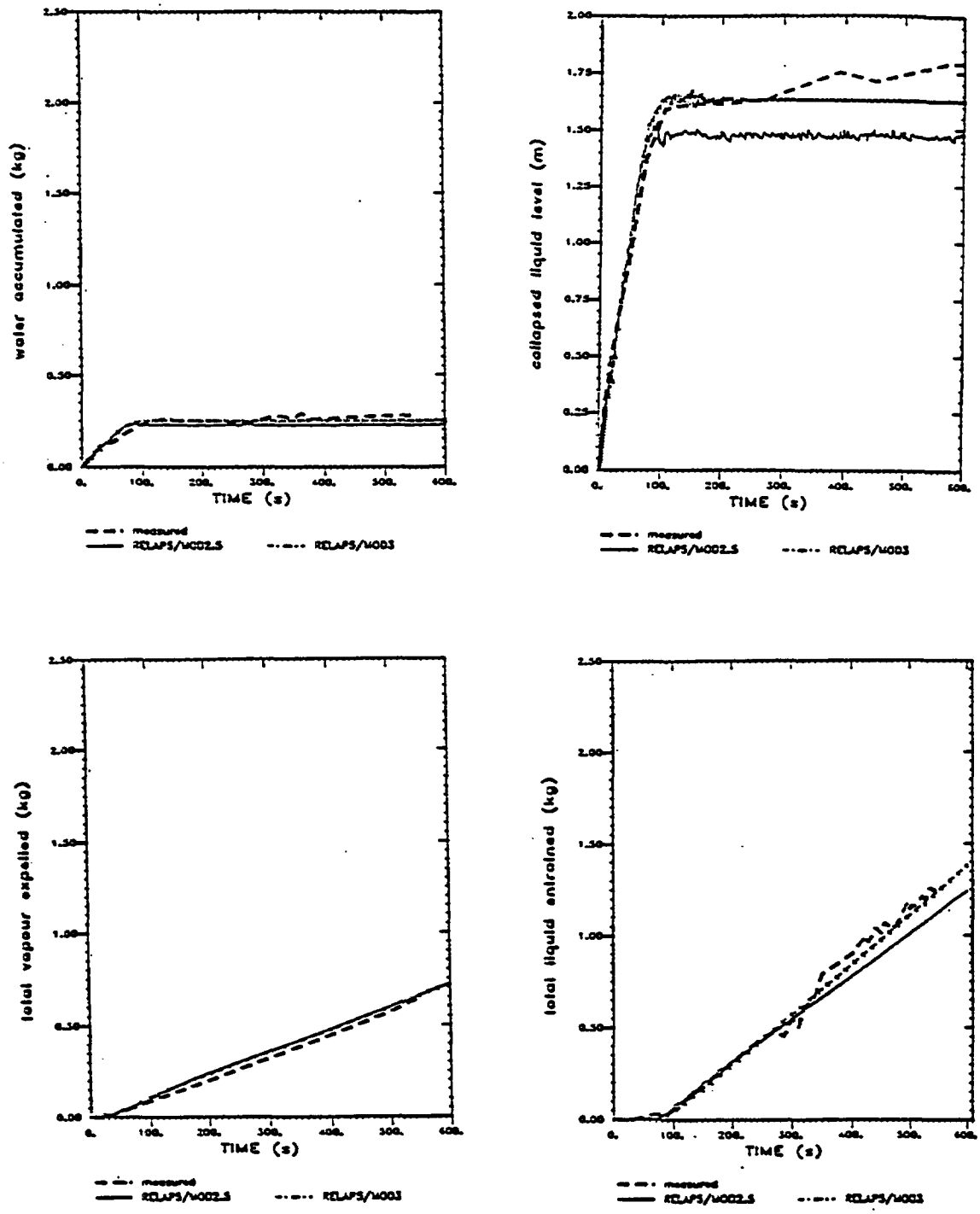


Figure 9: Comparison of the calculated accumulated mass, collapsed liquid level, vapour and liquid entrainment with the experimental data.

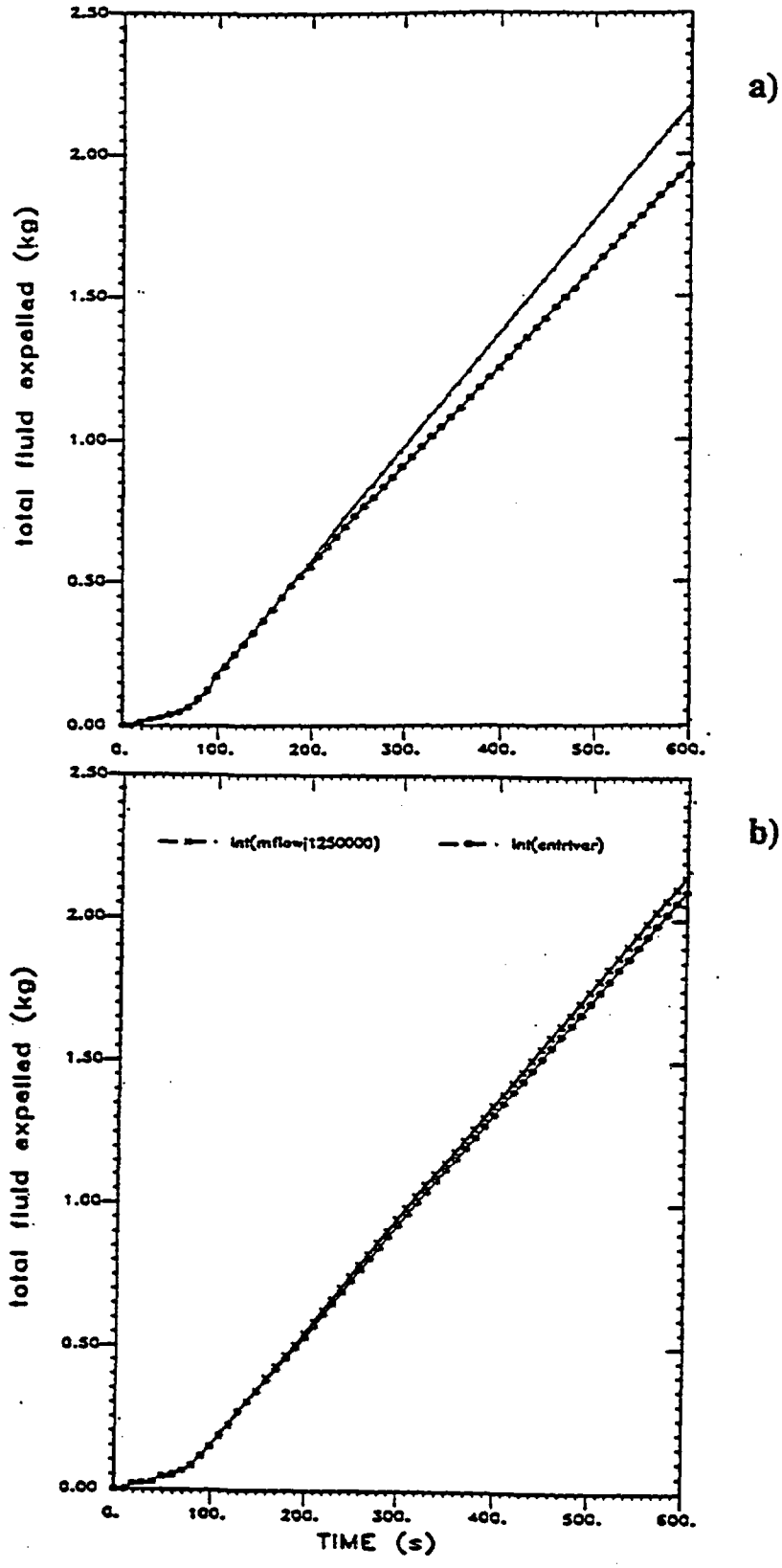


**Figure 10: Comparison of the calculated fluid expelled out of the test section by integrating directly the mass flow with that using control variables and the primitive variables (velocities, void fractions and densities): a) RELAP5/MOD2.5 and b) RELAP5/MOD3.**

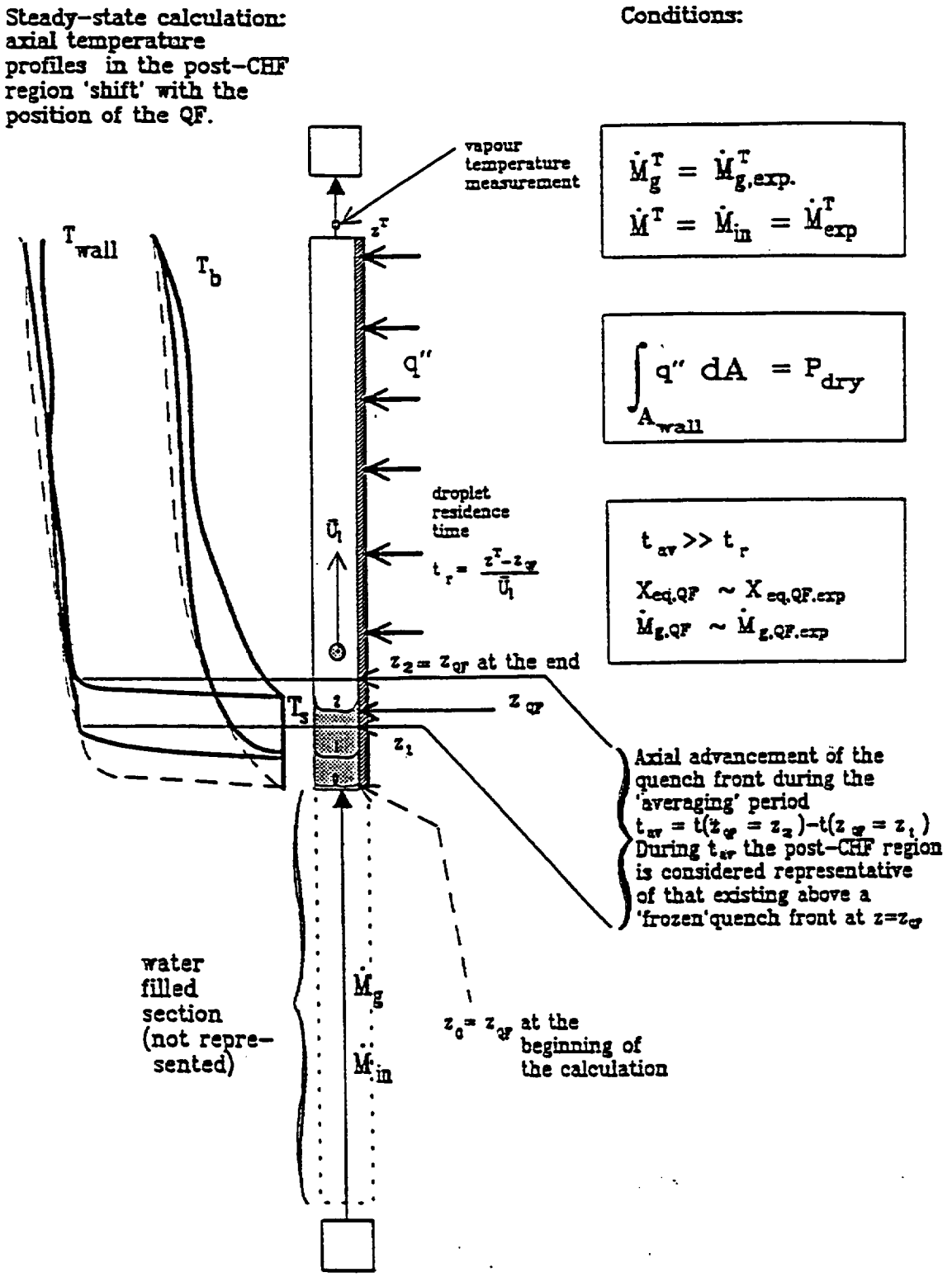


Figure 11: Prerequisites for the 'quasi steady-state' analysis of the post-CHF zone above a slowly advancing quench front (under these conditions the interfacial heat transfer model can be assessed

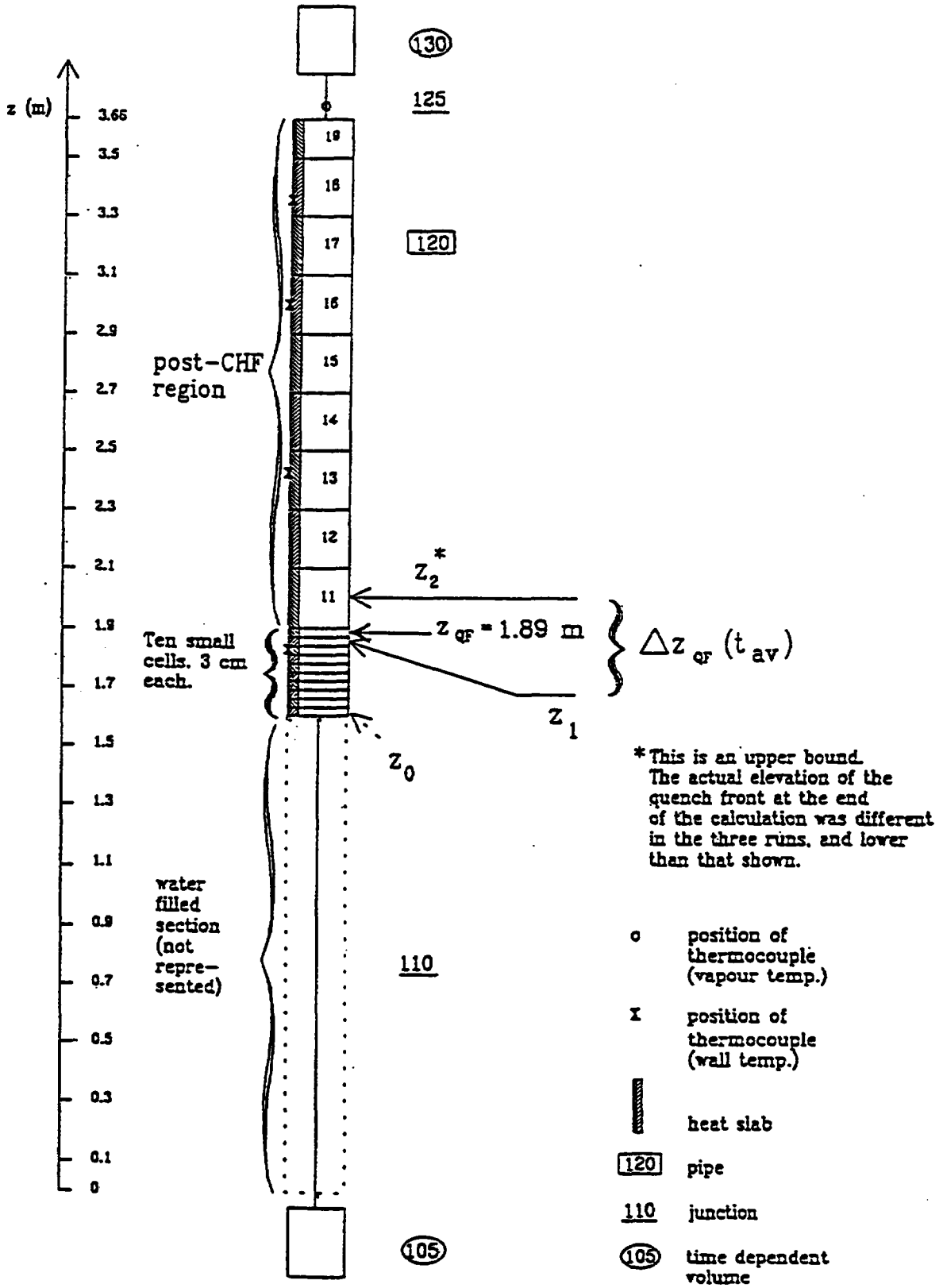


Figure 12: Nodalization used for the steady-state analysis of Run 3051 by RELAP5/MOD2.5.

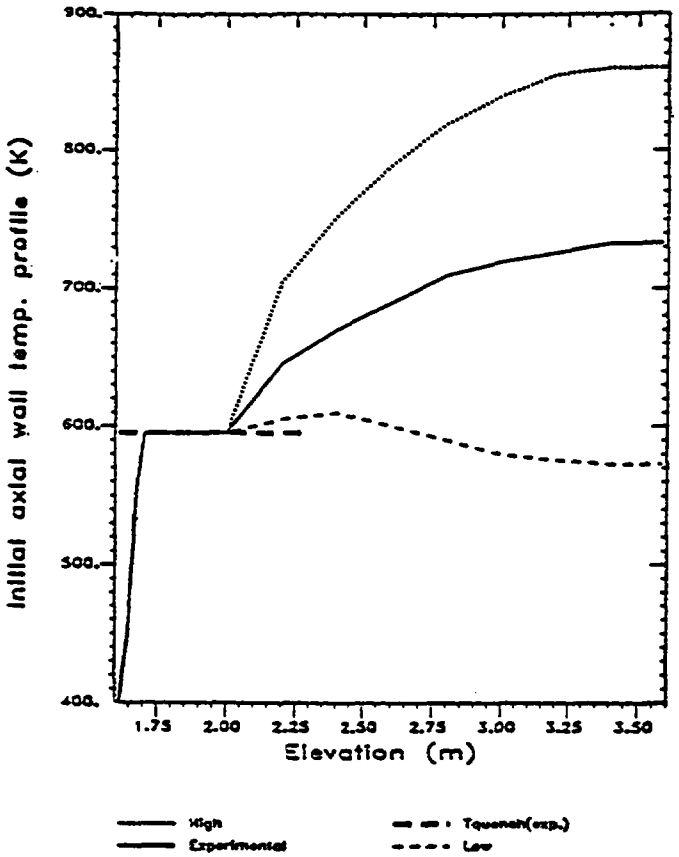


Figure 13: Initial axial wall temperature distributions used for the steady-state analysis of test 3051 at the time of the mid-height quench.

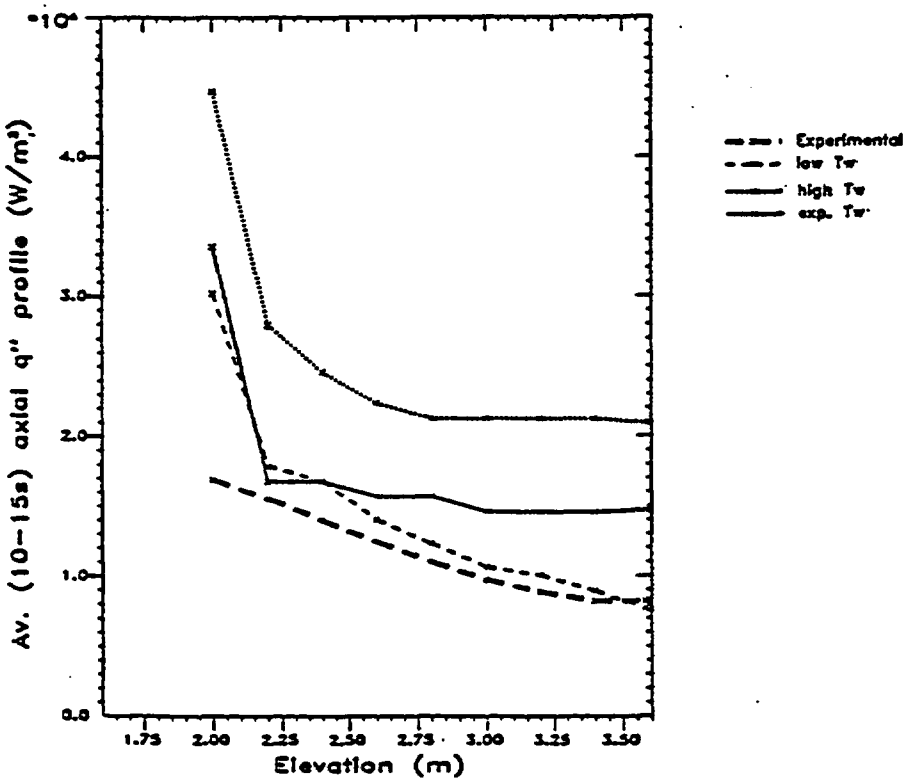


Figure 14: Average axial wall heat flux distributions during the time span 10-15 s for the three initial axial wall temperature distributions shown in Fig. 13.

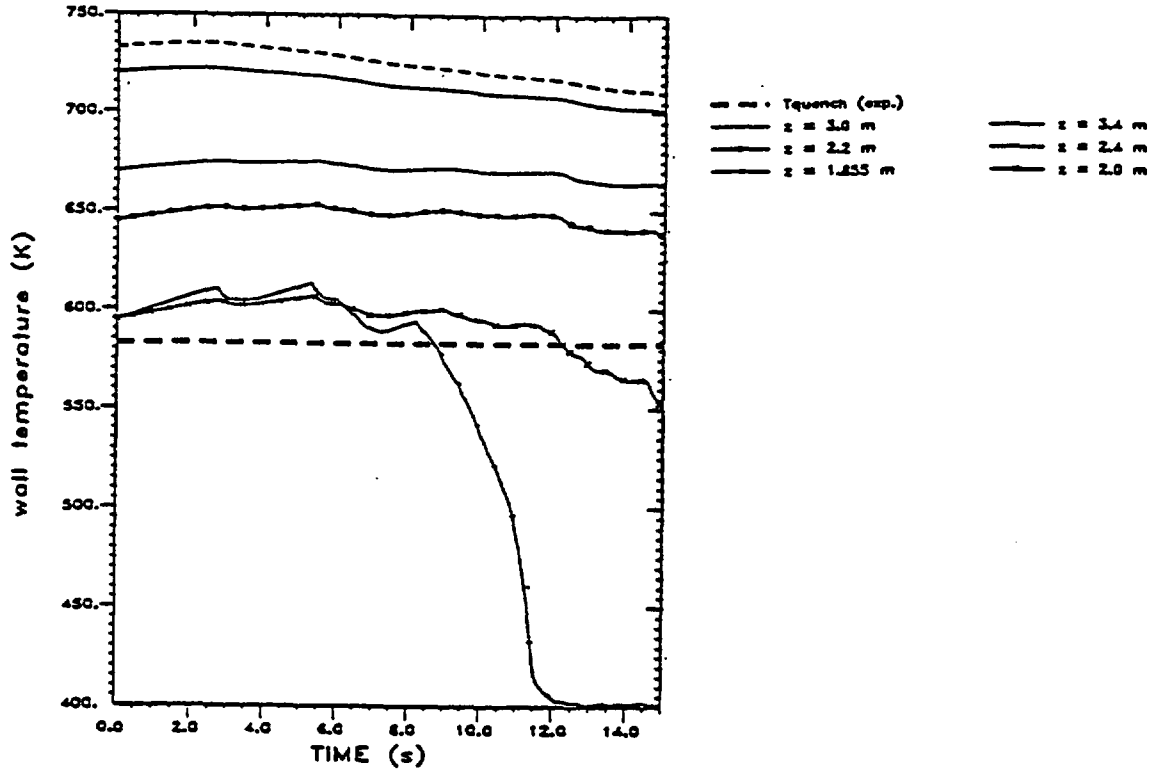


Figure 15: Calculated wall temperatures time-history at various elevations, when the experimental axial wall temperature distribution is imposed.

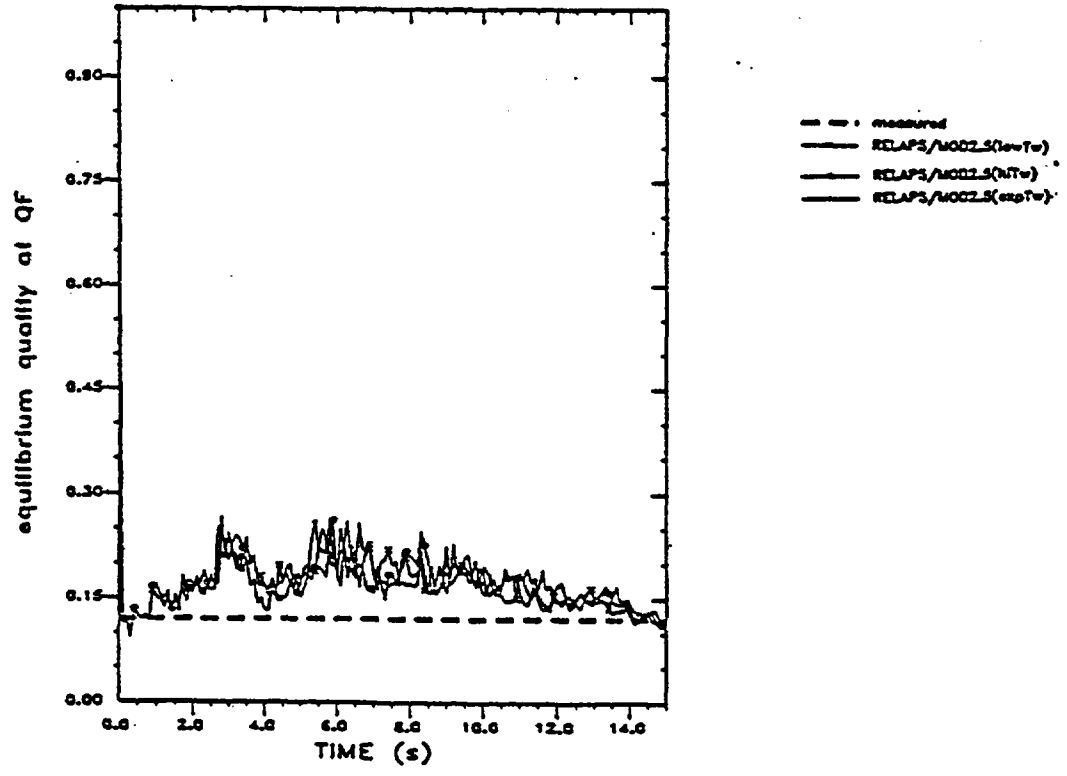


Figure 16: Equilibrium quality at the QF calculated using the three different initial wall temperature distributions (Fig. 13).

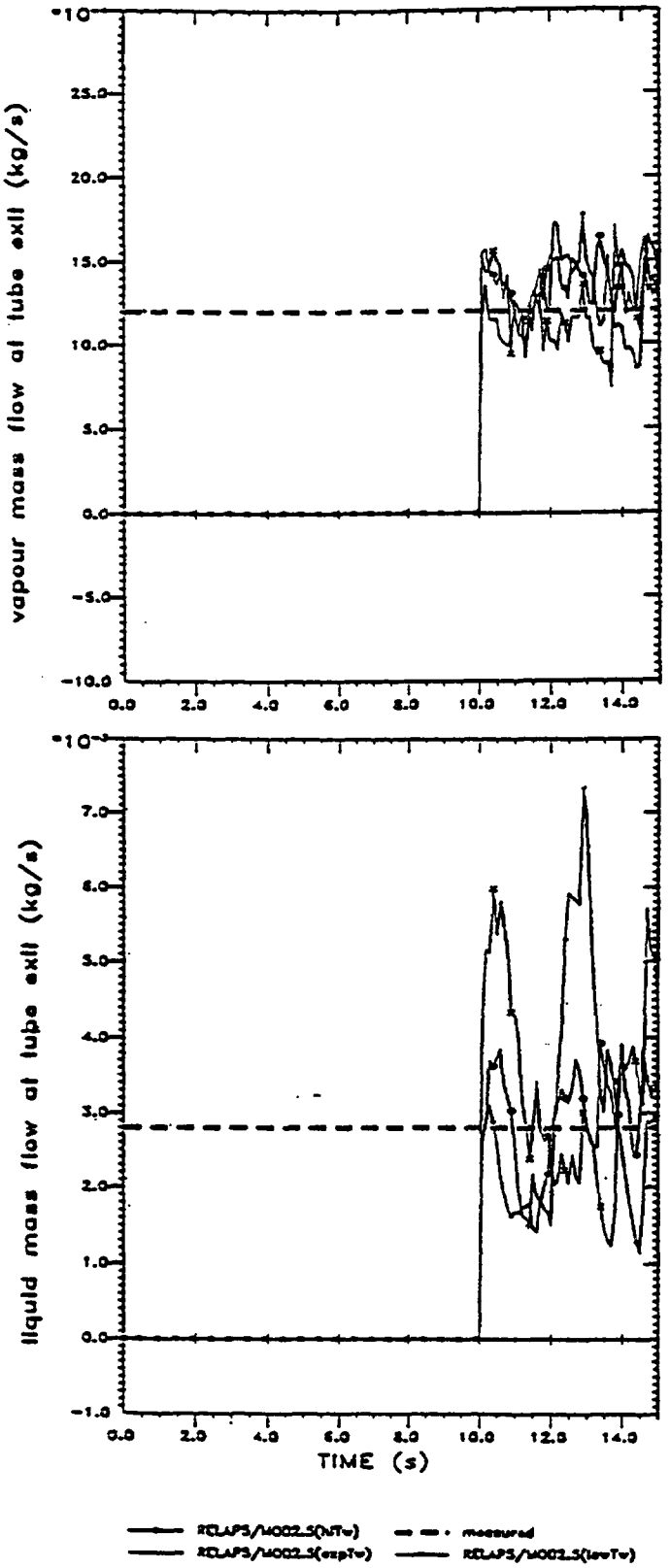


Figure 17: Vapour and liquid mass flow rates at the tube exit.

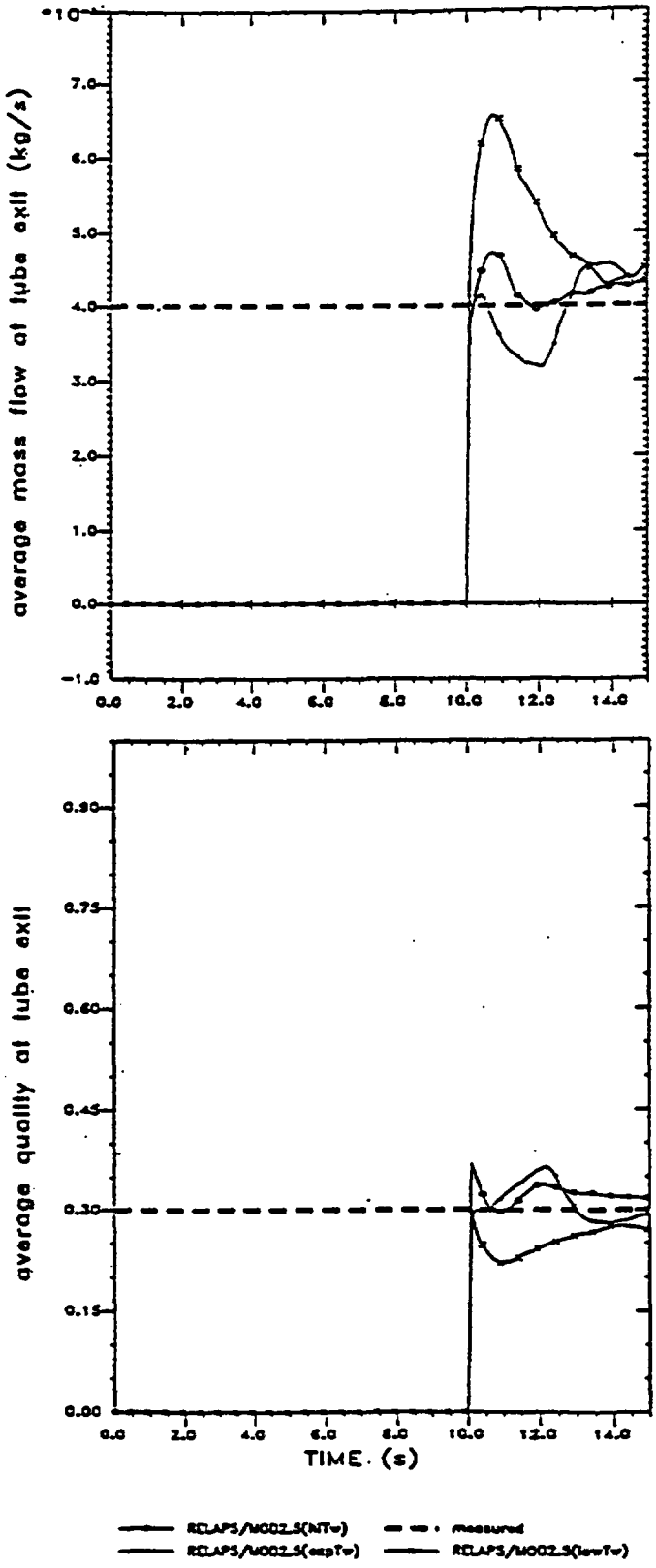


Figure 18: Average values of the total mass flow rates and exit quality over the time span 10-15 sec. The quantities to be averaged are calculated starting from 10 sec.

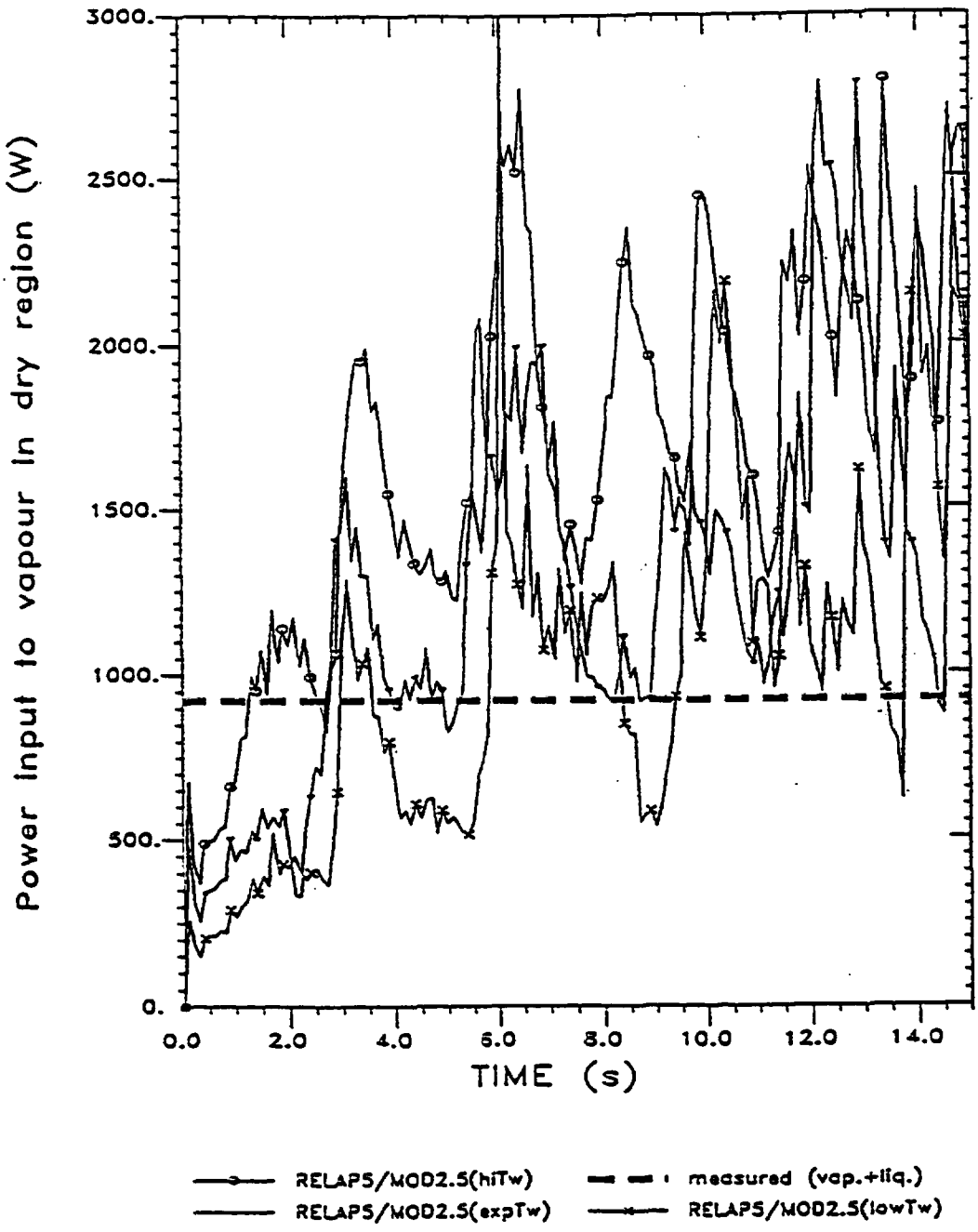


Figure 19: Comparison of the heat transfer rate to vapour with the total power input to the mixture measured in the experiment.

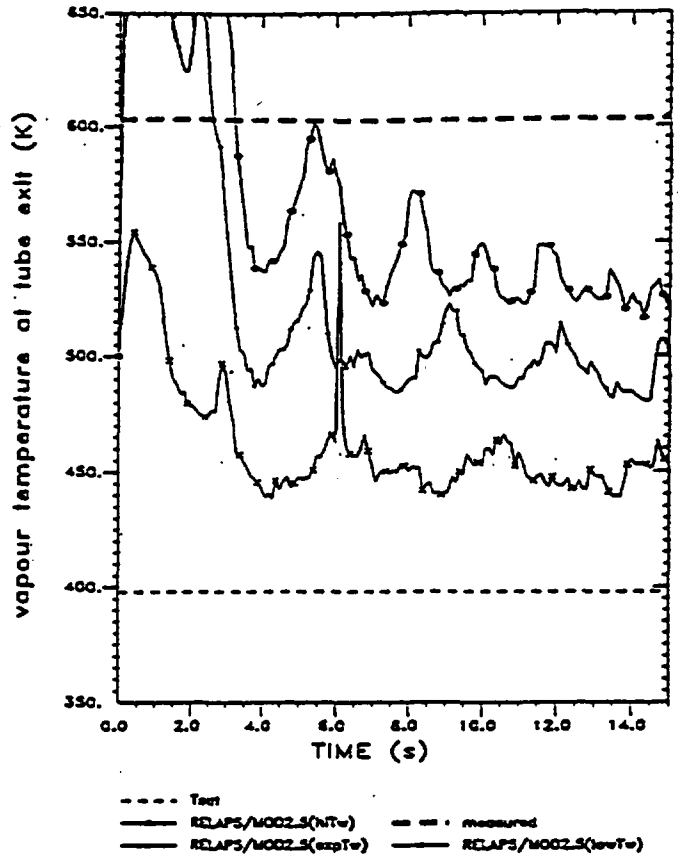


Figure 20: Comparison of the calculated vapour temperature at the tube exit with the experimental value at the time of the mid-height quench.

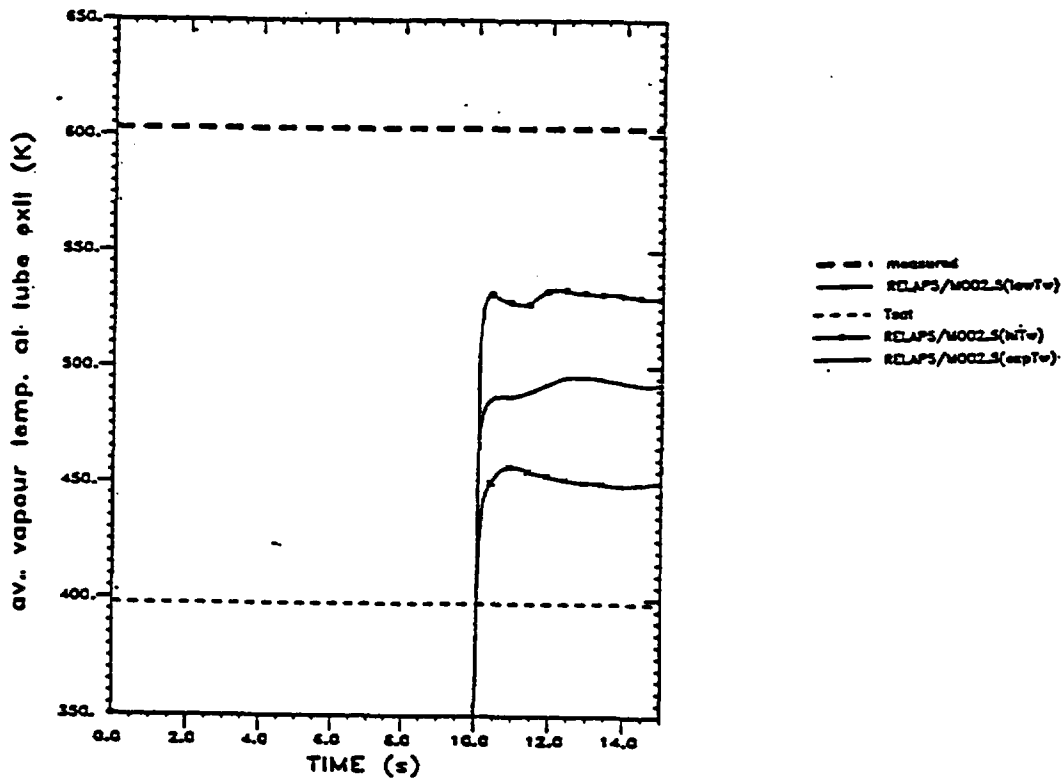


Figure 21: Time-average value of the vapour temperature at the tube exit.

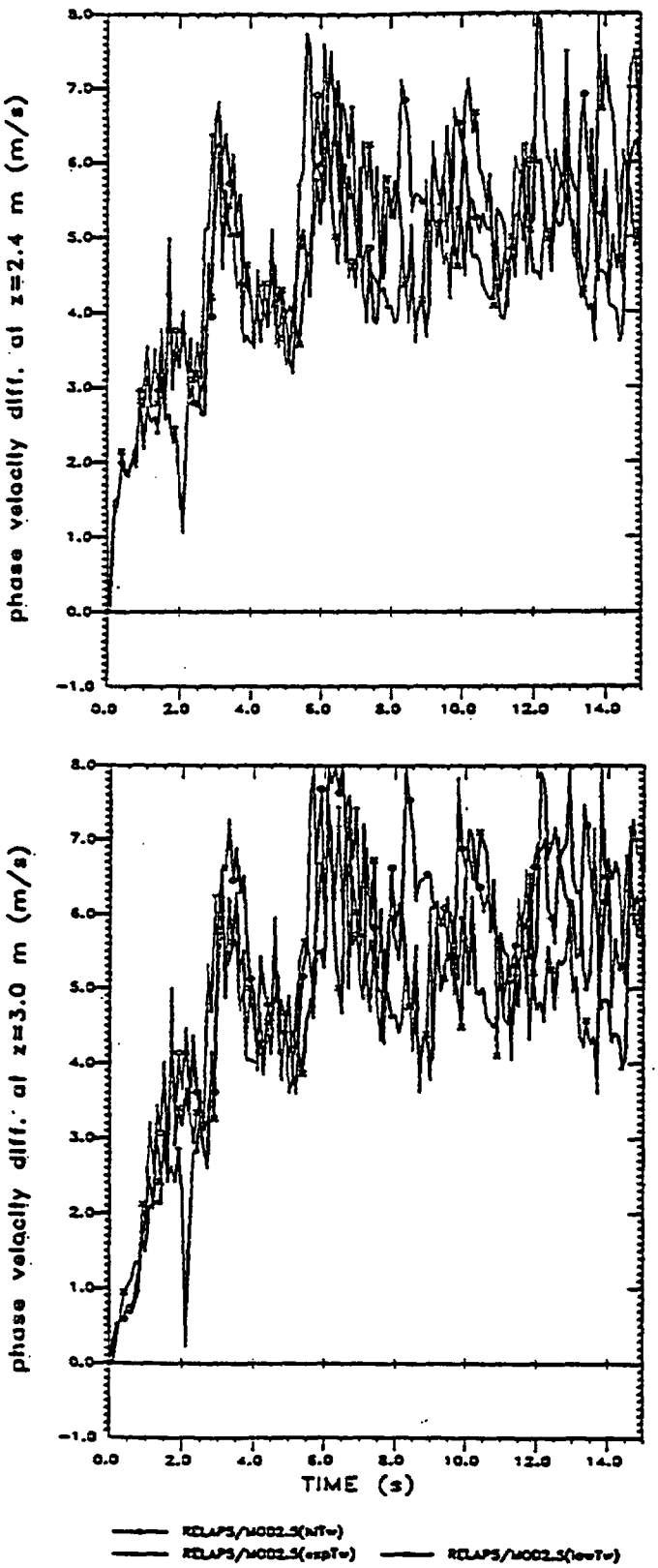


Figure 22: Phase velocity difference at z=2.4 m and z=3.0 m.

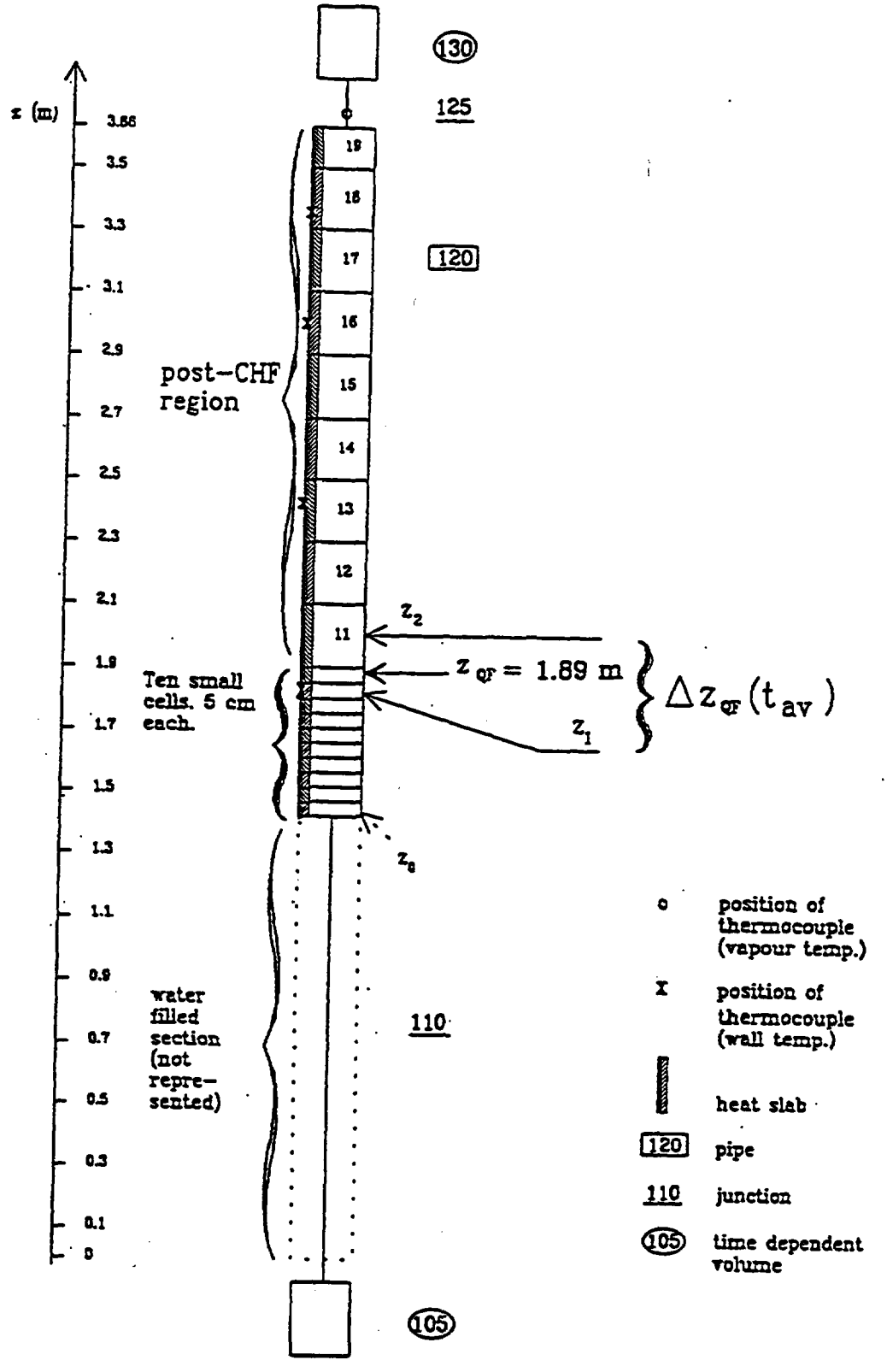


Figure 23: Nodalization used for the steady-state analysis of run 3051 by RELAP5/MOD3.

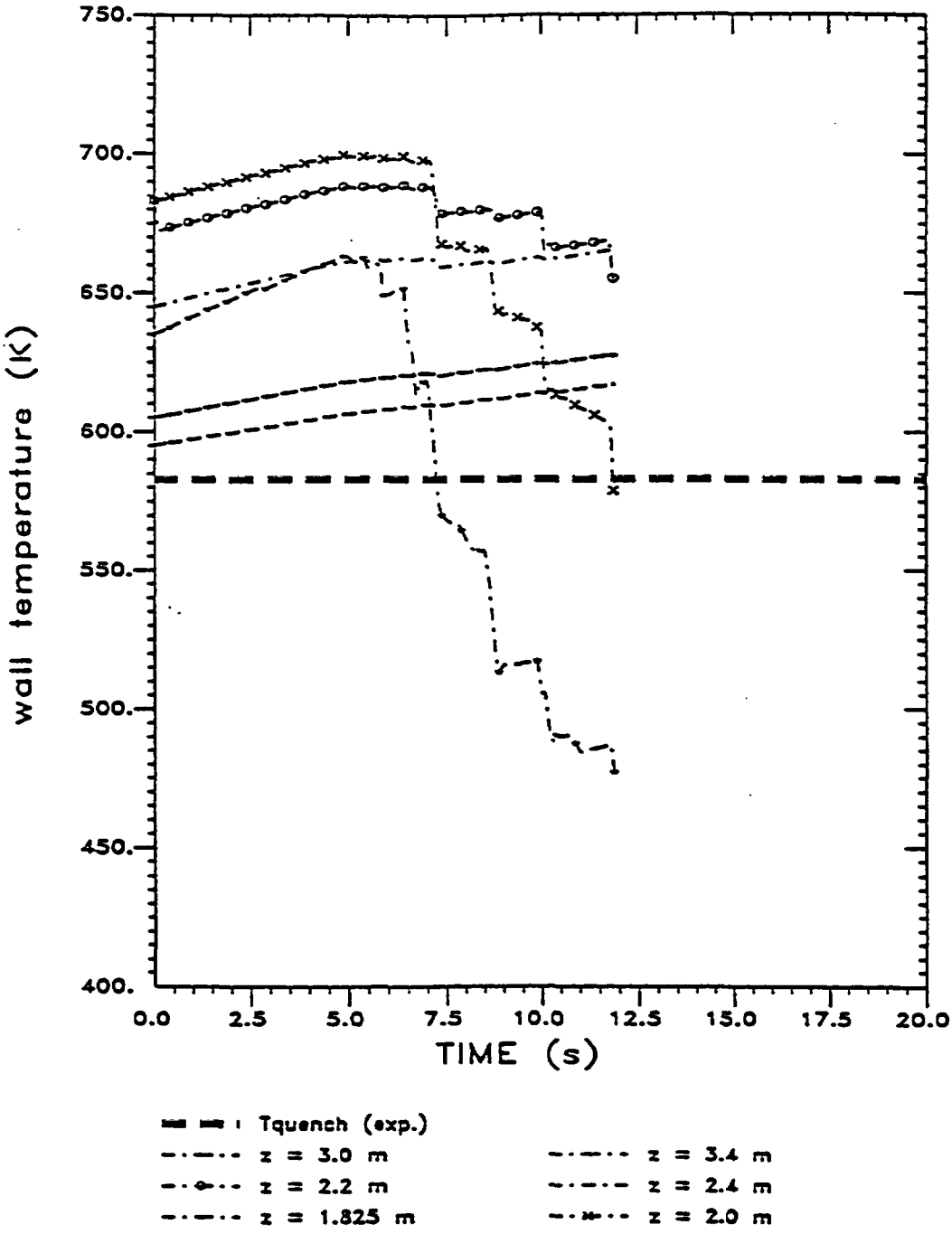


Figure 24: Wall temperatures at various elevations calculated by the frozen version of RELAP5/MOD3.

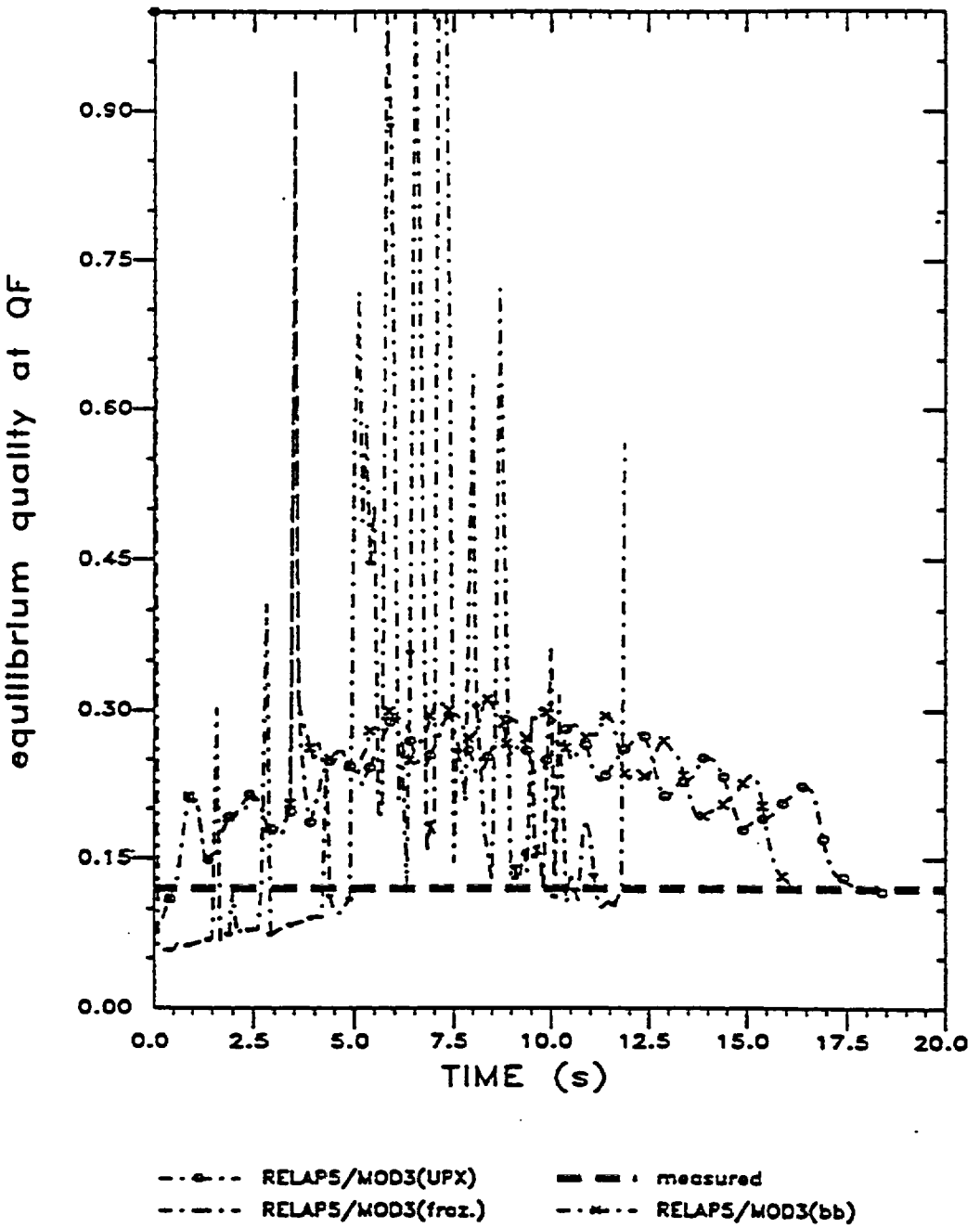


Figure 25: Equilibrium quality at the QF calculated by the frozen RELAP5/MOD3 (— · — · —), by a version (bb) including the PSI updates (— · × · — : Analytis, 1992) and an 'ad hoc' modification (version UPX) of the RELAP5/MOD3(bb) using a reduced value for the minimum droplet diameter and the correct drag coefficient for droplets (— · e · —).

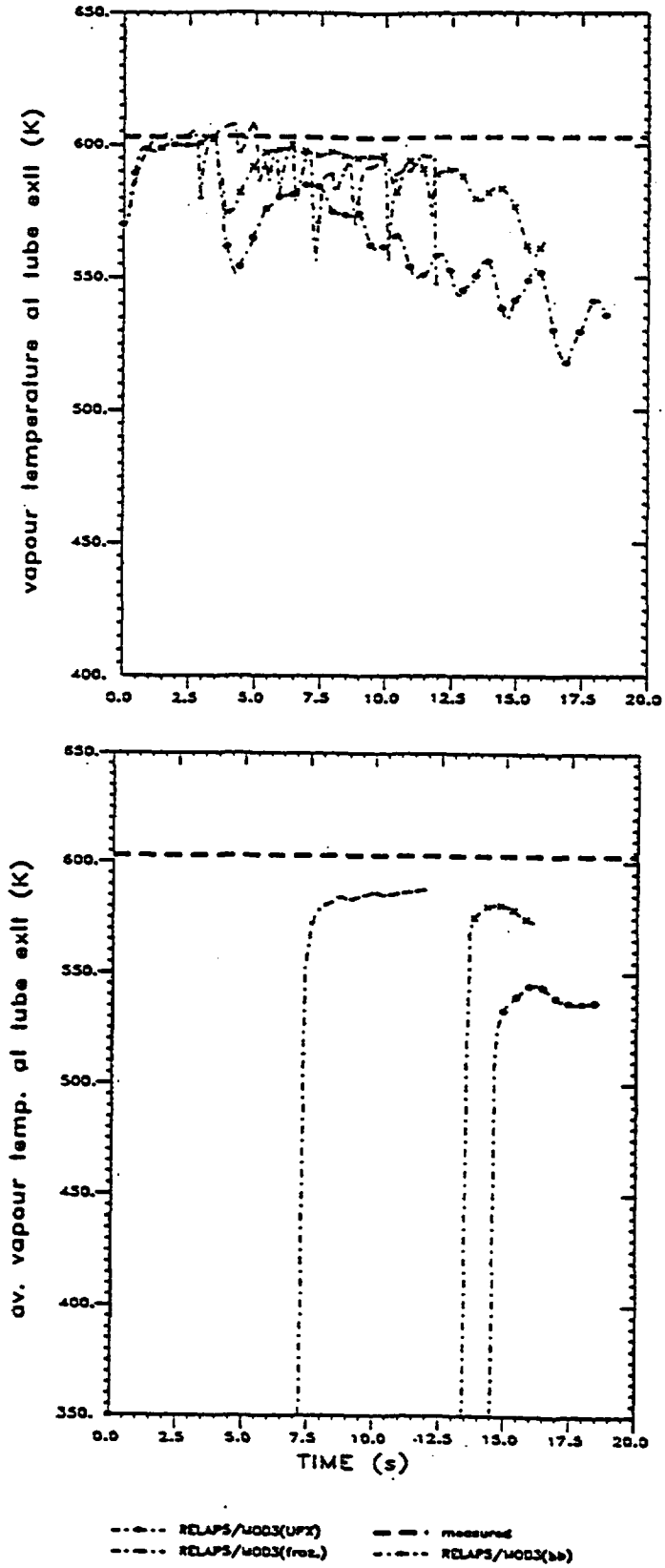


Figure 26: Vapour temperature at the tube exit calculated by three versions of RELAP5/MOD3 (see legend in Fig. 25).

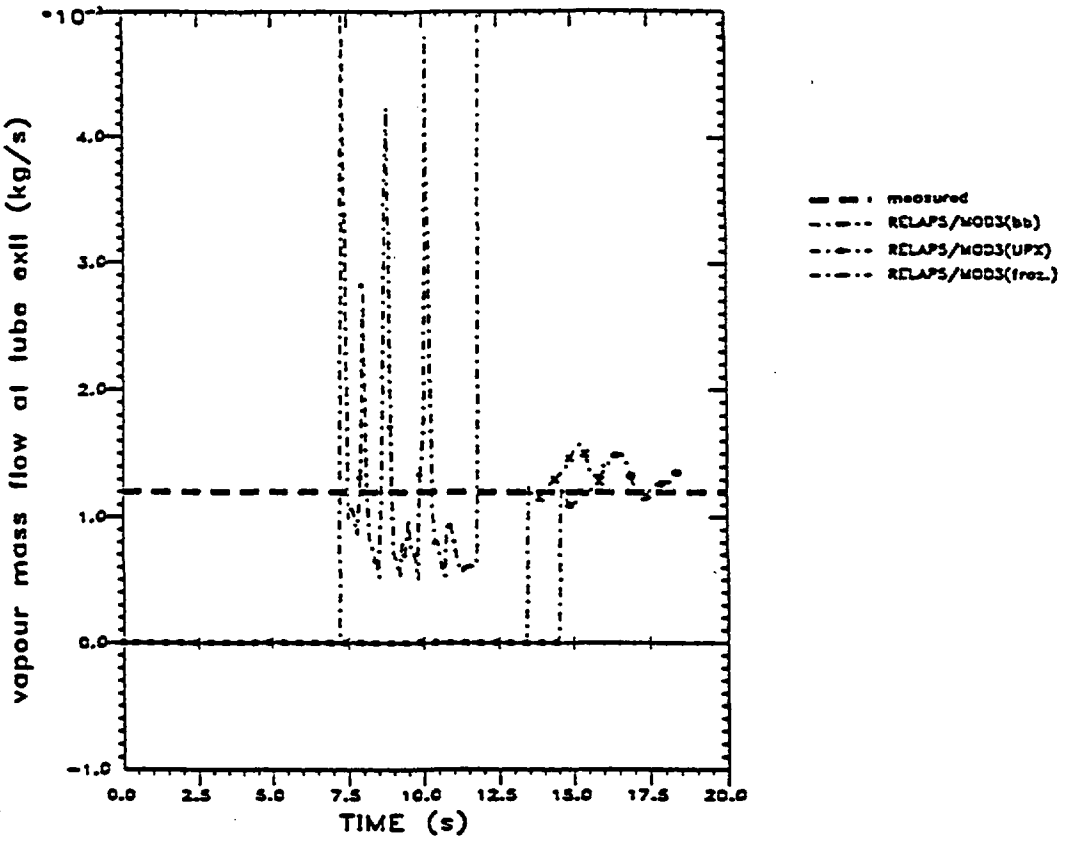


Figure 27: Vapour carry-out calculated by three versions of RELAP5/MOD3 (see legend in Fig. 25).

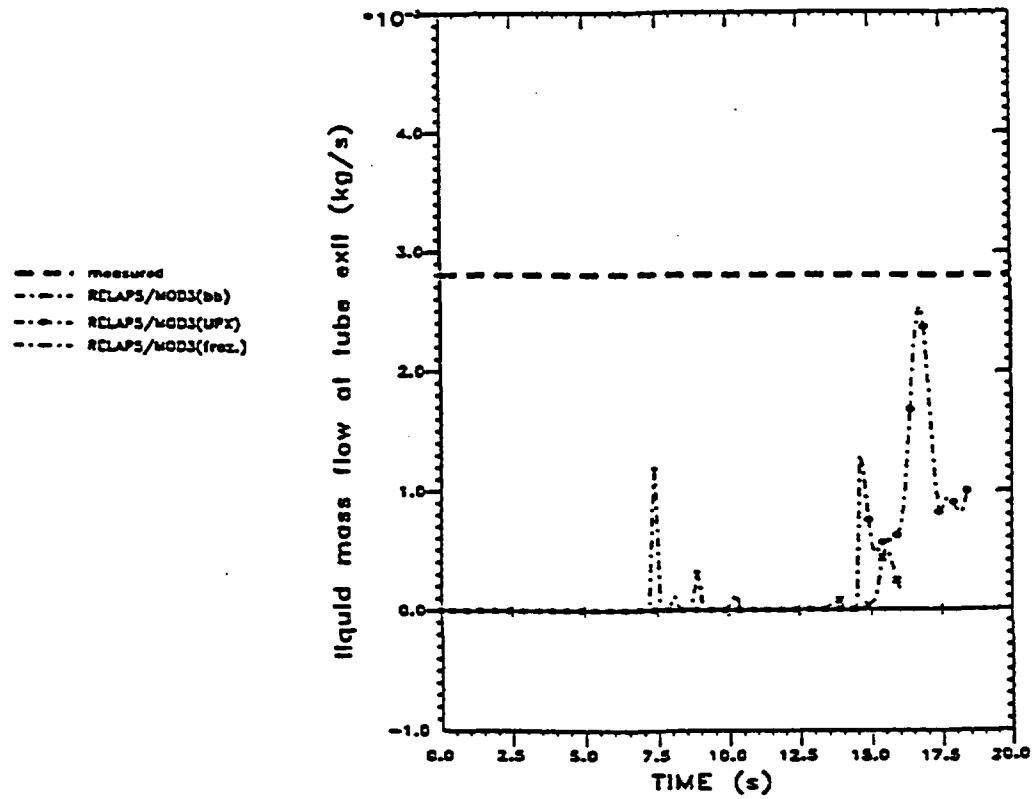


Figure 28: Liquid carry-out calculated by three versions of RELAP5/MOD3 (see legend in Fig. 25).

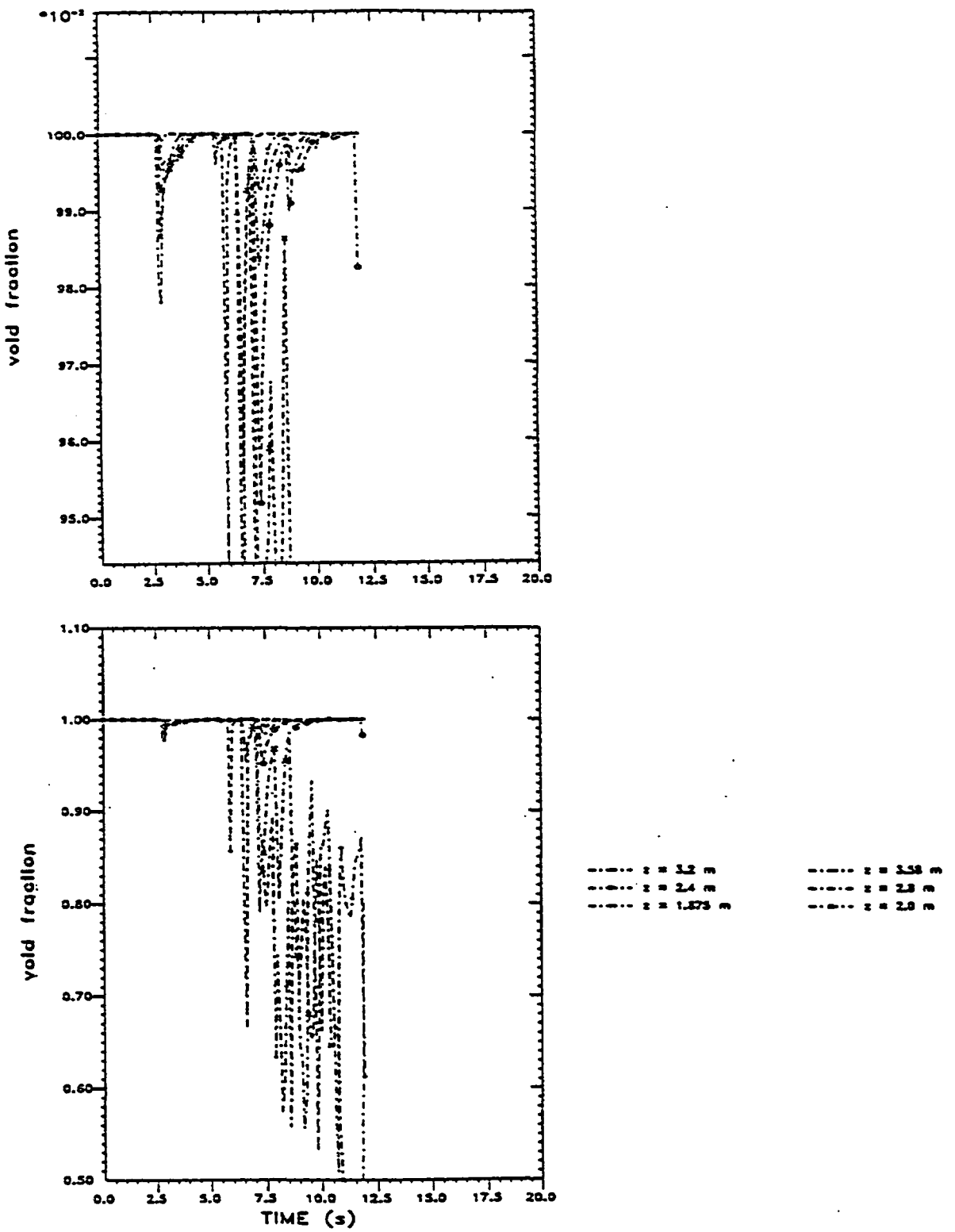


Figure 29: Void fractions (shown on two different scales) at various elevations calculated by the frozen version of RELAP5/MOD3.

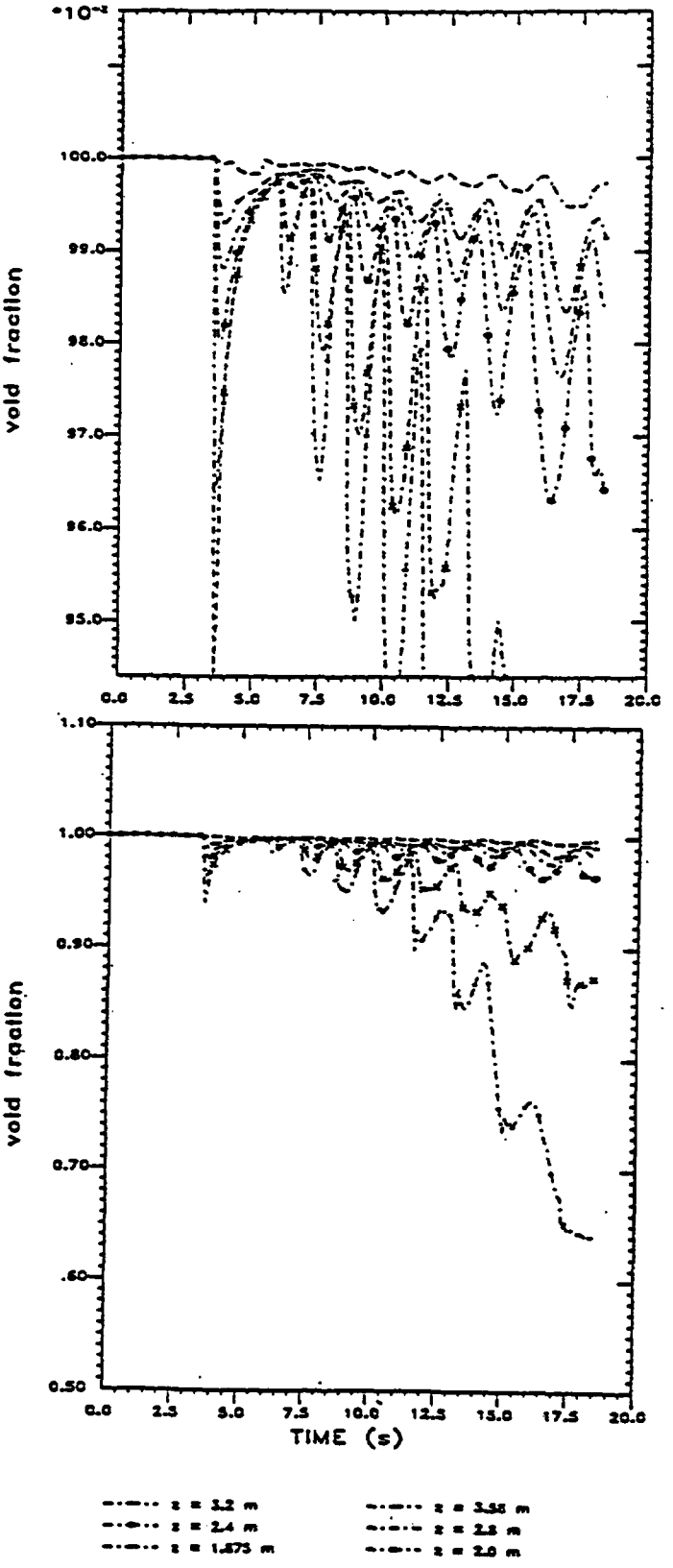


Figure 30: Void fractions (shown on two different scales) at various elevations calculated by RELAP5/MOD3+PSI updates (version bb).

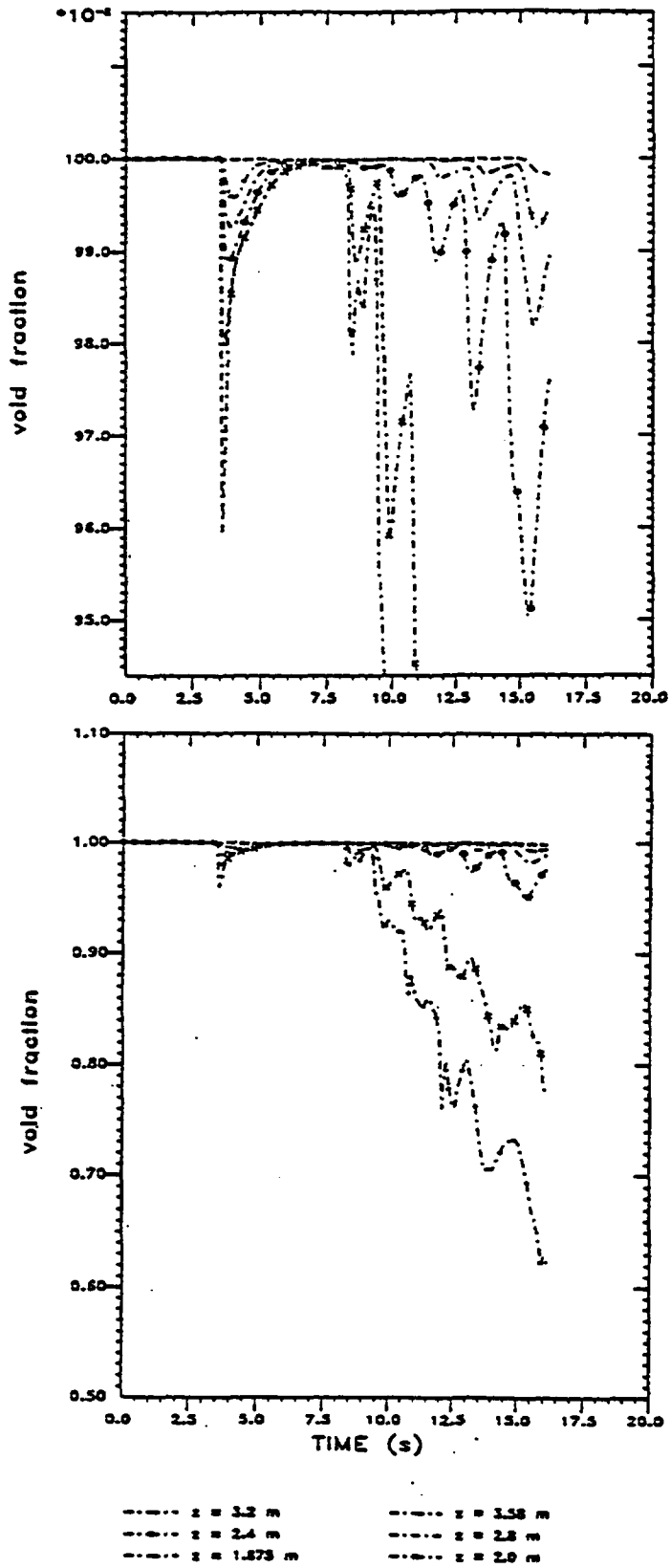


Figure 31: Void fractions (shown on two different scales) at various elevations calculated by RELAP5/MOD3+PSI updates+modified $C_D$ and $d_{min}$ = 1.25 mm (version UPX).

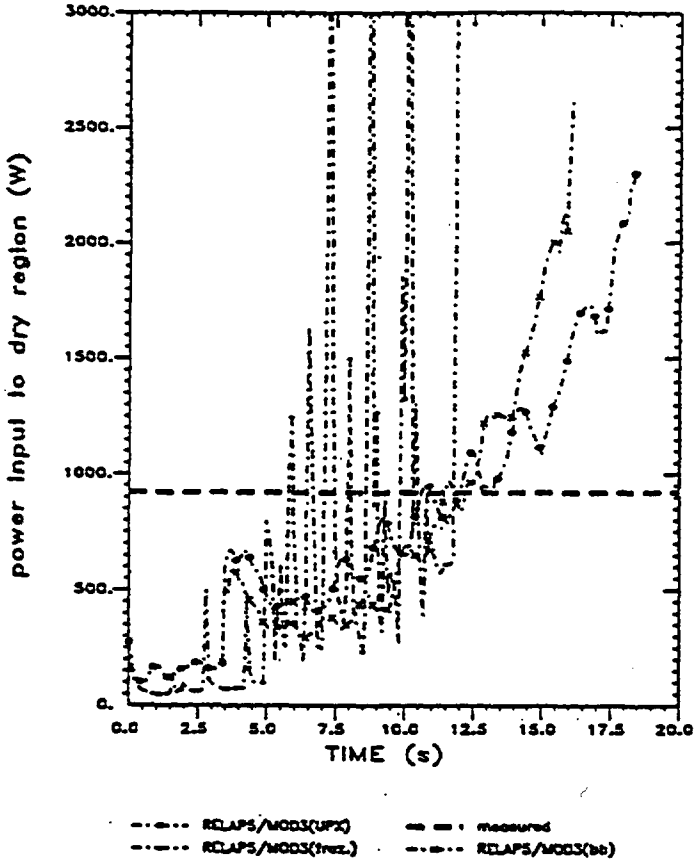


Figure 32: Power input to the mixture in the region above $z_{QF}$ for the three versions of RELAP5/MOD3 (see legend in Fig. 25).

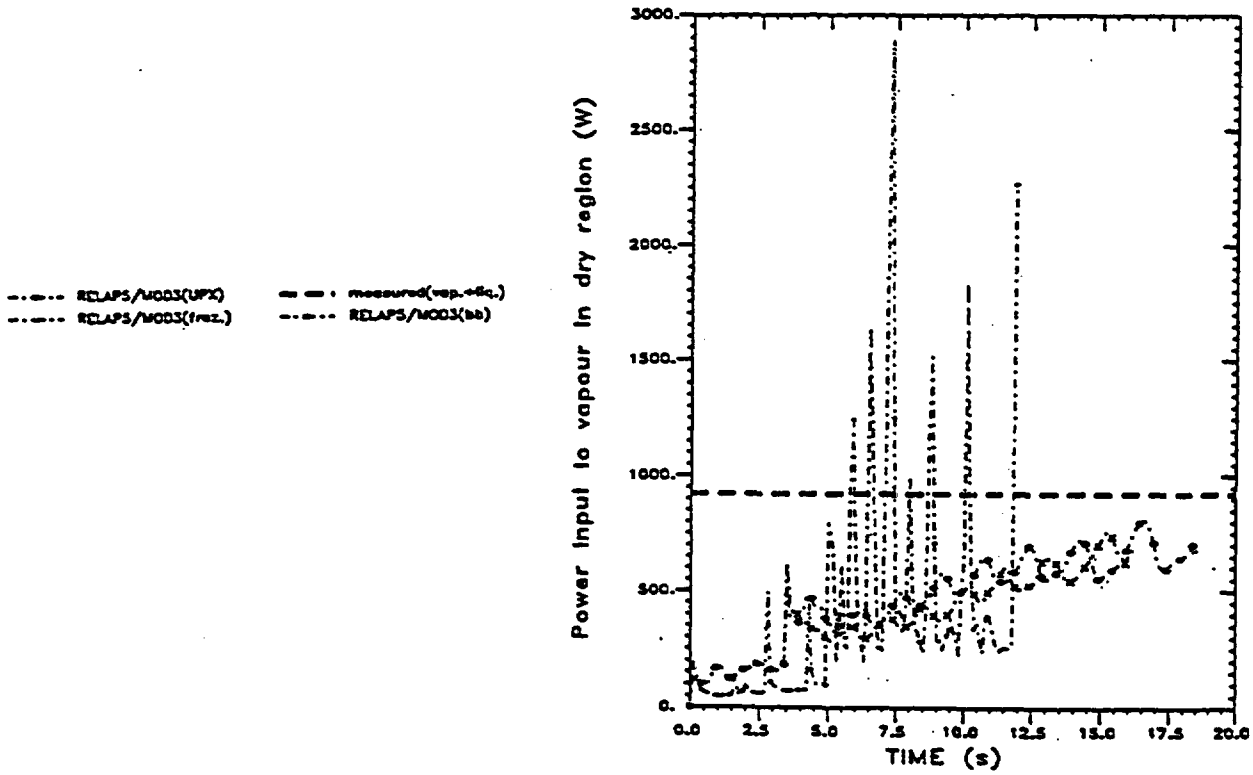


Figure 33: Heat transfer rate to the vapour alone for the three versions of RELAP5/MOD3 (legend in Fig. 25).

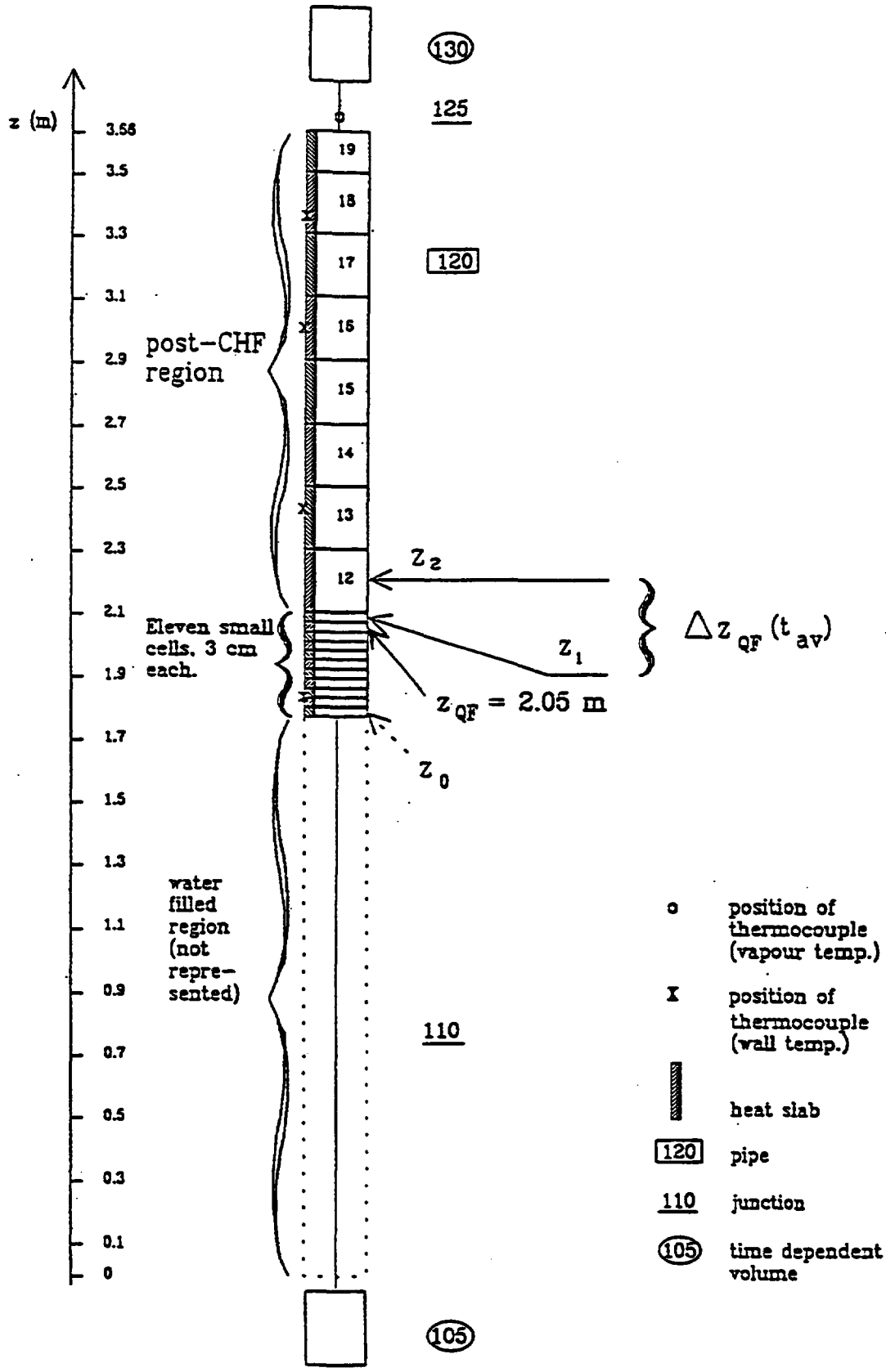


Figure 34: Nodalization used for the steady-state analysis of run 3053 by RELAP5/MOD2.5.

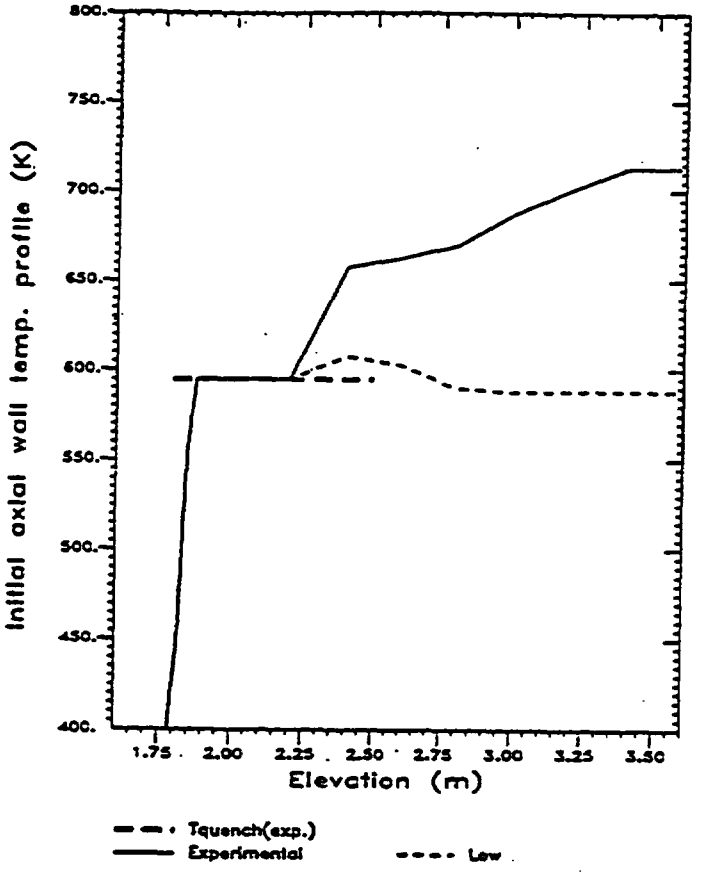


Figure 35: Initial axial wall temperature distributions used for the steady-state analysis of test 3053 at the time of the mid-height quench.

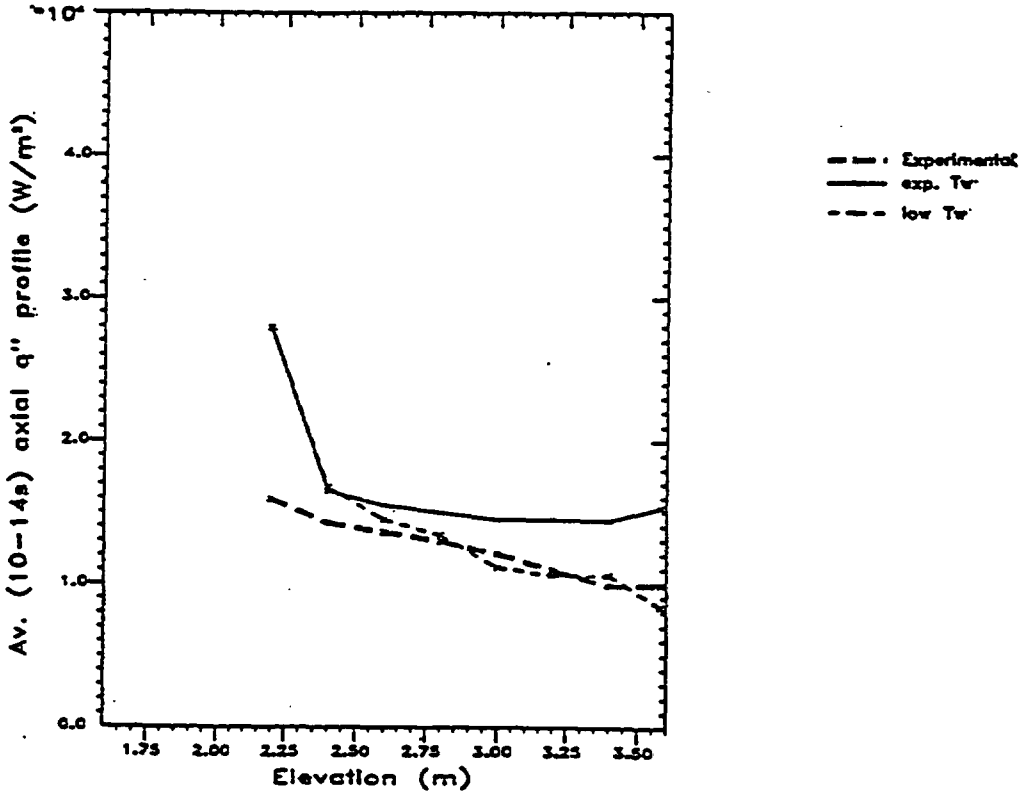


Figure 36: Average axial wall heat flux distributions during the time span 10-14 sec. for the two initial axial wall temperature distributions shown in Fig. 35.

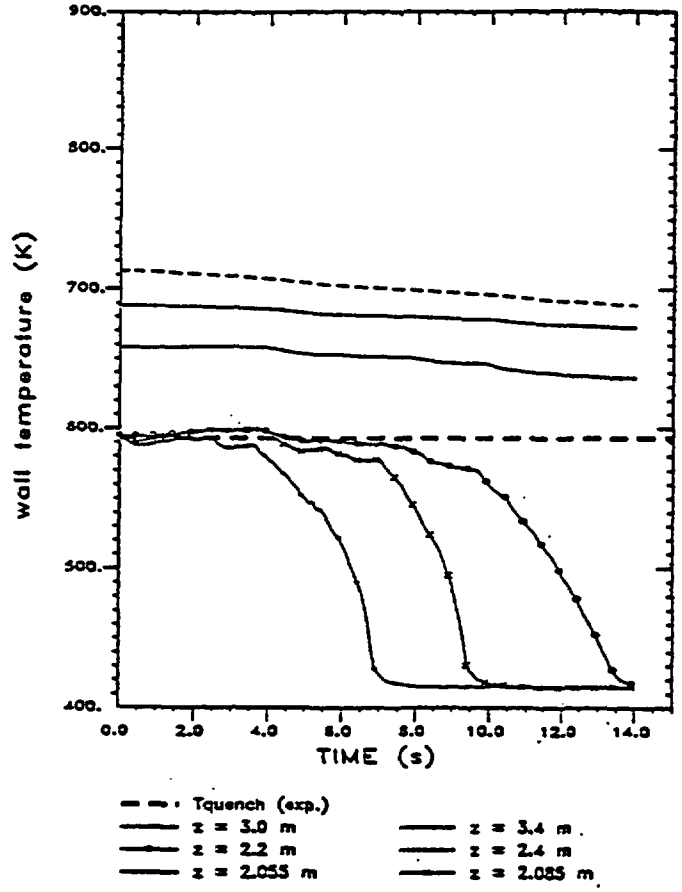


Figure 37: Wall temperatures at various elevations for test 3053 calculated by RELAP5/MOD2.5.

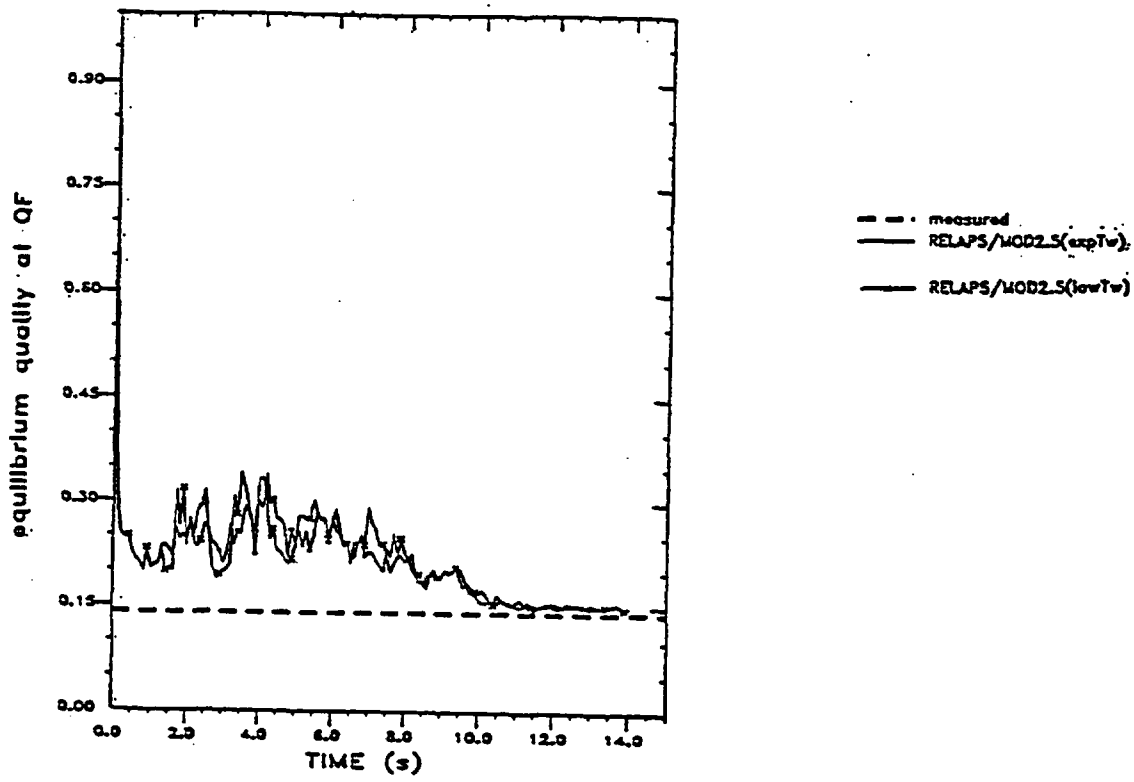


Figure 38: Equilibrium quality at the QF for the two different initial axial wall temperature profiles.

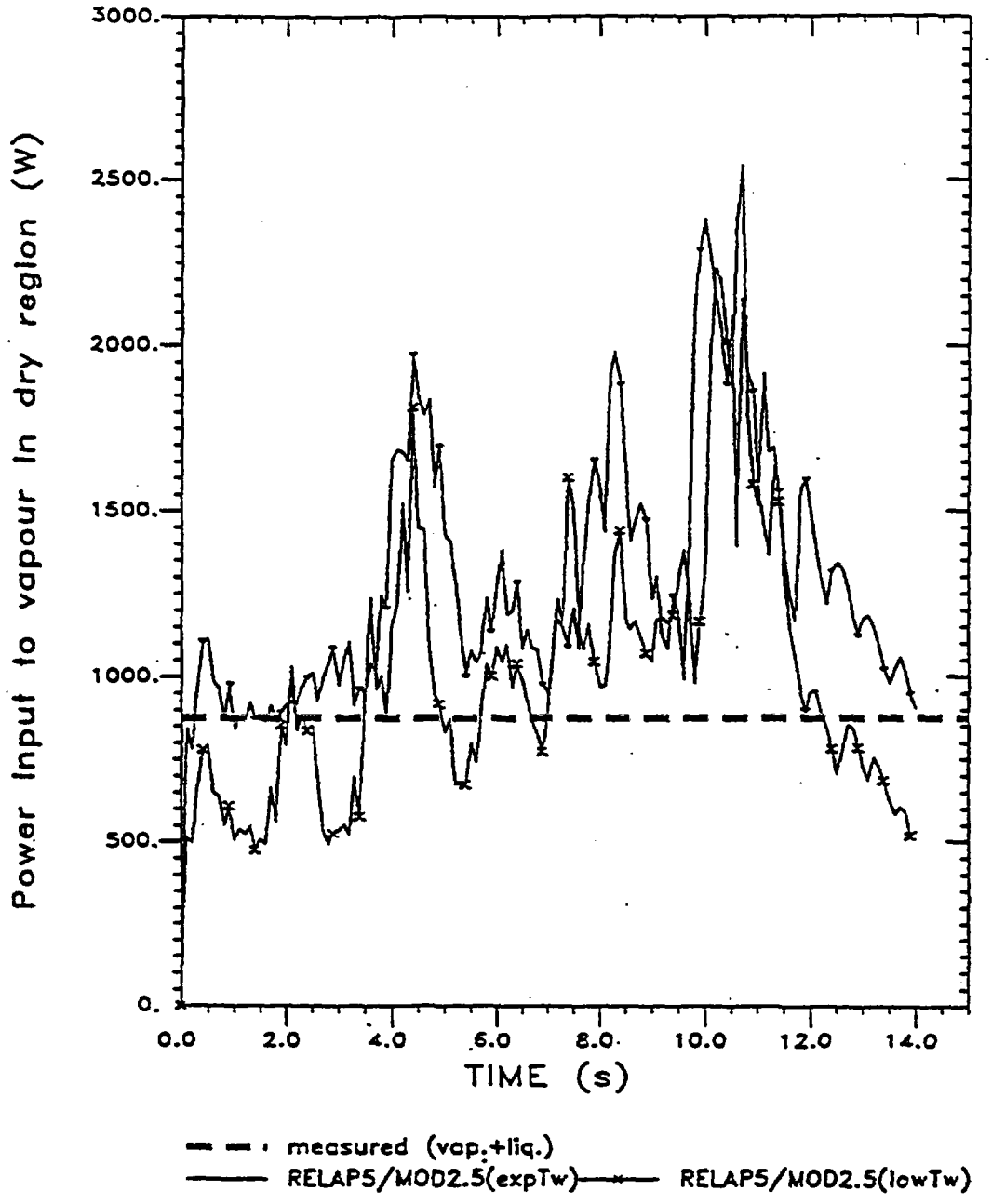


Figure 39: Heat transfer rate from wall to vapour in the post-dryout region for the two initial wall temperature distributions.

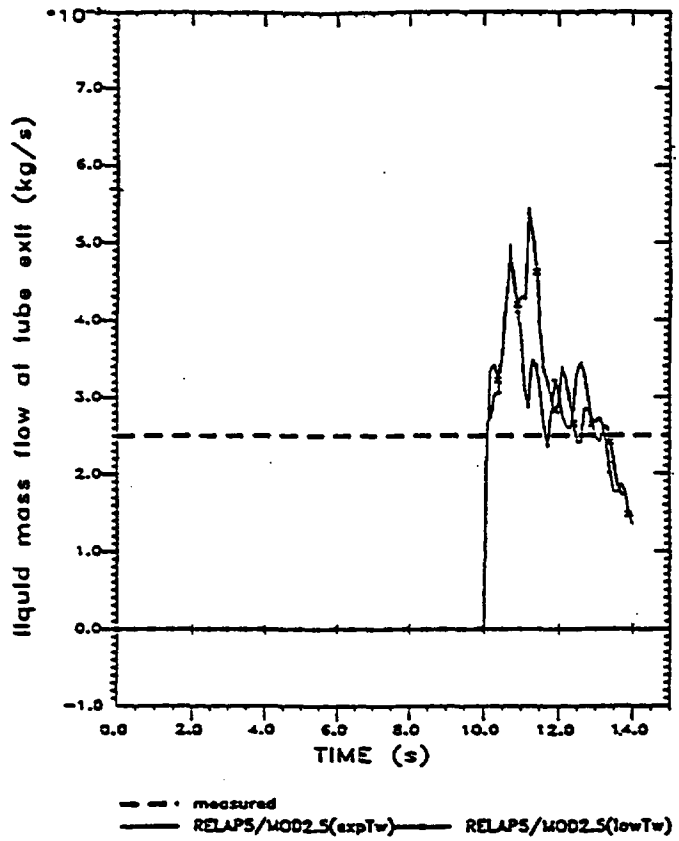


Figure 40: Liquid carry-out for the two initial axial wall temperature distributions.

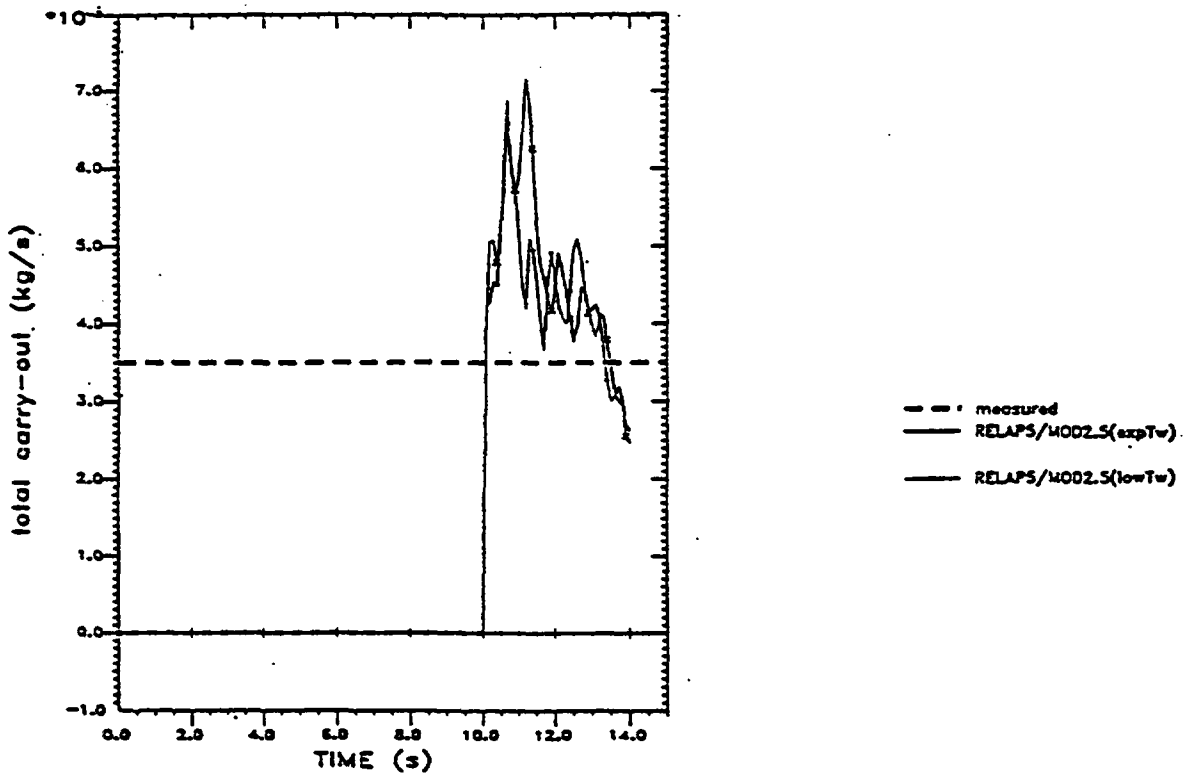


Figure 41: Total mass flow at the tube exit for the two initial axial wall temperature distributions.

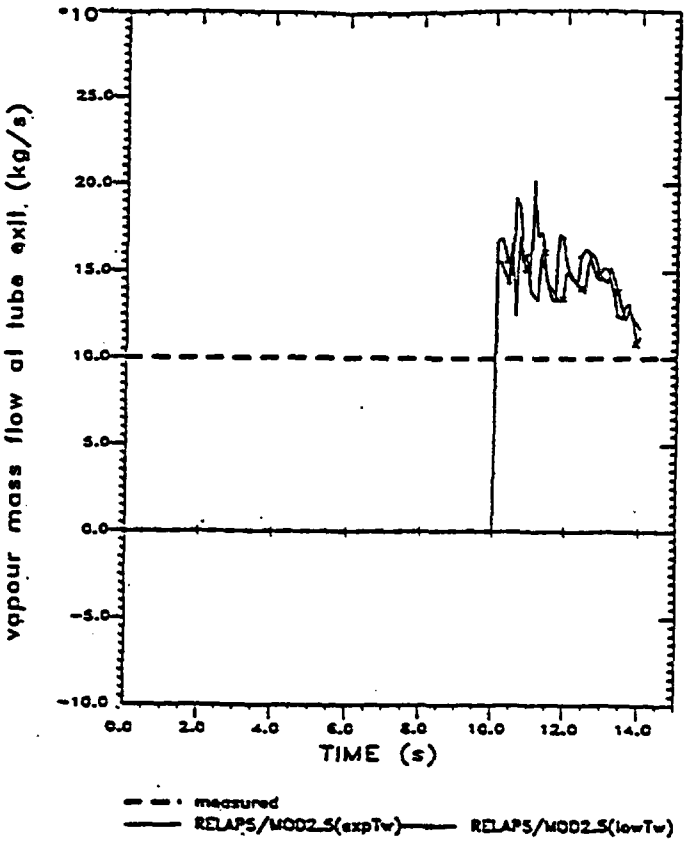


Figure 42: Vapour carry-out for the two initial axial wall temperature distributions.

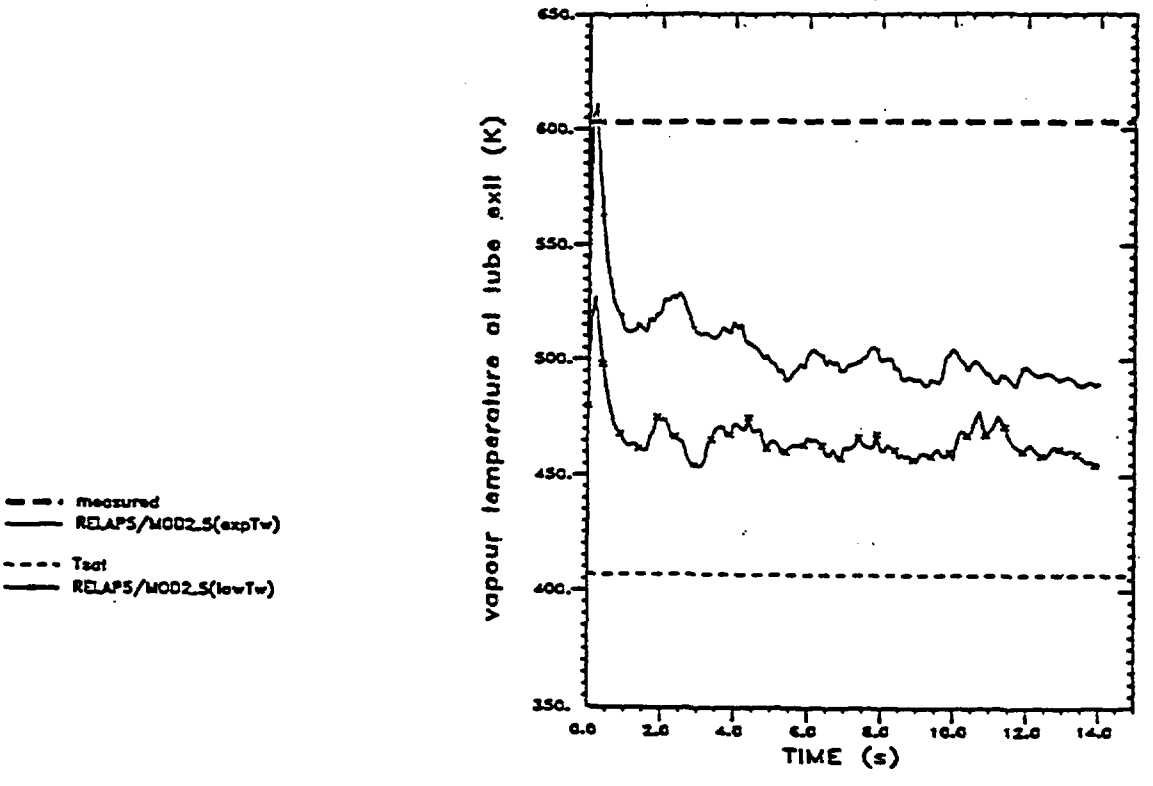


Figure 43: Vapour temperature at the tube exit calculated by RELAP5/MOD2.5 for the two initial wall temperature distributions.

# APPENDIX 1

## Input decks for transient calculations

# Appendix IA

## RELAP5/Mod 2.5 input deck

```
= UCB351
*
* UNIV. OF CALIFORNIA BERKELEY (UCB) TEST
*********************************************************************
* REFLOOD TEST IN SINGLE TUBE GEOMETRY
* UCB-3051: P=2 BAR, G=25.1 KG/M**2/S
*
* input : power and heat losses
*
* RELAP5/MOD3 calculation
*********************************************************************
*
00000100  new       transnt
00000101  run
*                           cpu-lim
00000105  1.0       2.0     3580.
*
*     TIME STEP CONTROL CARDS                          * REQUIRED
*         END TIME   MIN DT   MAX DT   OPTN   MNR   MJR  RST
00000201   10.       1.0-9    0.001    3      100   4000 4000
00000202   1000.     1.0-19   0.01     3      100   4000 4000
*
*$*$*$*$*$*$*$*$*$*$*$*$*$*$*$*$*$*$*$*$*$*$*$*$*$*$*$*$*$*$*$*$*$*$*
*
*                     MINOR EDIT REQUESTS
*
*$*$*$*$*$*$*$*$*$*$*$*$*$*$*$*$*$*$*$*$*$*$*$*$*$*$*$*$*$*$*$*$*$*$*
*
00000301  cputime   0
*
00000302  voidg     120010000
00000303  voidg     120020000
00000304  tempf     120010000
00000305  tempg     120010000
00000306  tempf     120020000
00000307  tempg     120020000
00000308  p         120010000
00000309  p         120020000
00000310  voidg     120120000
00000311  voidg     120130000
00000312  voidg     120140000
00000313  voidg     120150000
00000314  voidg     120170000
00000315  voidg     120190000
*
00000319  tempg     120190000
*
00000340  mflowj    125000000
*
00000342  cntrlvar  103
*
00000343  cntrlvar  112
00000344  cntrlvar  113
00000345  cntrlvar  114
00000346  cntrlvar  115
00000349  cntrlvar  122
00000350  cntrlvar  118
00000351  cntrlvar  119
*
00000363  cntrlvar  140
00000364  cntrlvar  141
00000365  cntrlvar  142
00000366  cntrlvar  143
*
00000370  cntrlvar  150
00000371  cntrlvar  151
00000372  cntrlvar  152
00000373  cntrlvar  161
00000374  cntrlvar  162
00000376  cntrlvar  169
*
```

```
00000380  floreg    120040000
00000381  floreg    120070000
00000382  floreg    120100000
00000383  floreg    120130000
00000386  floreg    120160000
00000388  floreg    120180000
*
00000390  httemp    120000401
00000391  httemp    120000701
00000392  httemp    120001001
00000393  httemp    120001301
00000394  httemp    120001601
00000395  httemp    120001801
*
*00000399  ztrwt     1200000
*
*$*$*$*$*$*$*$*$*$*$*$*$*$*$*$*$*$*$*$*$*$*$*$*$*$*$*$*$*$*$*$*$*$*$*$*$*
*
*                    TRIP COMPONENTS
*
*$*$*$*$*$*$*$*$*$*$*$*$*$*$*$*$*$*$*$*$*$*$*$*$*$*$*$*$*$*$*$*$*$*$*$*$*
*
500    time   0           gt   null    0.    600.    1 * end
*
502    time   0           gt   null    0.   0.       1 * start injection
*                                                      and reflood
600           500
*
*$*$*$*$*$*$*$*$*$*$*$*$*$*$*$*$*$*$*$*$*$*$*$*$*$*$*$*$*$*$*$*$*$*$*$*$*
*
*                    HYDRODYNAMIC COMPONENTS
*
*$*$*$*$*$*$*$*$*$*$*$*$*$*$*$*$*$*$*$*$*$*$*$*$*$*$*$*$*$*$*$*$*$*$*$*$*
*
*---- ----1---- ----1---- ----1---- ----1---- ----1---- ----1---- ----1-
* [105] feedwater tank - inlet thermodynamic conditions
*---- ----1---- ----1---- ----1---- ----1---- ----1---- ----1---- ----1-
1050000   'feedtan' tmdpvol
1050101   0.00015935  0.    1000.     0.  0.  0.  0.  0.  0
1050200   103        * i.c.:   p,T; subcooled water
1050201   0.         2.5e5    311.15
*---- ----1---- ----1---- ----1---- ----1---- ----1---- ----1---- ----1-
* [110] inlet junction - flow boundary conditions
*---- ----1---- ----1---- ----1---- ----1---- ----1---- ----1---- ----1-
1100000   'feedjun' tmdpjun
1100101   105000000 120000000 0.
1100200   1          502
1100201   0.         0.004007        0.000       0. *mcell=G*Acell
*---- ----1---- ----1---- ----1---- ----1---- ----1---- ----1---- ----1-
* [120] tube
*---- ----1---- ----1---- ----1---- ----1---- ----1---- ----1---- ----1-
1200000   'testsec'           pipe
1200001   19
1200101   0.00015935 19 * Avcell
1200201   0.         18 * Ajunct
1200301   0.1         1 * cell length dz
1200302   0.2        18 *
1200303   0.16       19
1200401   0.         19 * cell volume=dz*Avcell
1200501   0.         19 * hor. angle
1200601   90.        19 * vert. angle
1200701   0.1         1 * cell dz
1200702   0.2        18 *
1200703   0.16       19 *
1200801   1.-4      0.01425 19 * friction data
1200901   0.        0.      18 * loss coefficients
*1201002   100       11          * bundle correlation on
1201002   0         19          * tube correlation on
1201101   00000     18
1201201   3         2.00+5      812.        0. 0. 0.   19 * initial
*                                                       * conditions
```

```
*
1201300   1
1201301   0.              0.0           0.       18 * mass flows
*---- ----1---- ----1---- ----1---- ----1---- ----1---- ----1---- ----1-
* [125] outlet junction
*---- ----1---- ----1---- ----1---- ----1---- ----1---- ----1---- ----1-
1250000   'outljun' sngljun
1250101   120010000 130000000 0.         0.0        0.0       00000
1250201   1         0.        0.00       0.0
*---- ----1---- ----1---- ----1---- ----1---- ----1---- ----1---- ----1-
* [130] outlet tank
*---- ----1---- ----1---- ----1---- ----1---- ----1---- ----1---- ----1-
1300000   'outltan' tmdpvol
1300101   .01       0.     1000.     0.  0.  0.  0.  0.  0
1300200   003
1300201   0.        2.0+5     812.
*
*$*$*$*$*$*$*$*$*$*$*$*$*$*$*$*$*$*$*$*$*$*$*$*$*$*$*$*$*$*$*$*$*$*$*
*
*                    HEAT STRUCTURES
*
*$*$*$*$*$*$*$*$*$*$*$*$*$*$*$*$*$*$*$*$*$*$*$*$*$*$*$*$*$*$*$*$*$*$*
*
**---- ----1---- ----1---- ----1---- ----1---- ----1---- ----1---- ----1-*
** [1200] test section(tube)
**---- ----1---- ----1---- ----1---- ----1---- ----1---- ----1---- ----1-*
11200000  19        10          2          0          0.007125  502 0  32
11200100  0         1
11200101  9         0.00795 * outer tube radius
11200201  1         9
11200301  1.        9
11200400  0
11200401  812.      10 * temperatures of the nodes
11200501  120010000  0          1          1          0.1       1 * inner
11200502  120020000  10000      1          1          0.2      18 * surface
11200503  120190000  0          1          1          0.16     19 *
11200601  -120       0       4110          1          0.1       1 * outer
11200602  -120       0       4110          1          0.2      18 * surface
11200603  -120       0       4110          1          0.16     19 *
11200701    150          0.0273224   0.  0.       01 *  power distribution
11200702    150          0.0546448   0.  0.       18 *
11200703    150          0.0437158   0.  0.       19 *
*11200801  0         0.          0.          0.              19 * M2
11200801  0.        11.         11.        0. 0. 0. 0.  1. 19 * M3
*---- ----1---- ----1---- ----1---- ----1---- ----1---- ----1---- ----1-*
*
*$*$*$*$*$*$*$*$*$*$*$*$*$*$*$*$*$*$*$*$*$*$*$*$*$*$*$*$*$*$*$*$*$*$*
*
*                    CONTROL VARIABLES
*
*$*$*$*$*$*$*$*$*$*$*$*$*$*$*$*$*$*$*$*$*$*$*$*$*$*$*$*$*$*$*$*$*$*$*
*
*---- ----1---- ----1---- ----1---- ----1---- ----1---- ----1---- ----1-
* cv 103: collapsed liquid level in the test section (m)
*---- ----1---- ----1---- ----1---- ----1---- ----1---- ----1---- ----1-
*
20510300  collev    sum       1.        0.       1
20510301  0.
20510302  0.1       voidf     120010000
20510303  0.2       voidf     120020000
20510304  0.2       voidf     120030000
20510305  0.2       voidf     120040000
20510306  0.2       voidf     120050000
20510307  0.2       voidf     120060000
20510308  0.2       voidf     120070000
20510309  0.2       voidf     120080000
20510310  0.2       voidf     120090000
20510311  0.2       voidf     120100000
20510312  0.2       voidf     120110000
20510313  0.2       voidf     120120000
20510314  0.2       voidf     120130000
```

```
20510315  0.2       voidf     120140000
20510316  0.2       voidf     120150000
20510317  0.2       voidf     120160000
20510318  0.2       voidf     120170000
20510319  0.2       voidf     120180000
20510320  0.16      voidf     120190000
*
*---- ----1---- ----1---- ----1---- ----1---- ----1---- ----1---- ----1-
* cv 112: vapour mass flow from the test section (kg/s)
*---- ----1---- ----1---- ----1---- ----1---- ----1---- ----1---- ----1-
*
20511200  entgfl    mult      0.00015935          0.        0
20511201  rhogj     125000000
20511202  velgj     125000000
20511203  voidgj    125000000
*
*---- ----1---- ----1---- ----1---- ----1---- ----1---- ----1---- ----1-
* cv 113: liquid mass flow from the test section (kg/s)
*---- ----1---- ----1---- ----1---- ----1---- ----1---- ----1---- ----1-
*
20511300  entffl    mult      0.00015935          0.        0
20511301  rhofj     125000000
20511302  velfj     125000000
20511303  voidfj    125000000
*
*---- ----1---- ----1---- ----1---- ----1---- ----1---- ----1---- ----1-
* cv 114: total mass flow out of the test section  (kg/s)
*---- ----1---- ----1---- ----1---- ----1---- ----1---- ----1---- ----1-
*
20511400  entflow   sum       1.        1.       0
20511401  0.
20511402  1.        cntrlvar  112
20511403  1.        cntrlvar  113
*
*---- ----1---- ----1---- ----1---- ----1---- ----1---- ----1---- ----1-
* cv 115: quality at the tube exit
*---- ----1---- ----1---- ----1---- ----1---- ----1---- ----1---- ----1-
*
20511500  exitqual  div       1.         1.        0
20511501  cntrlvar  114       cntrlvar   112
*
*---- ----1---- ----1---- ----1---- ----1---- ----1---- ----1---- ----1-
* cv 118: integral of mass flow at tube exit (kg) (R5 var.)
*---- ----1---- ----1---- ----1---- ----1---- ----1---- ----1---- ----1-
*
20511800  intwgext  integral  1.        0.        0
20511801  mflowj    125000000
*
*---- ----1---- ----1---- ----1---- ----1---- ----1---- ----1---- ----1-
* cv 119: integral of mass flow at tube exit (kg) (cntrlvar)
*---- ----1---- ----1---- ----1---- ----1---- ----1---- ----1---- ----1-
*
20511900  intwgext   integral 1.         0.        0
20511901  cntrlvar   114
*
*---- ----1---- ----1---- ----1---- ----1---- ----1---- ----1---- ----1-
* cv 122: mass of water accumulated (kg)
*---- ----1---- ----1---- ----1---- ----1---- ----1---- ----1---- ----1-
*
20512200  accwater  sum     0.00015935  0.        0
20512201  0.
20512202  0.1     rho       120010000
20512203  0.2     rho       120020000
20512204  0.2     rho       120030000
20512205  0.2     rho       120040000
20512206  0.2     rho       120050000
20512207  0.2     rho       120060000
20512208  0.2     rho       120070000
20512209  0.2     rho       120080000
20512210  0.2     rho       120090000
20512211  0.2     rho       120100000
```

```
20512212  0.2     rho       120110000
20512213  0.2     rho       120120000
20512214  0.2     rho       120130000
20512215  0.2     rho       120140000
20512216  0.2     rho       120150000
20512217  0.2     rho       120160000
20512218  0.2     rho       120170000
20512219  0.2     rho       120180000
20512220  0.16    rho       120190000
*
*---- ----1---- ----1---- ----1---- ----1---- ----1---- ----1---- ----1-
* cv 140: integral of vapour mass flow at tube exit (kg)
*---- ----1---- ----1---- ----1---- ----1---- ----1---- ----1---- ----1-
*
20514000  intwgext   integral  1.          0.       0
20514001  cntrlvar   112
*
*---- ----1---- ----1---- ----1---- ----1---- ----1---- ----1---- ----1-
* cv 141: integral of liquid mass flow at tube exit (kg)
*---- ----1---- ----1---- ----1---- ----1---- ----1---- ----1---- ----1-
*
20514100  intwfext   integral  1.          0.       0
20514101  cntrlvar   113
*
*---- ----1---- ----1---- ----1---- ----1---- ----1---- ----1---- ----1-
* cv 142: sum of total mass accumulated and expelled (kg)
*---- ----1---- ----1---- ----1---- ----1---- ----1---- ----1---- ----1-
*
20514200  masstot    sum       1.        0.        0
20514201  0.
20514202  1.        cntrlvar  140
20514203  1.        cntrlvar  141
20514204  1.        cntrlvar  122
*
*---- ----1---- ----1---- ----1---- ----1---- ----1---- ----1---- ----1-
* cv 143: integral of liquid mass flow at tube inlet (kg)
*---- ----1---- ----1---- ----1---- ----1---- ----1---- ----1---- ----1-
*
20514300  intwfin  integral   1.          0.       0
20514301  mflowj   110000000
*
*---- ----1---- ----1---- ----1---- ----1---- ----1---- ----1---- ----1-
* cv 150: power input to wet portion of test section
*---- ----1---- ----1---- ----1---- ----1---- ----1---- ----1---- ----1-
*
20515000  qinwet    sum     1.          0.        1
20515001  0.
20515002  1.        q       120010000
20515003  1.        q       120020000
20515004  1.        q       120030000
20515005  1.        q       120040000
20515006  1.        q       120050000
20515007  1.        q       120060000
20515008  1.        q       120070000
20515009  1.        q       120080000
20515010  1.        q       120090000
20515011  1.        q       120100000
*
*---- ----1---- ----1---- ----1---- ----1---- ----1---- ----1---- ----1-
* cv 151: power input to dry portion of test section
*---- ----1---- ----1---- ----1---- ----1---- ----1---- ----1---- ----1-
*
20515100  qindry    sum     1.          0.        1         2    2000.
20515101  0.
20515102  1.        q       120110000
20515103  1.        q       120120000
20515104  1.        q       120130000
20515105  1.        q       120140000
20515106  1.        q       120150000
```

```
20515107  1.        q       120160000
20515108  1.        q       120170000
20515109  1.        q       120180000
20515110  1.        q       120190000
*
*---- ----1---- ----1---- ----1---- ----1---- ----1---- ----1---- ----1-
* cv 152: total power input to fluid in test section
*---- ----1---- ----1---- ----1---- ----1---- ----1---- ----1---- ----1-
*
20515200  qindry    sum      1.          0.        1
20515201  0.
20515202  1.        cntrlvar 150
20515203  1.        cntrlvar 151
*
*---- ----1---- ----1---- ----1---- ----1---- ----1---- ----1---- ----1-
* cv 161: power input above 2.4 m
*---- ----1---- ----1---- ----1---- ----1---- ----1---- ----1---- ----1-
*
20516100  qindry24  sum      1.          0.        1         2    2000.
20516101  0.
20516102  1.        q       120140000
20516103  1.        q       120150000
20516104  1.        q       120160000
20516105  1.        q       120170000
20516106  1.        q       120180000
20516107  1.        q       120190000
*
*---- ----1---- ----1---- ----1---- ----1---- ----1---- ----1---- ----1-
* cv 162: power input to vapour above 2.4 m
*---- ----1---- ----1---- ----1---- ----1---- ----1---- ----1---- ----1-
*
20516200  qvap24    sum      1.          0.        1         2    2000.
20516201  0.
20516202  1.        qwg      120140000
20516203  1.        qwg      120150000
20516204  1.        qwg      120160000
20516205  1.        qwg      120170000
20516206  1.        qwg      120180000
20516207  1.        qwg      120190000
*
*---- ----1---- ----1---- ----1---- ----1---- ----1---- ----1---- ----1-
* cv 169: heat transfer to vapour only in the dry region
*---- ----1---- ----1---- ----1---- ----1---- ----1---- ----1---- ----1-
*
20516900  qdryvap   sum      1.          0.        1
20516901  0.
20516902  1.        qwg      120110000
20516903  1.        qwg      120120000
20516904  1.        qwg      120130000
20516905  1.        qwg      120140000
20516906  1.        qwg      120150000
20516907  1.        qwg      120160000
20516908  1.        qwg      120170000
20516909  1.        qwg      120180000
20516910  1.        qwg      120190000
*
*$*$*$*$*$*$*$*$*$*$*$*$*$*$*$*$*$*$*$*$*$*$*$*$*$*$*$*$*$*$*$*$*$*$*
*   GENERAL TABLES
*$*$*$*$*$*$*$*$*$*$*$*$*$*$*$*$*$*$*$*$*$*$*$*$*$*$*$*$*$*$*$*$*$*$*
*
*---- ----1---- ----1---- ----1---- ----1---- ----1---- ----1----
* tab 110: heat losses
*---- ----1---- ----1---- ----1---- ----1---- ----1---- ----1----
*
20211000 htc-temp
20211001 300.   12.13582
20211002 350.   13.81509
20211003 400.   15.72673
20211004 425.   16.77957
20211005 450.   17.90288
```

```
20211006 475.   19.10140
20211007 500.   20.38016
20211008 520.   21.46453
20211009 540.   22.60660
20211010 560.   23.80943
20211011 580.   25.07626
20211012 600.   26.41051
20211013 620.   27.81574
20211014 630.   28.54614
20211015 640.   29.29573
20211016 650.   30.06500
20211017 660.   30.85448
20211018 670.   31.66468
20211019 680.   32.49616
20211020 690.   33.34947
20211021 700.   34.22519
20211022 710.   35.12390
20211023 720.   36.04622
20211024 730.   36.99275
20211025 740.   37.96413
20211026 750.   38.96103
20211027 760.   39.98410
20211028 770.   41.03404
20211029 780.   42.11154
20211030 790.   43.21734
20211031 800.   44.35218
20211032 810.   45.51682
20211033 820.   46.71204
20211034 830.   47.93864
20211035 840.   49.19745
20211036 850.   50.48932
20211037 860.   51.81511
20211038 870.   53.17572
20211039 880.   54.57205
20211040 890.   56.00505
20211041 900.   57.47568
20211042 910.   58.98492
20211043 920.   60.53380
20211044 930.   62.12335
20211045 940.   63.75463
20211046 950.   65.42876
20211047 960.   67.14684
20211048 970.   68.91004
20211049 980.   70.71953
20211050 990.   72.57655
20211051 1000.  74.48233
20211052 1010.  76.43815
20211053 1020.  78.44532
20211054 1030.  80.50520
20211055 1040.  82.61918
20211056 1050.  84.78866
20211057 1060.  87.01512
20211058 1070.  89.30003
20211059 1080.  91.64495
20211060 1090.  94.05144
20211061 1100.  96.52112
*
*---- ----1---- ----1---- ----1---- ----1---- ----1---- ----1----
* tab 120 ambient temperature
*---- ----1---- ----1---- ----1---- ----1---- ----1---- ----1----
*
20212000 temp
20212001 0.      294.26
20212002 1000.   294.26
*
```

```
*---- ----1---- ----1---- ----1---- ----1---- ----1---- ----1----
* tab 150 test section power
*---- ----1---- ----1---- ----1---- ----1---- ----1---- ----1----
*
20215000  power
20215001  0.       4326.
20215002  1000.    4326.
*
*$*$*$*$*$*$*$*$*$*$*$*$*$*$*$*$*$*$*$*$*$*$*$*$*$*$*$*$*$*$*$*$*
*
*   $$$$$$$$$$      HEAT STRUCTURE THERMAL PROPERTY DATA
*
* (s-steel and inconnel 600 from Bethsy, copper from TM-IN-816)
*
*$*$*$*$*$*$*$*$*$*$*$*$*$*$*$*$*$*$*$*$*$*$*$*$*$*$*$*$*$*$*$*$*
*
*---- ----1---- ----1---- ----1---- ----1---- ----1---- ----1----
20100100  tbl/fctn  1         1         * INCONEL-600
*---- ----1---- ----1---- ----1---- ----1---- ----1---- ----1----
*
*---- ----1---- ----1---- ----1---- ----1---- ----1---- ----1----
* INCONEL-600 - thermal conductivity    (W/m-K)    [tp002]
*---- ----1---- ----1---- ----1---- ----1---- ----1---- ----1----
20100101  0.        14.       294.0     14.8      * 1st - artiff.
20100102  373.0     15.7
20100103  473.0     17.3
20100104  573.0     18.9
20100105  673.0     20.6
20100106  773.0     22.2
20100107  873.0     23.8
20100108  973.0     25.7
20100109  1073.0    27.4
20100110  1173.0    29.3
20100111  1273.0    31.0
20100112  1373.0    32.7
20100113  1473.0    34.4
20100114  1573.0    36.1
*---- ----1---- ----1---- ----1---- ----1---- ----1---- ----1----
* INCONEL-600 - volumetric heat capacity     (J/m3-K)
*---- ----1---- ----1---- ----1---- ----1---- ----1---- ----1----
20100151  0.        3.7+6     294.0     3.740+6   * 1st - artiff.
20100152  373.0     3.900+6
20100153  473.0     4.060+6
20100154  573.0     4.180+6
20100155  673.0     4.330+6
20100156  773.0     4.510+6
20100157  873.0     4.650+6
20100158  973.0     4.830+6
20100159  1073.0    5.020+6
20100160  1173.0    5.200+6
20100161  1273.0    5.340+6
20100162  1373.0    5.630+6
20100163  1477.0    5.810+6
. *** END ***
```

# Appendix IB

# RELAP5/Mod 3 input deck

```
= UCB351
*
* UNIV. OF CALIFORNIA BERKELEY (UCB) TEST
*************************************************************************
* REFLOOD TEST IN SINGLE TUBE GEOMETRY
* UCB-3051: P=2 BAR, G=25.1 KG/M**2/S
*
* input : power and heat losses
*
* RELAP5/MOD2.5 calculation
* for RELAP5/MOD3 only the card nr. 11200801 has to be changed
*************************************************************************
*
00000100  new       transnt
00000101  run
*                           cpu-lim
00000105  1.0       2.0     3560.
*
*     TIME STEP CONTROL CARDS                          * REQUIRED
*         END TIME   MIN DT    MAX DT    OPTN   MNR    MJR  RST
00000201   10.       1.0-7     0.001     3      100    4000 4000
00000202   1000.     1.0-19    0.05      3      40     2000 2000
*
*$*$*$*$*$*$*$*$*$*$*$*$*$*$*$*$*$*$*$*$*$*$*$*$*$*$*$*$*$*$*$*$*$*$*$*
*
*                     MINOR EDIT REQUESTS
*
*$*$*$*$*$*$*$*$*$*$*$*$*$*$*$*$*$*$*$*$*$*$*$*$*$*$*$*$*$*$*$*$*$*$*$*
*
00000301  cputime   0
*
00000302  voidg     120070000
00000303  voidg     120130000
00000304  voidg     120190000
00000305  voidg     120250000
00000306  voidg     120310000
00000307  voidg     120340000
*
00000309  voidg     120160000
00000310  rhog      120160000
00000311  voidf     120160000
00000312  rhof      120160000
00000313  rho       120160000
*
00000319  tempg     120360000
*
00000340  mflowj    125000000
*
00000342  cntrlvar  103
*
00000343  cntrlvar  112
00000344  cntrlvar  113
00000345  cntrlvar  114
00000346  cntrlvar  115
00000347  cntrlvar  120
00000348  cntrlvar  121
00000349  cntrlvar  122
00000350  cntrlvar  118
00000351  cntrlvar  119
*
00000363  cntrlvar  140
00000364  cntrlvar  141
00000365  cntrlvar  142
00000366  cntrlvar  143
*
00000380  floreg    120070000
00000381  floreg    120130000
00000382  floreg    120190000
00000383  floreg    120250000
```

```
00000384  floreg    120310000
00000385  floreg    120340000
*
00000390  httemp    120000701
00000391  httemp    120001301
00000392  httemp    120001901
00000393  httemp    120002501
00000394  httemp    120003101
00000395  httemp    120003401
*
*00000399  ztrwt     1200000
*
*$*$*$*$*$*$*$*$*$*$*$*$*$*$*$*$*$*$*$*$*$*$*$*$*$*$*$*$*$*$*$*$*$*$*$*$*$*
*
*                    TRIP COMPONENTS
*
*$*$*$*$*$*$*$*$*$*$*$*$*$*$*$*$*$*$*$*$*$*$*$*$*$*$*$*$*$*$*$*$*$*$*$*$*$*
*
500    time   0           gt    null    0.    600.    1 * end
*
502    time   0           gt    null    0.    0.      1 * start injection
*                                                      and reflood
600           500
*
*$*$*$*$*$*$*$*$*$*$*$*$*$*$*$*$*$*$*$*$*$*$*$*$*$*$*$*$*$*$*$*$*$*$*$*$*$*
*
*                    HYDRODYNAMIC COMPONENTS
*
*$*$*$*$*$*$*$*$*$*$*$*$*$*$*$*$*$*$*$*$*$*$*$*$*$*$*$*$*$*$*$*$*$*$*$*$*$*
*
*---- ----1---- ----1---- ----1---- ----1---- ----1---- ----1---- ----1-
* [105] feedwater tank - inlet thermodynamic conditions
*---- ----1---- ----1---- ----1---- ----1---- ----1---- ----1---- ----1-
1050000   'feedtan' tmdpvol
1050101   0.00015935  0.    1000.     0.  0.  0.  0.  0.  0
1050200   103        * i.c.:   p,T; subcooled water
1050201   0.         2.5e5    311.15
*---- ----1---- ----1---- ----1---- ----1---- ----1---- ----1---- ----1-
* [110] inlet junction - flow boundary conditions
*---- ----1---- ----1---- ----1---- ----1---- ----1---- ----1---- ----1-
1100000   'feedjun' tmdpjun
1100101   105000000 120000000 0.
1100200   1          502
1100201   0.         0.004007        0.000       0. *mcell=G*Acell
*---- ----1---- ----1---- ----1---- ----1---- ----1---- ----1---- ----1-
* [120] tube
*---- ----1---- ----1---- ----1---- ----1---- ----1---- ----1---- ----1-
1200000   'testsec'            pipe
1200001   36
1200101   0.00015935 36 * Avcell
1200201   0.          35 * Ajunct
1200301   0.1          1 * cell length dz
1200302   0.1         35 *
1200303   0.16        36
1200401   0.          36 * cell volume=dz*Avcell
1200501   0.          36 * hor. angle
1200601   90.         36 * vert. angle
1200701   0.1          1 * cell dz
1200702   0.1         35 *
1200703   0.16        36 *
1200801   1.-4       0.01425 36 * friction data
1200901   0.         0.      35 * loss coefficients
*1201002   100        11         * bundle correlation on
1201002   0          36         * tube correlation on
1201101   00000      35
1201201   3          2.00+5      812.        0. 0. 0.    36 * initial
*                                                          * conditions
```

```
*
1201300   1
1201301   0.              0.0           0.       35 * mass flows
*---- ----1---- ----1---- ----1---- ----1---- ----1---- ----1---- ----1-
* [125] outlet junction
*---- ----1---- ----1---- ----1---- ----1---- ----1---- ----1---- ----1-
1250000   'outljun' snglju
1250101   120010000 130000000 0.        0.0       0.0       00000
1250201   1         0.        0.00      0.0
*---- ----1---- ----1---- ----1---- ----1---- ----1---- ----1---- ----1-
* [130] outlet tank
*---- ----1---- ----1---- ----1---- ----1---- ----1---- ----1---- ----1-
1300000   'outltan' tmdpvol
1300101   .01       0.    1000.     0.  0.  0.  0.  0.  0
1300200   003
1300201   0.        2.0+5     812.
*
*$*$*$*$*$*$*$*$*$*$*$*$*$*$*$*$*$*$*$*$*$*$*$*$*$*$*$*$*$*$*$*$*$*$*$*
*
*                    HEAT STRUCTURES
*
*$*$*$*$*$*$*$*$*$*$*$*$*$*$*$*$*$*$*$*$*$*$*$*$*$*$*$*$*$*$*$*$*$*$*$*
*
**---- ----1---- ----1---- ----1---- ----1---- ----1---- ----1---- ----1-*
** [1200] test section(tube)
**---- ----1---- ----1---- ----1---- ----1---- ----1---- ----1---- ----1-*
11200000  36        10          2          0          0.007125  502 0  16
11200100  0         1
11200101  9         0.00795 * outer tube radius
11200201  1         9
11200301  1.        9
11200400  0
11200401  812.      10 * temperatures of the nodes
11200501  120010000  0           1          1          0.1       1 * inner
11200502  120020000  10000       1          1          0.1      35 * surface
11200503  120190000  0           1          1          0.16     36 *
11200601  -120       0        4110          1          0.1       1 * outer
11200602  -120       0        4110          1          0.1      35 * surface
11200603  -120       0        4110          1          0.16     36 *
11200701    150           0.0273224   0.  0.        01 *  power distribution
11200702    150           0.0273224   0.  0.        35 *
11200703    150           0.0437158   0.  0.        36 *
11200801  0         0.          0.        0.                36 * M2
*11200801  0.        11.         11.        0. 0. 0. 0.  1. 18 * M3
*---- ----1---- ----1---- ----1---- ----1---- ----1---- ----1---- ----1-*
*
*$*$*$*$*$*$*$*$*$*$*$*$*$*$*$*$*$*$*$*$*$*$*$*$*$*$*$*$*$*$*$*$*$*$*$*
*
*                    CONTROL VARIABLES
*
*$*$*$*$*$*$*$*$*$*$*$*$*$*$*$*$*$*$*$*$*$*$*$*$*$*$*$*$*$*$*$*$*$*$*$*
*
*---- ----1---- ----1---- ----1---- ----1---- ----1---- ----1---- ----1-
* cv 101: collapsed liquid level in the test section  (lower part)
*---- ----1---- ----1---- ----1---- ----1---- ----1---- ----1---- ----1-
*
20510100  collevl   sum       1.        0.        1
20510101  0.
20510102  0.1     voidf     120010000
20510103  0.1     voidf     120020000
20510104  0.1     voidf     120030000
20510105  0.1     voidf     120040000
20510106  0.1     voidf     120050000
20510107  0.1     voidf     120060000
20510108  0.1     voidf     120070000
20510109  0.1     voidf     120080000
20510110  0.1     voidf     120090000
20510111  0.1     voidf     120100000
20510112  0.1     voidf     120110000
20510113  0.1     voidf     120120000
20510114  0.1     voidf     120130000
```

```
20510115  0.1     voidf     120140000
20510116  0.1     voidf     120150000
20510117  0.1     voidf     120160000
20510118  0.1     voidf     120170000
20510119  0.1     voidf     120180000
*
*---- ----1---- ----1---- ----1---- ----1---- ----1---- ----1---- ----1-
* cv 102: collapsed liquid level in the test section  (upper part)
*---- ----1---- ----1---- ----1---- ----1---- ----1---- ----1---- ----1-
*
20510200  collevu   sum       1.        0.        1
20510201  0.
20510202  0.1     voidf     120190000
20510203  0.1     voidf     120200000
20510204  0.1     voidf     120210000
20510205  0.1     voidf     120220000
20510206  0.1     voidf     120230000
20510207  0.1     voidf     120240000
20510208  0.1     voidf     120250000
20510209  0.1     voidf     120260000
20510210  0.1     voidf     120270000
20510211  0.1     voidf     120280000
20510212  0.1     voidf     120290000
20510213  0.1     voidf     120300000
20510214  0.1     voidf     120310000
20510215  0.1     voidf     120320000
20510216  0.1     voidf     120330000
20510217  0.1     voidf     120340000
20510218  0.1     voidf     120350000
20510219  0.16    voidf     120360000
*
*---- ----1---- ----1---- ----1---- ----1---- ----1---- ----1---- ----1-
* cv 103: collapsed liquid level in the test section (m)
*---- ----1---- ----1---- ----1---- ----1---- ----1---- ----1---- ----1-
*
20510300  collev    sum       1.        0.       0
20510301  0.
20510302  1.        cntrlvar  101
20510303  1.        cntrlvar  102
*
*---- ----1---- ----1---- ----1---- ----1---- ----1---- ----1---- ----1-
* cv 112: vapour mass flow from the test section (kg/s)
*---- ----1---- ----1---- ----1---- ----1---- ----1---- ----1---- ----1-
*
20511200  entgfl    mult      0.00015935          0.        1
20511201  rhogj     125000000
20511202  velgj     125000000
20511203  voidgj    125000000
*
*---- ----1---- ----1---- ----1---- ----1---- ----1---- ----1---- ----1-
* cv 113: liquid mass flow from the test section (kg/s)
*---- ----1---- ----1---- ----1---- ----1---- ----1---- ----1---- ----1-
*
20511300  entffl    mult      0.00015935          0.        1
20511301  rhofj     125000000
20511302  velfj     125000000
20511303  voidfj    125000000
*
*---- ----1---- ----1---- ----1---- ----1---- ----1---- ----1---- ----1-
* cv 114: total mass flow out of the test section  (kg/s)
*---- ----1---- ----1---- ----1---- ----1---- ----1---- ----1---- ----1-
*
20511400  entflow   sum       1.        1.       0
20511401  0.
20511402  1.        cntrlvar  112
20511403  1.        cntrlvar  113
*
```

```
*---- ----1---- ----1---- ----1---- ----1---- ----1---- ----1---- ----1-
* cv 115: quality at the tube exit
*---- ----1---- ----1---- ----1---- ----1---- ----1---- ----1---- ----1-
*
20511500  exitqual  div       1.          1.        0
20511501  cntrlvar  114       cntrlvar    112
*
*---- ----1---- ----1---- ----1---- ----1---- ----1---- ----1---- ----1-
* cv 118: integral of mass flow at tube exit (kg) (R5 var.)
*---- ----1---- ----1---- ----1---- ----1---- ----1---- ----1---- ----1-
*
20511800  intwgext  integral  1.          0.        0
20511801  mflowj    125000000
*
*---- ----1---- ----1---- ----1---- ----1---- ----1---- ----1---- ----1-
* cv 119: integral of mass flow at tube exit (kg) (cntrlvar)
*---- ----1---- ----1---- ----1---- ----1---- ----1---- ----1---- ----1-
*
20511900  intwgext   integral 1.          0.        0
20511901  cntrlvar   114
*
*---- ----1---- ----1---- ----1---- ----1---- ----1---- ----1---- ----1-
* cv 120: mass of water accumulated (lower part)
*---- ----1---- ----1---- ----1---- ----1---- ----1---- ----1---- ----1-
*
20512000  accwatl   sum      0.00015935  0.        0
20512001  0.
20512002  0.1      rho      120010000
20512003  0.1      rho      120020000
20512004  0.1      rho      120030000
20512005  0.1      rho      120040000
20512006  0.1      rho      120050000
20512007  0.1      rho      120060000
20512008  0.1      rho      120070000
20512009  0.1      rho      120080000
20512010  0.1      rho      120090000
20512011  0.1      rho      120100000
20512012  0.1      rho      120110000
20512013  0.1      rho      120120000
20512014  0.1      rho      120130000
20512015  0.1      rho      120140000
20512016  0.1      rho      120150000
20512017  0.1      rho      120160000
20512018  0.1      rho      120170000
20512019  0.1      rho      120180000
*
*---- ----1---- ----1---- ----1---- ----1---- ----1---- ----1---- ----1-
* cv 121: mass of water accumulated (upper part)
*---- ----1---- ----1---- ----1---- ----1---- ----1---- ----1---- ----1-
*
20512100  accwatu   sum      0.00015935  0.        0
20512101  0.
20512102  0.1      rho      120190000
20512103  0.1      rho      120200000
20512104  0.1      rho      120210000
20512105  0.1      rho      120220000
20512106  0.1      rho      120230000
20512107  0.1      rho      120240000
20512108  0.1      rho      120250000
20512109  0.1      rho      120260000
20512110  0.1      rho      120270000
20512111  0.1      rho      120280000
20512112  0.1      rho      120290000
20512113  0.1      rho      120300000
20512114  0.1      rho      120310000
20512115  0.1      rho      120320000
20512116  0.1      rho      120330000
20512117  0.1      rho      120340000
20512118  0.1      rho      120350000
20512119  0.16     rho      120360000
*
```

```
*---- ----1---- ----1---- ----1---- ----1---- ----1---- ----1---- ----1-
* cv 122: mass of water accumulated in the test section (kg)
*---- ----1---- ----1---- ----1---- ----1---- ----1---- ----1---- ----1-
*
20512200  accwater  sum       1.        0.       0
20512201  0.
20512202  1.        cntrlvar  120
20512203  1.        cntrlvar  121
*
*---- ----1---- ----1---- ----1---- ----1---- ----1---- ----1---- ----1-
* cv 140: integral of vapour mass flow at tube exit (kg)
*---- ----1---- ----1---- ----1---- ----1---- ----1---- ----1---- ----1-
*
20514000  intwgext   integral  1.         0.       0
20514001  cntrlvar   112
*
*---- ----1---- ----1---- ----1---- ----1---- ----1---- ----1---- ----1-
* cv 141: integral of liquid mass flow at tube exit (kg)
*---- ----1---- ----1---- ----1---- ----1---- ----1---- ----1---- ----1-
*
20514100  intwfext   integral  1.         0.       0
20514101  cntrlvar   113
*
*---- ----1---- ----1---- ----1---- ----1---- ----1---- ----1---- ----1-
* cv 142: sum of total mass accumulated and expelled (kg)
*---- ----1---- ----1---- ----1---- ----1---- ----1---- ----1---- ----1-
*
20514200  intwtext   sum       1.       0.        0
20514201  0.
20514202  1.        cntrlvar  140
20514203  1.        cntrlvar  141
20514204  1.        cntrlvar  122
*
*---- ----1---- ----1---- ----1---- ----1---- ----1---- ----1---- ----1-
* cv 143: integral of liquid mass flow at tube inlet (kg)
*---- ----1---- ----1---- ----1---- ----1---- ----1---- ----1---- ----1-
*
20514300  intwfin  integral   1.         0.       0
20514301  mflowj   110000000
*
*$*$*$*$*$*$*$*$*$*$*$*$*$*$*$*$*$*$*$*$*$*$*$*$*$*$*$*$*$*$*$*$*$*$*
*   GENERAL TABLES
*$*$*$*$*$*$*$*$*$*$*$*$*$*$*$*$*$*$*$*$*$*$*$*$*$*$*$*$*$*$*$*$*$*$*
*
*---- ----1---- ----1---- ----1---- ----1---- ----1---- ----1----
* tab 110: heat losses
*---- ----1---- ----1---- ----1---- ----1---- ----1---- ----1----
*
20211000 htc-temp
20211001 300.   12.13582
20211002 350.   13.81509
20211003 400.   15.72673
20211004 425.   16.77957
20211005 450.   17.90288
20211006 475.   19.10140
20211007 500.   20.38016
20211008 520.   21.46453
20211009 540.   22.60660
20211010 560.   23.80943
20211011 580.   25.07626
20211012 600.   26.41051
20211013 620.   27.81574
20211014 630.   28.54614
20211015 640.   29.29573
20211016 650.   30.06500
20211017 660.   30.85448
20211018 670.   31.66468
20211019 680.   32.49616
20211020 690.   33.34947
20211021 700.   34.22519
```

```
20211022 710.   35.12390
20211023 720.   36.04622
20211024 730.   36.99275
20211025 740.   37.96413
20211026 750.   38.96103
20211027 760.   39.98410
20211028 770.   41.03404
20211029 780.   42.11154
20211030 790.   43.21734
20211031 800.   44.35218
20211032 810.   45.51682
20211033 820.   46.71204
20211034 830.   47.93864
20211035 840.   49.19745
20211036 850.   50.48932
20211037 860.   51.81511
20211038 870.   53.17572
20211039 880.   54.57205
20211040 890.   56.00505
20211041 900.   57.47568
20211042 910.   58.98492
20211043 920.   60.53380
20211044 930.   62.12335
20211045 940.   63.75463
20211046 950.   65.42876
20211047 960.   67.14684
20211048 970.   68.91004
20211049 980.   70.71953
20211050 990.   72.57655
20211051 1000.  74.48233
20211052 1010.  76.43815
20211053 1020.  78.44532
20211054 1030.  80.50520
20211055 1040.  82.61918
20211056 1050.  84.78866
20211057 1060.  87.01512
20211058 1070.  89.30003
20211059 1080.  91.64495
20211060 1090.  94.05144
20211061 1100.  96.52112
*
*---- ----1---- ----1---- ----1---- ----1---- ----1---- ----1----
* tab 120 ambient temperature
*---- ----1---- ----1---- ----1---- ----1---- ----1---- ----1----
*
20212000 temp
20212001 0.      294.26
20212002 1000.   294.26
*
*---- ----1---- ----1---- ----1---- ----1---- ----1---- ----1----
* tab 150 test section power
*---- ----1---- ----1---- ----1---- ----1---- ----1---- ----1----
*
20215000  power
20215001  0.       4326.
20215002  1000.    4326.
*
```

```
*$*$*$*$*$*$*$*$*$*$*$*$*$*$*$*$*$*$*$*$*$*$*$*$*$*$*$*$*$*$*$*$*$*$*$*$*$*$*
*
*   $$$$$$$$$$      HEAT STRUCTURE THERMAL PROPERTY DATA
*
* (s-steel and inconnel 600 from Bethsy, copper from TM-IN-816)
*
*$*$*$*$*$*$*$*$*$*$*$*$*$*$*$*$*$*$*$*$*$*$*$*$*$*$*$*$*$*$*$*$*$*$*$*$*$*$*
*
*---- ----1---- ----1---- ----1---- ----1---- ----1---- ----1----
20100100  tbl/fctn  1         1          * INCONEL-600
*---- ----1---- ----1---- ----1---- ----1---- ----1---- ----1----
*
*---- ----1---- ----1---- ----1---- ----1---- ----1---- ----1----
* INCONEL-600 - thermal conductivity    (W/m-K)    [tp002]
*---- ----1---- ----1---- ----1---- ----1---- ----1---- ----1----
20100101  0.        14.       294.0     14.8       * 1st - artiff.
20100102  373.0     15.7
20100103  473.0     17.3
20100104  573.0     18.9
20100105  673.0     20.6
20100106  773.0     22.2
20100107  873.0     23.8
20100108  973.0     25.7
20100109  1073.0    27.4
20100110  1173.0    29.3
20100111  1273.0    31.0
20100112  1373.0    32.7
20100113  1473.0    34.4
20100114  1573.0    36.1
*---- ----1---- ----1---- ----1---- ----1---- ----1---- ----1----
* INCONEL-600 - volumetric heat capacity     (J/m3-K)
*---- ----1---- ----1---- ----1---- ----1---- ----1---- ----1----
20100151  0.        3.7+6     294.0     3.740+6    * 1st - artiff.
20100152  373.0     3.900+6
20100153  473.0     4.060+6
20100154  573.0     4.180+6
20100155  673.0     4.330+6
20100156  773.0     4.510+6
20100157  873.0     4.650+6
20100158  973.0     4.830+6
20100159  1073.0    5.020+6
20100160  1173.0    5.200+6
20100161  1273.0    5.340+6
20100162  1373.0    5.630+6
20100163  1477.0    5.810+6
. *** END ***
```

# Appendix II

## Sample input deck for quasi-steady state analysis

```
= UCB351
*
* UNIV. OF CALIFORNIA BERKELEY (UCB) TEST
*************************************************************************
* REFLOOD TEST IN SINGLE TUBE GEOMETRY
* UCB-3051: P=2 BAR, G=25.1 KG/M**2/S, XQ-=0.09
*
* GOAL: CALCULATION OF THE AXIAL VAPOUR
*       TEMPERATURE DISTRIBUTION WHEN THE QUENCH FRONT
*       IS AT HALF-LENGTH ELEVATION (Z=1.89 M)
*
*       REPRESENTATION OF THE SECTION ABOVE QUENCH FRONT ONLY (Z>1.8 M)
*       REFLOODING OPTION USED
*
* input: Power and heat losses
*
* RELAP5/MOD2.5 calculation
* for RELAP5/MOD3 only the card nr. 11200801 has to be changed
*************************************************************************
*
00000100  new       transnt
00000101  run
*                           cpu-lim
00000105  5.0       10.0      880.
00000110  nitrogen
*
*     TIME STEP CONTROL CARDS                        * REQUIRED
*          END TIME   MIN DT    MAX DT    OPTN   MNR    MJR  RST
00000201   15         1.0-9     0.01         3   10     400  400
*
*$*$*$*$*$*$*$*$*$*$*$*$*$*$*$*$*$*$*$*$*$*$*$*$*$*$*$*$*$*$*$*$*$*$*$*
*
*                     MINOR EDIT REQUESTS
*
*$*$*$*$*$*$*$*$*$*$*$*$*$*$*$*$*$*$*$*$*$*$*$*$*$*$*$*$*$*$*$*$*$*$*$*
*
00000301  cputime   0
*
00000308  voidg     120100000
00000309  voidg     120110000
00000310  voidg     120120000
00000311  voidg     120130000
00000312  voidg     120140000
00000313  voidg     120150000
00000314  voidg     120170000
00000315  voidg     120190000
*
00000319  tempg     120190000
*
00000320  q         120110000
00000321  qwg       120110000
00000322  q         120120000
00000323  qwg       120120000
00000324  qwg       120130000
00000325  qwg       120140000
00000326  qwg       120150000
00000327  qwg       120160000
00000328  qwg       120170000
00000329  qwg       120180000
00000330  qwg       120190000
*
00000331  mflowj    120110000
00000332  mflowj    120120000
00000333  mflowj    120130000
00000334  mflowj    120140000
00000335  mflowj    120150000
00000336  mflowj    120160000
00000337  mflowj    120170000
```

```
00000338  mflowj    120180000
00000340  mflowj    125000000
*
00000342  cntrlvar  101
*
00000343  cntrlvar  102
00000344  cntrlvar  103
00000345  cntrlvar  104
00000346  cntrlvar  105
00000348  cntrlvar  106
00000349  cntrlvar  110
00000351  cntrlvar  111
00000352  cntrlvar  115
00000353  cntrlvar  120
00000356  cntrlvar  125
00000357  cntrlvar  128
00000358  cntrlvar  129
00000359  cntrlvar  133
00000360  cntrlvar  134
00000361  cntrlvar  138
00000362  cntrlvar  139
00000363  cntrlvar  143
00000364  cntrlvar  144
00000365  cntrlvar  149
00000370  cntrlvar  150
00000371  cntrlvar  151
00000372  cntrlvar  152
00000373  cntrlvar  166
00000374  cntrlvar  167
00000375  cntrlvar  168
00000376  cntrlvar  169
00000377  cntrlvar  173
00000378  cntrlvar  182
*
00000380  floreg    120100000
00000381  floreg    120110000
00000382  floreg    120120000
00000383  floreg    120130000
00000384  floreg    120140000
00000385  floreg    120150000
00000386  floreg    120160000
00000387  floreg    120170000
00000388  floreg    120180000
00000389  floreg    120190000
*
00000391  httemp    120001001
00000392  httemp    120001101
00000393  httemp    120001301
00000394  httemp    120001601
00000395  httemp    120001801
*
*00000397  ztrwt     1200000
*
*$*$*$*$*$*$*$*$*$*$*$*$*$*$*$*$*$*$*$*$*$*$*$*$*$*$*$*$*$*$*$*$*$*$*$*$*
*
*                    TRIP COMPONENTS
*
*$*$*$*$*$*$*$*$*$*$*$*$*$*$*$*$*$*$*$*$*$*$*$*$*$*$*$*$*$*$*$*$*$*$*$*$*
*
500    time   0           gt   null    0.    400.    1 * end
*
501    quale  120180000   le   null    0.   20.00001 1 * full
*
502    time   0           gt   null    0.   0.      1 * start injection
*                                                      and reflood
503    time   0           gt   null    0.   10.     1 * start averaging
600           500
*
```

```
*$*$*$*$*$*$*$*$*$*$*$*$*$*$*$*$*$*$*$*$*$*$*$*$*$*$*$*$*$*$*$*$*$*$*$*$*$*$*
*
*                    HYDRODYNAMIC COMPONENTS
*
*$*$*$*$*$*$*$*$*$*$*$*$*$*$*$*$*$*$*$*$*$*$*$*$*$*$*$*$*$*$*$*$*$*$*$*$*$*$*
*
*---- ----1---- ----1---- ----1---- ----1---- ----1---- ----1---- ----1---- ----1-
* [105] feedwater tank - inlet thermodynamic conditions
*---- ----1---- ----1---- ----1---- ----1---- ----1---- ----1---- ----1---- ----1-
1050000   'feedtan' tmdpvol
1050101   0.00015935  0.    1000.      0.  0.  0.  0.  0.  0
1050200   002         * i.c.:   p,X; saturated
1050201   0.          2.15+5    .008
*---- ----1---- ----1---- ----1---- ----1---- ----1---- ----1---- ----1---- ----1-
* [110] inlet junction - flow boundary conditions
*---- ----1---- ----1---- ----1---- ----1---- ----1---- ----1---- ----1---- ----1-
1100000   'feedjun' tmdpjun
1100101   105000000 120000000 0.
1100200   1         502       time       0
1100201  -1.        0.0              0.0            0.
1100202   0.        0.0              0.0            0.
1100203   0.0001    0.003707         0.00030        0.
1100204 100.0       0.003707         0.00030        0. *mcell=G*Acell
*---- ----1---- ----1---- ----1---- ----1---- ----1---- ----1---- ----1---- ----1-
* [120] tube
*---- ----1---- ----1---- ----1---- ----1---- ----1---- ----1---- ----1---- ----1-
1200000   'testsec'           pipe
1200001   19
1200101   0.00015935 19 * Avcell
1200201   0.          18 * Ajunct
1200301   0.03        10 * cell length dz
1200302   0.2         18 *
1200303   0.16        19
1200401   0.          19 * cell volume=dz*Avcell
1200501   0.          19 * hor. angle
1200601   90.         19 * vert. angle
1200701   0.03        10 * cell dz
1200702   0.2         18 *
1200703   0.16        19 *
1200801   1.-4      0.01425 19 * friction data
1200901   0.        0.      18 * loss coefficients
*1201002   100       11          * bundle correlation on
1201002   0         19          * tube correlation on
1201101   00000     18
1201201   2         2.00+5      1.          0. 0. 0.    1 * initial
1201202   2         2.00+5      1.          0. 0. 0.    2 * conditions
1201203   2         2.00+5      1.          0. 0. 0.    3
1201204   2         2.00+5      1.          0. 0. 0.    4
1201205   2         2.00+5      1.          0. 0. 0.    5
1201206   2         2.00+5      1.          0. 0. 0.    6
1201207   2         2.00+5      1.          0. 0. 0.    7
1201208   2         2.00+5      1.          0. 0. 0.    8
1201209   2         2.00+5      1.          0. 0. 0.    9
1201210   2         2.00+5      1.          0. 0. 0.    10
1201211   3         2.0+5       420.           0. 0. 0.    11
1201212   3         2.0+5       430.           0. 0. 0.    12
1201213   3         2.0+5       440.           0. 0. 0.    13
1201214   3         2.0+5       450.           0. 0. 0.    14
1201215   3         2.0+5       460.           0. 0. 0.    15
1201216   3         2.0+5       470.           0. 0. 0.    16
1201217   3         2.0+5       480.           0. 0. 0.    17
1201218   3         2.0+5       490.           0. 0. 0.    18
1201219   3         2.0+5       500.           0. 0. 0.    19
*
1201300   1
1201301   0.              0.00030       0.          1 * mass flows
1201302   0.              0.00035       0.          2
1201303   0.              0.00037       0.          3
```

```
1201304   0.              0.00039       0.        4
1201305   0.              0.00040       0.        5
1201306   0.              0.00041       0.        6
1201307   0.              0.00042       0.        7
1201308   0.              0.00043       0.        8
1201309   0.              0.00045       0.        9
1201310   0.              0.00047       0.        10
1201311   0.              0.00052             0.        11
1201312   0.              0.00058             0.        12
1201313   0.              0.00063             0.        13
1201314   0.              0.00066             0.        14
1201315   0.              0.00069             0.        15
1201316   0.              0.00072             0.        16
1201317   0.              0.00075             0.        17
1201318   0.              0.00078             0.        18
*---- ----1---- ----1---- ----1---- ----1---- ----1---- ----1---- ----1-
* [125] outlet junction
*---- ----1---- ----1---- ----1---- ----1---- ----1---- ----1---- ----1-
1250000   'outljun' sngljun
1250101   120010000 130000000 0.        0.0       0.0      00000
1250201   1         0.        0.00078   0.0
*---- ----1---- ----1---- ----1---- ----1---- ----1---- ----1---- ----1-
* [130] outlet tank
*---- ----1---- ----1---- ----1---- ----1---- ----1---- ----1---- ----1-
1300000   'outltan' tmdpvol
1300101   .01       0.    1000.     0.  0.  0.  0.  0.  0
1300200   003
1300201   0.        2.0+5     480.
*
*$*$*$*$*$*$*$*$*$*$*$*$*$*$*$*$*$*$*$*$*$*$*$*$*$*$*$*$*$*$*$*$*$*$*
*
*                    HEAT STRUCTURES
*
*$*$*$*$*$*$*$*$*$*$*$*$*$*$*$*$*$*$*$*$*$*$*$*$*$*$*$*$*$*$*$*$*$*$*
*
**---- ----1---- ----1---- ----1---- ----1---- ----1---- ----1---- ----1-*
** [1200] test section(tube) - above quench front
**---- ----1---- ----1---- ----1---- ----1---- ----1---- ----1---- ----1-*
11200000  19        10         2         0         0.007125  502   0   64
11200100  0         1
11200101  9         0.00795 * outer tube radius
11200201  1         9
11200301  1.        9
11200400  -1
11200401  400.   400. 400. 400. 400. 400. 400. * initial
+         400.   400. 400.                     * temperatures of
11200402  450.   450. 450. 450. 450. 450. 450. * the nodes
+         450.   450. 450.                     *
11200403  555.   555. 555. 555. 555. 555. 555. *
+         555.   555. 555.                     *
11200404  575.   575. 575. 575. 575. 575. 575. *
+         575.   575. 575.                     *
11200405  595.   595. 595. 595. 595. 595. 595. *
+         595.   595. 595.                     *
11200406  595.   595. 595. 595. 595. 595. 595. *
+         595.   595. 595.                     *
11200407  595.   595. 595. 595. 595. 595. 595. *
+         595.   595. 595.                     *
11200408  595.   595. 595. 595. 595. 595. 595. *
+         595.   595. 595.                     *
11200409  595.   595. 595. 595. 595. 595. 595. *
+         595.   595. 595.                     *
11200410  595.   595. 595. 595. 595. 595. 595. *
+         595.   595. 595.                     *
11200411  595.   595. 595. 595. 595. 595. 595. ** (above QF)
+         595.   595. 595.                     **
11200412  645.   645. 645. 645. 645. 645. 645. **
+         645.   645. 645.                     **
```

```
11200413  670.    670. 670. 670. 670. 670. 670. **
+         670.    670. 670.                      **
11200414  690.    690. 690. 690. 690. 690. 690. **
+         690.    690. 690.                      **
11200415  710.    710. 710. 710. 710. 710. 710. **
+         710.    710. 710.                      **
11200416  720.    720. 720. 720. 720. 720. 720. **
+         720.    720. 720.                      **
11200417  726.    726. 726. 726. 726. 726. 726. **
+         726.    726. 726.                      **
11200418  733.    733. 733. 733. 733. 733. 733. **
+         733.    733. 733.                      **
11200419  733.    733. 733. 733. 733. 733. 733. **
+         733.    733. 733.                      **
11200501  120010000  10000      1        1         0.03     10 * inner surf
11200502  120110000  10000      1        1         0.2      18 **
11200503  120190000  0          1        1         0.16     19 **
11200601  0              0      0        1         0.03     10 * outer surf
11200602  0              0   2121        1         0.2      11 *
11200603  0              0   2122        1         0.2      12 *
11200604  0              0   2123        1         0.2      13 *
11200605  0              0   2124        1         0.2      14 *
11200606  0              0   2125        1         0.2      15 *
11200607  0              0   2126        1         0.2      16  *
11200608  0              0   2127        1         0.2      17 *
11200609  0              0   2128        1         0.2      18 *
11200610  0              0   2129        1         0.16     19 *
11200701    150          0.00819672  0.  0.       10 * power distribution
11200702    150          0.0546448   0.  0.       18 *
11200703    150          0.0437158   0.  0.       19 *
11200801  0          0.        0.        0.              19 * M2
*11200801  0.        11.       11.       0. 0. 0. 0.  1. 19 * M3
*---- ----1---- ----1---- ----1---- ----1---- ----1---- ----1---- ----1-*
*
*$*$*$*$*$*$*$*$*$*$*$*$*$*$*$*$*$*$*$*$*$*$*$*$*$*$*$*$*$*$*$*$*$*$*$*
*
*                    CONTROL VARIABLES
*
*$*$*$*$*$*$*$*$*$*$*$*$*$*$*$*$*$*$*$*$*$*$*$*$*$*$*$*$*$*$*$*$*$*$*$*
*
*---- ----1---- ----1---- ----1---- ----1---- ----1---- ----1---- ----1-
* cv 101: collapsed liquid level in the test section
*---- ----1---- ----1---- ----1---- ----1---- ----1---- ----1---- ----1-
*
20510100  collev    sum       1.        0.        1
20510101  0.
20510102  0.03      voidf     120010000
20510103  0.03      voidf     120020000
20510104  0.03      voidf     120030000
20510105  0.03      voidf     120040000
20510106  0.03      voidf     120050000
20510107  0.03      voidf     120060000
20510108  0.03      voidf     120070000
20510109  0.03      voidf     120080000
20510110  0.03      voidf     120090000
20510111  0.03      voidf     120100000
20510112  0.2       voidf     120110000
20510113  0.2       voidf     120120000
20510114  0.2       voidf     120130000
20510115  0.2       voidf     120140000
20510116  0.2       voidf     120150000
20510117  0.2       voidf     120160000
20510118  0.2       voidf     120170000
20510119  0.2       voidf     120180000
20510120  0.16      voidf     120190000
*
```

```
*---- ----1---- ----1---- ----1---- ----1---- ----1---- ----1---- ----1-
* cv 102: vapour mass flow from the test section
*---- ----1---- ----1---- ----1---- ----1---- ----1---- ----1---- ----1-
*
20510200  entgfl    mult      0.00015935          0.        1
20510201  rhogj     125000000
20510202  velgj     125000000
20510203  voidgj    125000000
20510204  cntrlvar  153
*
*---- ----1---- ----1---- ----1---- ----1---- ----1---- ----1---- ----1-
* cv 103: liquid mass flow from the test section
*---- ----1---- ----1---- ----1---- ----1---- ----1---- ----1---- ----1-
*
20510300  entffl    mult      0.00015935          0.        1
20510301  rhofj     125000000
20510302  velfj     125000000
20510303  voidfj    125000000
20510304  cntrlvar  153
*
*---- ----1---- ----1---- ----1---- ----1---- ----1---- ----1---- ----1-
* cv 104: total mass flow out of the test section
*---- ----1---- ----1---- ----1---- ----1---- ----1---- ----1---- ----1-
*
20510400  entflow   sum       1.        1.-10     1         1     1.-10
20510401  0.
20510402  1.        cntrlvar  102
20510403  1.        cntrlvar  103
*
*---- ----1---- ----1---- ----1---- ----1---- ----1---- ----1---- ----1-
* cv 105: quality at the tube exit
*---- ----1---- ----1---- ----1---- ----1---- ----1---- ----1---- ----1-
*
20510500  exitqual  div       1.         0.        1
20510501  cntrlvar  104       cntrlvar   102
*
*---- ----1---- ----1---- ----1---- ----1---- ----1---- ----1---- ----1-
* cv 106: phase velocity difference in volume 13
*---- ----1---- ----1---- ----1---- ----1---- ----1---- ----1---- ----1-
*
20510600  diffv13   sum       1.        0.        1
20510601  0.
20510602  1.        velg      120130000
20510603  -1.       velf      120130000
*
*---- ----1---- ----1---- ----1---- ----1---- ----1---- ----1---- ----1-
* cv 107:
*---- ----1---- ----1---- ----1---- ----1---- ----1---- ----1---- ----1-
*
20510700  abscv106  stdfnctn  1.        0.        1
20510701  abs       cntrlvar  106
*
*---- ----1---- ----1---- ----1---- ----1---- ----1---- ----1---- ----1-
* cv 108:
*---- ----1---- ----1---- ----1---- ----1---- ----1---- ----1---- ----1-
*
20510800  cv107s10  mult      1.        0.        1
20510801  cntrlvar  153       cntrlvar  107
*
*---- ----1---- ----1---- ----1---- ----1---- ----1---- ----1---- ----1-
* cv 109:
*---- ----1---- ----1---- ----1---- ----1---- ----1---- ----1---- ----1-
*
20510900  cv107int   integral 1.         0.        1
20510901  cntrlvar   108
*
```

```
*---- ----1---- ----1---- ----1---- ----1---- ----1---- ----1---- ----1-
* cv 110: average phase velocity difference (10-20s) in cell 13
*---- ----1---- ----1---- ----1---- ----1---- ----1---- ----1---- ----1-
*
20511000  avdv13    div       1.        0.        1
20511001  cntrlvar  154       cntrlvar  109
*
*---- ----1---- ----1---- ----1---- ----1---- ----1---- ----1---- ----1-
* cv 111: phase velocity difference in volume 16
*---- ----1---- ----1---- ----1---- ----1---- ----1---- ----1---- ----1-
*
20511100  diffv16   sum       1.        0.        1
20511101  0.
20511102  1.        velg      120160000
20511103  -1.       velf      120160000
*
*---- ----1---- ----1---- ----1---- ----1---- ----1---- ----1---- ----1-
* cv 112:
*---- ----1---- ----1---- ----1---- ----1---- ----1---- ----1---- ----1-
*
20511200  abscv111  stdfnctn  1.        0.        1
20511201  abs       cntrlvar  111
*
*---- ----1---- ----1---- ----1---- ----1---- ----1---- ----1---- ----1-
* cv 113:
*---- ----1---- ----1---- ----1---- ----1---- ----1---- ----1---- ----1-
*
20511300  cv112s10  mult      1.        0.        1
20511301  cntrlvar  153       cntrlvar  112
*
*---- ----1---- ----1---- ----1---- ----1---- ----1---- ----1---- ----1-
* cv 114:
*---- ----1---- ----1---- ----1---- ----1---- ----1---- ----1---- ----1-
*
20511400  cv113int   integral 1.         0.        1
20511401  cntrlvar   113
*
*---- ----1---- ----1---- ----1---- ----1---- ----1---- ----1---- ----1-
* cv 115: average phase velocity difference (10-20s) in cell 16
*---- ----1---- ----1---- ----1---- ----1---- ----1---- ----1---- ----1-
*
20511500  avdv16    div       1.        0.        1
20511501  cntrlvar  154       cntrlvar 114
*
*---- ----1---- ----1---- ----1---- ----1---- ----1---- ----1---- ----1-
* cv 118: vapour mass flow at junction 10
*---- ----1---- ----1---- ----1---- ----1---- ----1---- ----1---- ----1-
*
20511800  entgj10    mult      0.00015935          0.        1
20511801  rhogj     120100000
20511802  velgj     120100000
20511803  voidgj    120100000
*
*---- ----1---- ----1---- ----1---- ----1---- ----1---- ----1---- ----1-
* cv 119: liquid mass flow at junction 10
*---- ----1---- ----1---- ----1---- ----1---- ----1---- ----1---- ----1-
*
20511900  entfj10    mult      0.00015935          0.        1
20511901  rhofj     120100000
20511902  velfj     120100000
20511903  voidfj    120100000
*
*---- ----1---- ----1---- ----1---- ----1---- ----1---- ----1---- ----1-
* cv 120: total mass flow at junction 10
*---- ----1---- ----1---- ----1---- ----1---- ----1---- ----1---- ----1-
*
20512000  mflowj10   sum       1.        0.        1
20512001  0.
```

```
20512002  1.         cntrlvar  118
20512003  1.         cntrlvar  119
*
*---- ----1---- ----1---- ----1---- ----1---- ----1---- ----1---- ----1-
* cv 121: quality at junction 10
*---- ----1---- ----1---- ----1---- ----1---- ----1---- ----1---- ----1-
*
20512100  qualj10   div       1.          0.         1
20512101  cntrlvar  120       cntrlvar    118
*
*---- ----1---- ----1---- ----1---- ----1---- ----1---- ----1---- ----1-
* cv 122: vapour mass flow at junction 11
*---- ----1---- ----1---- ----1---- ----1---- ----1---- ----1---- ----1-
*
20512200  entgj11    mult      0.00015935          0.         1
20512201  rhogj     120110000
20512202  velgj     120110000
20512203  voidgj    120110000
20512204  cntrlvar  153
*
*---- ----1---- ----1---- ----1---- ----1---- ----1---- ----1---- ----1-
* cv 123: liquid mass flow at junction 11
*---- ----1---- ----1---- ----1---- ----1---- ----1---- ----1---- ----1-
*
20512300  entfj11    mult      0.00015935          0.         1
20512301  rhofj     120110000
20512302  velfj     120110000
20512303  voidfj    120110000
20512304  cntrlvar  153
*
*---- ----1---- ----1---- ----1---- ----1---- ----1---- ----1---- ----1-
* cv 124: total mass flow at junction 11
*---- ----1---- ----1---- ----1---- ----1---- ----1---- ----1---- ----1-
*
20512400  mflowj11  sum       1.         1.-10     1          1      1.-10
20512401  0.
20512402  1.         cntrlvar  122
20512403  1.         cntrlvar  123
*
*---- ----1---- ----1---- ----1---- ----1---- ----1---- ----1---- ----1-
* cv 125: quality at junction 11
*---- ----1---- ----1---- ----1---- ----1---- ----1---- ----1---- ----1-
*
20512500  qualj11   div       1.          0.         1
20512501  cntrlvar  124       cntrlvar    122
*
*---- ----1---- ----1---- ----1---- ----1---- ----1---- ----1---- ----1-
* cv 126: vapour mass flow at junction 16
*---- ----1---- ----1---- ----1---- ----1---- ----1---- ----1---- ----1-
*
20512600  entgj16   mult      0.00015935          0.         1
20512601  rhogj     120160000
20512602  velgj     120160000
20512603  voidgj    120160000
20512604  cntrlvar  153
*
*---- ----1---- ----1---- ----1---- ----1---- ----1---- ----1---- ----1-
* cv 127: liquid mass flow at junction 16
*---- ----1---- ----1---- ----1---- ----1---- ----1---- ----1---- ----1-
*
20512700  entfj16   mult      0.00015935          0.         1
20512701  rhofj     120160000
20512702  velfj     120160000
20512703  voidfj    120160000
20512704  cntrlvar  153
*
```

```
*---- ----1---- ----1---- ----1---- ----1---- ----1---- ----1---- ----1-
* cv 128: total mass flow at junction 16
*---- ----1---- ----1---- ----1---- ----1---- ----1---- ----1---- ----1-
*
20512800  mflowj16  sum       1.        1.-10     1         1     1.-10
20512801  0.
20512802  1.        cntrlvar  126
20512803  1.        cntrlvar  127
*
*---- ----1---- ----1---- ----1---- ----1---- ----1---- ----1---- ----1-
* cv 129: quality at junction 16
*---- ----1---- ----1---- ----1---- ----1---- ----1---- ----1---- ----1-
*
20512900  qualj16   div       1.         0.        1
20512901  cntrlvar  128       cntrlvar   126
*
*---- ----1---- ----1---- ----1---- ----1---- ----1---- ----1---- ----1-
* cv 130: integral of vapour mass flow at junction 11
*---- ----1---- ----1---- ----1---- ----1---- ----1---- ----1---- ----1-
*
20513000  intwgj11   integral  1.         0.        0
20513001  cntrlvar   122
*
*---- ----1---- ----1---- ----1---- ----1---- ----1---- ----1---- ----1-
* cv 131: integral of liquid mass flow at junction 11
*---- ----1---- ----1---- ----1---- ----1---- ----1---- ----1---- ----1-
*
20513100  intwfj11   integral  1.         0.        0
20513101  cntrlvar   123
*
*---- ----1---- ----1---- ----1---- ----1---- ----1---- ----1---- ----1-
* cv 132: integral of total mass flow at junction 11
*---- ----1---- ----1---- ----1---- ----1---- ----1---- ----1---- ----1-
*
20513200  intwtj11   sum       1.        1.-10     1         1     1.-10
20513201  0.
20513202  1.        cntrlvar  130
20513203  1.        cntrlvar  131
*
*---- ----1---- ----1---- ----1---- ----1---- ----1---- ----1---- ----1-
* cv 133: average total mass flow at junction 11
*---- ----1---- ----1---- ----1---- ----1---- ----1---- ----1---- ----1-
*
20513300  avwtj11   div       1.         0.        0
20513301  cntrlvar 154        cntrlvar   132
*
*---- ----1---- ----1---- ----1---- ----1---- ----1---- ----1---- ----1-
* cv 134: average quality at junction 11
*---- ----1---- ----1---- ----1---- ----1---- ----1---- ----1---- ----1-
*
20513400  avxaj11   div       1.        0.        0
20513401  cntrlvar  132       cntrlvar  130
*
*---- ----1---- ----1---- ----1---- ----1---- ----1---- ----1---- ----1-
* cv 135: integral of vapour mass flow at junction 16
*---- ----1---- ----1---- ----1---- ----1---- ----1---- ----1---- ----1-
*
20513500  intwgj16   integral  1.         0.        0
20513501  cntrlvar   126
*
*---- ----1---- ----1---- ----1---- ----1---- ----1---- ----1---- ----1-
* cv 136: integral of liquid mass flow at junction 16
*---- ----1---- ----1---- ----1---- ----1---- ----1---- ----1---- ----1-
*
20513600  intwfj16   integral  1.         0.        0
20513601  cntrlvar   127
*
```

```
*---- ----1---- ----1---- ----1---- ----1---- ----1---- ----1---- ----1-
* cv 137: integral of total mass flow at junction 16
*---- ----1---- ----1---- ----1---- ----1---- ----1---- ----1---- ----1-
*
20513700  intwtj16   sum       1.       1.-10     1         1     1.-10
20513701  0.
20513702  1.         cntrlvar  135
20513703  1.         cntrlvar  136
*
*---- ----1---- ----1---- ----1---- ----1---- ----1---- ----1---- ----1-
* cv 138: average total mass flow at junction 16
*---- ----1---- ----1---- ----1---- ----1---- ----1---- ----1---- ----1-
*
20513800  avwtj16   div       1.         0.       0
20513801  cntrlvar 154        cntrlvar  137
*
*---- ----1---- ----1---- ----1---- ----1---- ----1---- ----1---- ----1-
* cv 139: average quality at junction 16
*---- ----1---- ----1---- ----1---- ----1---- ----1---- ----1---- ----1-
*
20513900  avxaj16   div       1.        0.       0
20513901  cntrlvar  137       cntrlvar  135
*
*---- ----1---- ----1---- ----1---- ----1---- ----1---- ----1---- ----1-
* cv 140: integral of vapour mass flow at tube exit
*---- ----1---- ----1---- ----1---- ----1---- ----1---- ----1---- ----1-
*
20514000  intwgext   integral  1.         0.       0
20514001  cntrlvar   102
*
*---- ----1---- ----1---- ----1---- ----1---- ----1---- ----1---- ----1-
* cv 141: integral of liquid mass flow at tube exit
*---- ----1---- ----1---- ----1---- ----1---- ----1---- ----1---- ----1-
*
20514100  intwfext   integral  1.         0.       0
20514101  cntrlvar   103
*
*---- ----1---- ----1---- ----1---- ----1---- ----1---- ----1---- ----1-
* cv 142: integral of total mass flow at tube exit
*---- ----1---- ----1---- ----1---- ----1---- ----1---- ----1---- ----1-
*
20514200  intwtext   sum       1.       1.-10     1         1     1.-10
20514201  0.
20514202  1.         cntrlvar  140
20514203  1.         cntrlvar  141
*
*---- ----1---- ----1---- ----1---- ----1---- ----1---- ----1---- ----1-
* cv 143: average total mass flow at tube exit
*---- ----1---- ----1---- ----1---- ----1---- ----1---- ----1---- ----1-
*
20514300  avwtext   div       1.         0.       0
20514301  cntrlvar 154        cntrlvar  142
*
*---- ----1---- ----1---- ----1---- ----1---- ----1---- ----1---- ----1-
* cv 144: average quality at tube exit
*---- ----1---- ----1---- ----1---- ----1---- ----1---- ----1---- ----1-
*
20514400  avxaext   div       1.        0.       0
20514401  cntrlvar  142       cntrlvar  140
*
*---- ----1---- ----1---- ----1---- ----1---- ----1---- ----1---- ----1-
* cv 149: equilibrium quality at the quench front
*---- ----1---- ----1---- ----1---- ----1---- ----1---- ----1---- ----1-
*
20514900  xeqqf     sum       1.        1.       0.       0
20514901  0.075
20514902  1.13355258-4        cntrlvar  150
*
```

```
*---- ----1---- ----1---- ----1---- ----1---- ----1---- ----1---- ----1-
* cv 150: power input to wet portion of test section
*---- ----1---- ----1---- ----1---- ----1---- ----1---- ----1---- ----1-
*
20515000  qinwet    sum       1.        0.       1
20515001  0.
20515002  1.        q         120010000
20515003  1.        q         120020000
20515004  1.        q         120030000
20515005  1.        q         120040000
20515006  1.        q         120050000
20515007  1.        q         120060000
20515008  1.        q         120070000
20515009  1.        q         120080000
20515010  1.        q         120090000
20515011  1.        q         120100000
*
*---- ----1---- ----1---- ----1---- ----1---- ----1---- ----1---- ----1-
* cv 151: power input to dry portion of test section
*---- ----1---- ----1---- ----1---- ----1---- ----1---- ----1---- ----1-
*
20515100  qindry    sum       1.        0.       1
20515101  0.
20515102  1.        q         120110000
20515103  1.        q         120120000
20515104  1.        q         120130000
20515105  1.        q         120140000
20515106  1.        q         120150000
20515107  1.        q         120160000
20515108  1.        q         120170000
20515109  1.        q         120180000
20515110  1.        q         120190000
*
*---- ----1---- ----1---- ----1---- ----1---- ----1---- ----1---- ----1-
* cv 152: total heat input to fluid in test section
*---- ----1---- ----1---- ----1---- ----1---- ----1---- ----1---- ----1-
*
20515200  qintot    sum       1.        0.       1
20515201  0.
20515202  1.        cntrlvar  150
20515203  1.        cntrlvar  151
*
*---- ----1---- ----1---- ----1---- ----1---- ----1---- ----1---- ----1-
* cv 153: trip unit
*---- ----1---- ----1---- ----1---- ----1---- ----1---- ----1---- ----1-
*
20515300  trip      tripunit  1.        0.        0
20515301  503
*
*---- ----1---- ----1---- ----1---- ----1---- ----1---- ----1---- ----1-
* cv 154: delay
*---- ----1---- ----1---- ----1---- ----1---- ----1---- ----1---- ----1-
20515400  delay     sum       1.        0.0000001 1
20515401  -10.
20515402  1.        time      0
*
*---- ----1---- ----1---- ----1---- ----1---- ----1---- ----1---- ----1-
* cv 160: heat added to wet part (after 10 s)
*---- ----1---- ----1---- ----1---- ----1---- ----1---- ----1---- ----1-
*
20516000  htwet10   mult      1.        0.        0
20516001  cntrlvar  150       cntrlvar  153
*
*---- ----1---- ----1---- ----1---- ----1---- ----1---- ----1---- ----1-
* cv 161: heat added to dry part (after 10 s)
*---- ----1---- ----1---- ----1---- ----1---- ----1---- ----1---- ----1-
```

```
*
20516100  htdry10   mult      1.        0.        0
20516101  cntrlvar  151       cntrlvar  153
*
*---- ----1---- ----1---- ----1---- ----1---- ----1---- ----1---- ----1-
* cv 162: heat added to fluid (after 10 s)
*---- ----1---- ----1---- ----1---- ----1---- ----1---- ----1---- ----1-
*
20516200  httot10   mult      1.        0.        0
20516201  cntrlvar  152       cntrlvar  153
*
*---- ----1---- ----1---- ----1---- ----1---- ----1---- ----1---- ----1-
* cv 163: total heat added to fluid in wet region (after 10 s)
*---- ----1---- ----1---- ----1---- ----1---- ----1---- ----1---- ----1-
*
20516300  htinwet   integral  1.        0.        1
20516301  cntrlvar  160
*
*---- ----1---- ----1---- ----1---- ----1---- ----1---- ----1---- ----1-
* cv 164: total heat added to fluid in dry region (after 10 s)
*---- ----1---- ----1---- ----1---- ----1---- ----1---- ----1---- ----1-
*
20516400  htindry   integral  1.        0.        1
20516401  cntrlvar  161
*
*---- ----1---- ----1---- ----1---- ----1---- ----1---- ----1---- ----1-
* cv 165: total heat added to fluid (after 10 s)
*---- ----1---- ----1---- ----1---- ----1---- ----1---- ----1---- ----1-
*
20516500  htintot   integral  1.        0.        1
20516501  cntrlvar  162
*
*---- ----1---- ----1---- ----1---- ----1---- ----1---- ----1---- ----1-
* cv 166: average heat transfer rate in wet region (10-20 s)
*---- ----1---- ----1---- ----1---- ----1---- ----1---- ----1---- ----1-
*
20516600  avhtwet   div       1.        0.        0
20516601  cntrlvar  154       cntrlvar  163
*
*---- ----1---- ----1---- ----1---- ----1---- ----1---- ----1---- ----1-
* cv 167: average heat transfer rate in dry region (10-20 s)
*---- ----1---- ----1---- ----1---- ----1---- ----1---- ----1---- ----1-
*
20516700  avhtdry   div       1.        0.        0
20516701  cntrlvar  154       cntrlvar  164
*
*---- ----1---- ----1---- ----1---- ----1---- ----1---- ----1---- ----1-
* cv 168: average heat transfer rate to fluid (10-20 s)
*---- ----1---- ----1---- ----1---- ----1---- ----1---- ----1---- ----1-
*
20516800  avhttot   div       1.        0.        0
20516801  cntrlvar  154       cntrlvar  165
*
*---- ----1---- ----1---- ----1---- ----1---- ----1---- ----1---- ----1-
* cv 169: heat transfer to vapour only in the dry region
*---- ----1---- ----1---- ----1---- ----1---- ----1---- ----1---- ----1-
*
20516900  qdryvap   sum       1.        0.        1
20516901  0.
20516902  1.        qwg       120110000
20516903  1.        qwg       120120000
20516904  1.        qwg       120130000
20516905  1.        qwg       120140000
20516906  1.        qwg       120150000
20516907  1.        qwg       120160000
20516908  1.        qwg       120170000
20516909  1.        qwg       120180000
20516910  1.        qwg       120190000
*
```

```
*---- ----1---- ----1---- ----1---- ----1---- ----1---- ----1---- ----1-
* cv 171: heat added to vapour in dry region (after 10 s)
*---- ----1---- ----1---- ----1---- ----1---- ----1---- ----1---- ----1-
*
20517100  htdry10   mult      1.        0.       0
20517101  cntrlvar  169       cntrlvar  153
*
*---- ----1---- ----1---- ----1---- ----1---- ----1---- ----1---- ----1-
* cv 172: total heat added to vapour in dry region (after 10 s)
*---- ----1---- ----1---- ----1---- ----1---- ----1---- ----1---- ----1-
*
20517200  htgdry    integral  1.        0.       1
20517201  cntrlvar  171
*
*---- ----1---- ----1---- ----1---- ----1---- ----1---- ----1---- ----1-
* cv 173: average heat transfer rate to vapour in dry region (10-20 s)
*---- ----1---- ----1---- ----1---- ----1---- ----1---- ----1---- ----1-
*
20517300  avqwgdry  div       1.        0.       0
20517301  cntrlvar  154       cntrlvar  172
*
*---- ----1---- ----1---- ----1---- ----1---- ----1---- ----1---- ----1-
* cv 180: vapour temperature after 10 s
*---- ----1---- ----1---- ----1---- ----1---- ----1---- ----1---- ----1-
*
20518000  tempg10   mult      1.        0.       0
20518001  tempg     120190000 cntrlvar  153
*
*---- ----1---- ----1---- ----1---- ----1---- ----1---- ----1---- ----1-
* cv 181:
*---- ----1---- ----1---- ----1---- ----1---- ----1---- ----1---- ----1-
*
20518100  tempint   integral  1.        0.       0
20518101  cntrlvar  180
*
*---- ----1---- ----1---- ----1---- ----1---- ----1---- ----1---- ----1-
* cv 182: average temperature (10-20 s)
*---- ----1---- ----1---- ----1---- ----1---- ----1---- ----1---- ----1-
*
20518200  avtemp    div       1.        0.       0
20518201  cntrlvar  154       cntrlvar  181
*
*$*$*$*$*$*$*$*$*$*$*$*$*$*$*$*$*$*$*$*$*$*$*$*$*$*$*$*$*$*$*$*$*$*$*
*   GENERAL TABLES
*$*$*$*$*$*$*$*$*$*$*$*$*$*$*$*$*$*$*$*$*$*$*$*$*$*$*$*$*$*$*$*$*$*$*
*
*---- ----1---- ----1---- ----1---- ----1---- ----1---- ----1----
* tab 110-129 heat losses and heat fluxes
*---- ----1---- ----1---- ----1---- ----1---- ----1---- ----1----
*
20211000 htrnrate
20211001 0.      26402.
20211002 1000.   26402.
*
20211100 htrnrate
20211101 0.      16930.
20211102 1000.   16930.
*
20211200 htrnrate
20211201 0.      15470.
20211202 1000.   15470.
*
20211300 htrnrate
20211301 0.      13930.
20211302 1000.   13930.
*
20211400 htrnrate
20211401 0.      12395.
20211402 1000.   12395.
```

```
*
20211500 htrnrate
20211501 0.       10980.
20211502 1000.    10980.
*
20211600 htrnrate
20211601 0.       9700.
20211602 1000.    9700.
*
20211700 htrnrate
20211701 0.       8843.
20211702 1000.    8843.
*
20211800 htrnrate
20211801 0.       8195.
20211802 1000.    8195.
*
20211900 htrnrate
20211901 0.       8195.
20211902 1000.    8195.
*
20212100 htrnrate
20212101 0.       8494.
20212102 1000.    8494.
*
20212200 htrnrate
20212201 0.       9802.
20212202 1000.    9802.
*
20212300 htrnrate
20212301 0.       11174.
20212302 1000.    11174.
*
20212400 htrnrate
20212401 0.       12553.
20212402 1000.    12553.
*
20212500 htrnrate
20212501 0.       13823.
20212502 1000.    13823.
*
20212600 htrnrate
20212601 0.       14973.
20212602 1000.    14973.
*
20212700 htrnrate
20212701 0.       15737.
20212702 1000.    15737.
*
20212800 htrnrate
20212801 0.       16317.
20212802 1000.    16317.
*
20212900 htrnrate
20212901 0.       16317.
20212902 1000.    16317.
*
*---- ----1---- ----1---- ----1---- ----1---- ----1---- ----1----
* tab 150 test section power
*---- ----1---- ----1---- ----1---- ----1---- ----1---- ----1----
*
20215000  power
20215001  0.        4326.
20215002  1000.     4326.
*
```

```
*$*$*$*$*$*$*$*$*$*$*$*$*$*$*$*$*$*$*$*$*$*$*$*$*$*$*$*$*$*$*$*$*$*$*$*$*$*$*
*
*   $$$$$$$$$$      HEAT STRUCTURE THERMAL PROPERTY DATA
*
* (s-steel and inconnel 600 from Bethsy, copper from TM-IN-816)
*
*$*$*$*$*$*$*$*$*$*$*$*$*$*$*$*$*$*$*$*$*$*$*$*$*$*$*$*$*$*$*$*$*$*$*$*$*$*$*
*
*---- ----1---- ----1---- ----1---- ----1---- ----1---- ----1----
20100100  tbl/fctn  1          1          * INCONEL-600
*---- ----1---- ----1---- ----1---- ----1---- ----1---- ----1----
*
*---- ----1---- ----1---- ----1---- ----1---- ----1---- ----1----
* INCONEL-600 - thermal conductivity     (W/m-K)    [tp002]
*---- ----1---- ----1---- ----1---- ----1---- ----1---- ----1----
20100101  0.        14.       294.0     14.8       * 1st - artiff.
20100102  373.0     15.7
20100103  473.0     17.3
20100104  573.0     18.9
20100105  673.0     20.6
20100106  773.0     22.2
20100107  873.0     23.8
20100108  973.0     25.7
20100109  1073.0    27.4
20100110  1173.0    29.3
20100111  1273.0    31.0
20100112  1373.0    32.7
20100113  1473.0    34.4
20100114  1573.0    36.1
*---- ----1---- ----1---- ----1---- ----1---- ----1---- ----1----
* INCONEL-600 - volumetric heat capacity      (J/m3-K)
*---- ----1---- ----1---- ----1---- ----1---- ----1---- ----1----
20100151  0.        3.7+6     294.0     3.740+6    * 1st - artiff.
20100152  373.0     3.900+6
20100153  473.0     4.060+6
20100154  573.0     4.180+6
20100155  673.0     4.330+6
20100156  773.0     4.510+6
20100157  873.0     4.650+6
20100158  973.0     4.830+6
20100159  1073.0    5.020+6
20100160  1173.0    5.200+6
20100161  1273.0    5.340+6
20100162  1373.0    5.630+6
20100163  1477.0    5.810+6
. *** END ***
```

NRC FORM 335 (2-89) NRCM 1102, 3201, 3202

U.S. NUCLEAR REGULATORY COMMISSION

# BIBLIOGRAPHIC DATA SHEET

*(See instructions on the reverse)*

1. REPORT NUMBER (Assigned by NRC, Add Vol., Supp., Rev., and Addendum Numbers, if any.)

NUREG/IA-0163

2. TITLE AND SUBTITLE

A Study of the Dispersed Flow Interfacial Heat Transfer Model of RELAP5/MOD2.5 and RELAP5/MOD3

3. DATE REPORT PUBLISHED

| MONTH | YEAR |
|---|---|
| April | 1999 |

4. FIN OR GRANT NUMBER

D6227

5. AUTHOR(S)

M. Andreani*
G. Th. Analytis
S. N. Aksan

6. TYPE OF REPORT

7. PERIOD COVERED *(Inclusive Dates)*

8. PERFORMING ORGANIZATION - NAME AND ADDRESS *(If NRC, provide Division, Office or Region, U.S. Nuclear Regulatory Commission, and mailing address; if contractor, provide name and mailing address.)*

Thermal-Hydraulics Laboratory
Paul Scherrer Institute (PSI)
CH-5232 Villigen PSI, Switzerland

*ETHZ, Nuclear Engineering Laboratory
Swiss Federal Institute of Technology
8092 Zurich Switzerland

9. SPONSORING ORGANIZATION - NAME AND ADDRESS *(If NRC, type "Same as above"; if contractor, provide NRC Division, Office or Region, U.S. Nuclear Regulatory Commission, and mailing address.)*

Office of Nuclear Regulatory Research
U.S. Nuclear Regulatory Commission
Washington, DC 20555-0001

10. SUPPLEMENTARY NOTES

G. Rhee, NRC Project Manager

11. ABSTRACT *(200 words or less)*

For conditions of low quality at the quench front and low mass flux, the interfacial heat transfer calculated assuming a uniform distribution of droplets over the cross-sectional area of the channel is necessarily overpredicted, and the vapour superheat is strongly underpredicted. The purpose of the present paper is to show that limitations of the 1-D approach, obtained from the steady-state analyses of slow reflooding experiments, has some impact on the performance of the 1-D transient computer codes like RELAP5/MOD2.5 and RELAP5/MOD3. As an example, the transient analysis of a low flooding rate experiment in a tube was performed. An early completion of the quench process and a fast desuperheating of the vapour at the tube exit was obtained by both codes. The too high quench front velocity (four times higher than in the experiment) could not, however, be put univocally in relation to the underprediction of the vapour temperature, and the consequent increase of the precursory cooling, as many coupled thermal and hydraulic transient effects prevailed. Quasi steady-state analyses of two runs, where the boundary conditions for the post-dryout region could be better controlled for a predetermined position of the quench front, were thus performed. These analyses show that the vapour superheat at the tube exit is strongly underpredicted, confirming the limitations of the 1-D model for interfacial heat transfer in the dispersed flow region.

12. KEY WORDS/DESCRIPTORS *(List words or phrases that will assist researchers in locating the report.)*

Assessment of RELAP5, Reflood Heat Transfer
Dispersed Flow, Post-CHF Heat Transfer
Interfacial Heat Transfer Model
RELAP5/MOD2.5
RELAP5/MOD3

13. AVAILABILITY STATEMENT

unlimited

14. SECURITY CLASSIFICATION

*(This Page)* unclassified

*(This Report)* unclassified

15. NUMBER OF PAGES

16. PRICE


Federal Recycling Program